Numerical analysis of an interior penalty discontinuous Galerkin scheme for two phase flow in heterogeneous porous media with discontinuous dynamic capillary pressure effects

Stefan Karpinski

PhD Thesis

Promoters:
Prof. Dr. Iuliu Sorin Pop, University of Hasselt, Belgium
Prof. Dr. Florin Adrian Radu, Bergen University, Norway

Doctoral committee members:
Prof. Dr. Rainer Helmig, University of Stuttgart, Germany
Prof. Dr. Iuliu Sorin Pop, University of Hasselt, Belgium
Prof. Dr. Florin Adrian Radu, Bergen University, Norway
Prof. Dr. Jochen Schütz, University of Hasselt, Belgium

Hasselt University

Faculty of Sciences
Discipline group Mathematics and statistics
Research group Computational mathematics

Dedicated to my loving wife,
without whom I wouldn't have written this...

Acknowledgments

I am extremely thankful to my supervisor Prof. Dr. Sorin Pop for his readiness to accept me as his student despite the challenges of guiding an external thesis. I am grateful for his constant support, compassion, and encouragement that reinforced my belief in my ability to finalize this thesis. I couldn't have wished for a better supervisor!

I am also grateful to Prof. Dr. Florin Adrian Radu for agreeing to supervise my thesis together with Sorin, and for helping to find a good direction to take my thesis forward. I want to thank Prof. Dr. Jochen Schütz for his detailed and diligent proof-reading of my thesis. I also acknowledge the support of Prof. Dr. Barbara Wohlmuth and Prof. Dr. Rainer Helmig for introducing me to this interesting topic, guiding me through the first years of PhD, and introducing me to Sorin.

I take this opportunity to also thank Dr. Roman Rojko for showing interest and support in my thesis, and for mentoring me in my first years of work in the industry. My thanks also to Dr. Stefan Zaprianov and all my colleagues at ESPRiT Engineering GmbH. Working with them is an enjoyable and a valuable experience.

I also thank my parents for encouraging me to pursue academics, for supporting me through my studies, and for being there when ever I needed them.

Special thanks to all my friends for being my sanity in hard times and for always being there for a beer or a game of Munchkin or Borderlands as and when the occasion demanded it!

Lastly, and more importantly, I want to thank my loving and amazing wife Shubhangi Gupta. She helped me wherever she could and encouraged me through all my different phases throughout the PhD. Be it moral support, scientific discussion, or just a hug when things got too stressful, she was alway there for me. Without her I would probably become a boring, miserable, grumpy old man. For this, and everything else, I thank her very much.

Abstract

We present an interior penalty discontinuous Galerkin scheme for a two-phase flow model in heterogeneous porous media. The model includes dynamic effects and discontinuities in the capillary pressure. We define the interface conditions arising across material interfaces in heterogeneous media and show how to account for capillary barriers. We numerically approximate the mass-conservation laws without reformulation, i.e. without introducing a global pressure. We prove the existence of a solution to the emerging fully discrete systems, show the convergence of the numerical scheme, and obtain error-estimates for sufficiently smooth data. We also present a linearization scheme for the non-linear algebraic system resulting from the fully discrete discontinuous Galerkin approximation of the model. The linearization scheme does not require any regularization step. Additionally, in contrast with Newton or Picard methods, the linearization scheme does not involve computation of derivatives. Finally, to validate our theoretical findings and to show the scope of the applicability of the scheme, we present $1D$ and $2D$ numerical examples in realistic settings for homogeneous as well as heterogeneous porous media. We rigorously prove that the scheme is robust and linearly convergent.

Contents

Chapter 1

Introduction

Flow and transport processes in porous media are of high interest in many different fields of application, e.g., geological CO_2-storage [Nordbotten and Celia, 2011], environmental pollution [Radu and Pop, 2011], designing of diapers [Diersch et al., 2010], filters, etc. In light of their relevance, it is essential to develop a better understanding of such systems. Experimental studies are an important and indispensable tool to understand the behaviour of these processes. However, experimental studies are not always possible, nor feasible. Mathematical modelling and simulation tools, relying on mathematical and numerical analysis, provide an attractive alternative towards studying these processes with minimal societal and environmental impact.

In this context, porous media models have been developed for describing flow and transport processes at various scales [Bear, 2013; Helmig, 1997], and many different simulation and discretization techniques have been proposed in the literature. An important property of the porous media flow models is the *local mass conservation*. It is, therefore, desirable that the numerical schemes used for approximating these models reflect this property. Important classes of methods that are locally mass-conservative include finite volume methods [Eymard et al., 2003; Helmig, 1997], mixed finite element methods [Durlofsky, 1993; Radu and Pop, 2011; Radu et al., 2015a], and discontinuous Galerkin methods [Bastian, 2014; Bastian and Riviere, 2003; Ern et al., 2010; Sun and Wheeler, 2005].

Most of the standard models for two phase flow in porous media were traditionally developed for large scale reservoir simulations, and typically assumed equilibrium conditions between the two phases. In these models, it is common to neglect the capillary effects, or to model the capillary effect using nonlinear algebraic relationships between the phase pressure difference and the saturation of one of the phases (commonly, the wetting phase). Such relationships are obtained experimentally, typically based on measurements that were made over long times so that the phases are in equilibrium [Helmig, 1997; Nordbotten and Celia, 2011]. Over the last couple of decades, applications involving smaller scales, like laboratory scale, have increasingly attracted attention, particularly from the scientific community, which has lead to efforts in developing new modelling and discretization approaches. The flow behaviour at these small scales is different from the large field or reservoir scales in the

sense that it is essentially dynamic, characterized by *non-standard effects* like hysteresis and dynamic capillarity. Such effects can explain experimental results like saturation overshoot [Di Carlo, 2004] that are ruled out by standard models.

In this thesis, we are particularly interested in the dynamic capillarity effects, and consider the models where the pressure difference - saturation relationship additionally involves a dynamic term, as proposed in [Fucik and Mikyska, 2011; Hassanizadeh and Beliaev, 2001; Hassanizadeh and Gray, 1993; Hassanizadeh et al., 2002]. We refer to these models as *non-standard models*. In contrast to standard, equilibrium based porous media flow models, dynamic (or non-equilibrium) models, i.e. non-standard models, can explain effects like saturation overshoot and finger-pattern formation, which have been observed experimentally. The ability of non-equilibrium models to explain the small-scale experimental results as mentioned above has been proved by means of mathematical analysis. For example, the occurrence of non-monotonic travelling wave profiles depending on the magnitude of the dynamic capillarity effects has been analyzed rigorously in [van Duijn et al., 2013]. The existence and uniqueness of weak solutions for such types of models has been proved in [Cao and Pop, 2015, 2016; Fan and Pop, 2011; Koch et al., 2013; Mikelic, 2010; Rätz and Schweizer, 2014] or [van Duijn et al., 2016].

Compared to the standard models, the non-equilibrium based models encounter additional problems arising from the non-linear, possibly degenerate equations, which change their type depending on the choice of the unknowns. Further, the parameters and non-linearities are location dependent for realistic models in porous media and major difficulties arise when modelling the coupling between two homogeneous domains since the properties become discontinuous over the interface of the homogeneous domains. In order to obtain a consistent model for this case, it becomes necessary to impose proper and well designed interface conditions to account for the flux and mass conservation as well as the behaviour of the primary and secondary variables over the interface. The details and a mathematical derivation of these conditions can be found in [de Neef and Molenaar, 1997; van Duijn and de Neef, 1998; van Duijn et al., 1995].

Apart from mathematical modelling, the numerical solution of such models is also a challenging task. Firstly, rigorously designed numerical approximations are necessary to deal with the highly nonlinear, possibly degenerate models on each homogeneous subdomain. The numerical approximations for the homogeneous case have been studied over the last decades with techniques such as finite difference methods [Peszynska and Yi, 2008] finite volume methods [Cao et al., 2015; Eymard et al., 2003, 2010; Helmig, 1997; Helmig et al., 2007, 2009], finite element methods [Chavent and Jaffre, 1986; Chen, 2001; Koch et al., 2013; Rätz and Schweizer, 2014], mixed finite element methods [Durlofsky, 1993; Radu and Pop, 2011; Radu et al., 2015a], and discontinuous Galerkin methods [Bastian, 2014; Bastian and Riviere, 2003; Epshteyn and Riviere, 2009; Ern et al., 2010; Karpinski and Pop, 2017; Sun and Wheeler, 2005]. Secondly, in order to account for the material discontinuities over the interface, a proper and consistent communication between the homogeneous domains must be incorporated into the numerical model, as shown by [Kueper and Frind, 1991a,b]. The material discontinuities lead to discontinuities in the numerical solution.Pressures, and saturation can and will show discontinuities over some interface and these have to be properly resolved, which imposes additional restriction on the techniques and approximation methods that can

be used. There are different approaches to deal with this issue, like finite volume methods, finite element techniques extended by mortar methods [Arzanfudi et al., 2014; Cancès et al., 2009; Enchéry et al., 2006; Helmig et al., 2009; Hoteit and Firoozabadi, 2008], and discontinuous Galerkin (dG) methods [Bastian, 2014; Ern et al., 2010; Mozolevski and Schuh, 2013]. A major benefit of dG methods is, that the scheme, in general, provides a discontinuous solution, and inherently includes inter-elemental interface conditions. Therefore, extending the dG methods to the context of coupling of multiple homogeneous porous medium domains can be done naturally. The dG methods also have a direct advantage over the cG (continuous Galerkin) methods which are continuous over inter-elemental interfaces, and thus, lead to either oscillations or unnecessarily smeared out solutions. The dG methods have grown more popular in the last decades due to their versatility and easy adaptation to include heterogeneities, parallelization, and hp-adaptivity. These methods are well developed for standard, equilibrium based two-phase flow problems [Epshteyn and Riviere, 2009]. In this thesis, we analyze and implement an interior penalty discontinuous Galerkin (IPdG) method for the non-standard porous media models involving two phase flow with dynamic capillarity effects. We also discuss an extension of the IPdG approximation to deal with possible discontinuities when solving two phase flow problems in heterogeneous porous media. The spatial discretization is built on [Bastian, 2014; Ern et al., 2010], and is extended to include dynamic capillary pressure effects as in [Karpinski and Pop, 2017; Karpinski et al., 2017]. For time discretization, an implicit Euler approximation is used in order to avoid restrictions on the timestep size due the temporal discretization. We obtain a numerical scheme which is capable of a proper approximation of heterogeneous porous media, which is comparable to the results in [Helmig et al., 2007, 2009].

A common approach when dealing with two phase flow models, both standard and non-standard, is to employ the so-called global pressure, which allows rewriting the system in a way that some nonlinear factors in the higher order terms become linear [Chavent and Jaffre, 1986]. The advantage of this approach is that the a priori estimates can be obtained separately for each of the transformed pressures, which can then be used to estimate the saturation. This approach is detailed in [Epshteyn and Riviere, 2009]. The drawback of this approach lies in the fact that the global pressure is not a physical quantity, and one needs to post-process the results for extracting information that is relevant for the actual application. This is often quite cumbersome for realistic problems. If the mass balance equations are not reformulated in terms of the global pressure, the model with the original physical unknowns leads to a strong coupling of the mass balance equations, making it impossible to obtain the a priori estimate for the pressures directly. Instead, both pressure and saturation need to be estimated simultaneously, as done by [Eymard et al., 2003] and [Koch et al., 2013]. In [Eymard et al., 2003], the estimates were derived for a standard model using finite volume approach, while in [Koch et al., 2013], the estimates were derived for non-standard model with dynamic capillarity effects using finite element approach. In this thesis, we derive estimates for phase pressures and saturation and provide a rigorous convergence proof for an IPdG approximation for a non-standard two-phase flow model with dynamic capillarity.

The mathematical model in our case is highly non-linear and therefore, very demanding in terms of the numerical solution. To resolve the non-linearities, the usual methods include Newton or Picard methods, see e.g. [Bergamaschi and Putti, 1999; Celia et al., 1990; Neumann et al., 2013], a combination of Newton and Picard methods [Lehmann and Ackerer,

1998; List and Radu, 2016], or iterative IMPES (implicit pressure explicit saturation) [Kou and Sun, 2010a,b]. The Newton method shows a local convergence with quadratic order, but only if the initial guess is close enough to the solution, while Picard-iterations are more robust but show only a linear convergence. For designing Newton or Picard methods for degenerate problems, as appearing in porous media flows, it also becomes necessary to include a regularization step. Another noteworthy alternative to Newton's method, especially for multi-component flows, is the semi-smooth Newton method [Kraeutle, 2011]. This method has the advantage that it includes the equilibrium conditions within the nonlinear solver, which leads to a stable solution strategy. Its drawback, however, is in its relatively high implementation cost.

As mentioned, the Newton-scheme shows a high convergence order which makes it very attractive for solving nonlinear problems. However, the Newton-method requires the calculation of the Jacobian matrix (or at least a proper approximation of it) for any iteration step, which, in general, is computationally expensive. Additionally, to guarantee the convergence of the iterations, the initial guess should be close enough to the solution. This aspect was analyzed in e.g. [Park, 1995] for the mixed finite element discretization for nonlinear elliptic problems, where they show that the difference between the initial guess and the exact solution should be of order h^d (h being the mesh size and d the dimension of the domain) for convergence. For parabolic partial differential equations, a straightforward choice for the initial guess is the solution obtained at the previous time-step. Nevertheless, to ensure that this is indeed close enough, the time-step must be chosen sufficiently small, again of order h^d. This restriction becomes more severe when degenerate parabolic problems are considered. In this case, in locations where one of the phases is not present, the permeability of this phase vanishes leading to singular Jacobian matrices and ill-conditioned linear systems. To avoid this, it becomes necessary to regularize the problem, i.e. to consider perturbations assuring that the problem remains non-degenerate. This is an additional source of errors in the system. More importantly, the restriction on the time step becomes even more severe in this case, as it additionally involves a small regularization parameter (see [Radu et al., 2006]). Similar issues appear for reactive flow models with non-Lipschitz rates [Radu and Pop, 2011]. These issues with the Newton method have motivated the linearization schemes proposed in [List and Radu, 2016; Pop et al., 2004; Radu et al., 2015a,b; Slodička, 2002, 2005a,b; Yong and Pop, 1996] for the finite element, finite volume, and the mixed finite element discretization of porous media flow models. The idea of the linearization scheme is to add an additional term in the form of

$$L \cdot (Solution\_Current\_Iteration - Solution\_Old\_Iteration),$$

with L being a parameter that has to be chosen sufficiently large. The robustness of such schemes (also called L-schemes) for standard porous media flow models is proved in the papers mentioned above. Although the L-schemes show only a linear convergence, they may become faster than the Newton method as they do not require the computation of derivatives. Additionally, the L-schemes do not involve any regularization step, and lead to better conditioned linear systems within each iteration (see [List and Radu, 2016], where also the possibility of combining the L-scheme with the Newton iteration has been discussed). The L-schemes may even involve the same matrix for the linear algebraic system, which offers the possibility to compute its factorization only once per time step.

Inspired by the above results, in this thesis we also propose a linearly convergent iterative L-scheme for our model, i.e. a non-standard two phase porous media model of pseudo parabolic type involving a dynamic term in the phase pressure difference - saturation relationship (the dynamic capillarity). The model formulation for developing this scheme does not involve any global or complementary pressure, as opposed to the case in [Radu et al., 2015a,b]. We present a rigorous convergence proof for the L-scheme, and provide numerical experiments confirming the theoretical findings. These experiments also include heterogeneous media. To the best of our knowledge, this is the first time when such a scheme has been tested for the case of a heterogeneous medium.

Layout of the thesis

In Chapter 2, we introduce our mathematical model for a two phase flow in homogeneous and heterogeneous porous media with dynamic and discontinuous capillary pressure effects. In Chapter 3, we develop an interior penalty discontinuous Galerkin (IPdG) based numerical discretization scheme for our mathematical model. Next, in Chapter 4, we analyze our discretization scheme and prove the existence of a discrete solution, the energy estimate for the discrete solution, and the convergence of the scheme. In Chapter 5, we propose a new linearization method for our IPdG scheme to resolve the non-linearities in the discrete model. The proposed scheme is based on [Radu et al., 2015b] and [List and Radu, 2016]. Following this we prove the convergence of the linearization scheme by estimating the errors of the iteration step with the solution at the next time step. Finally, in Chapter 6, we present several $1D$ and $2D$ numerical examples in heterogeneous porous media with and without discontinuous capillary pressure effects to show the capabilities of our numerical scheme. We conclude the thesis by summarizing our work and presenting an outlook on the various possibilities for extending this work in future in Chapter 7.

List of publications

The following journal publications have resulted from this PhD work:

1. Stefan Karpinski, Iuliu Sorin Pop, *Analysis of an interior penalty discontinuous Galerkin scheme for two phase flow in porous media with dynamic capillary effects*, Numerische Mathematik, 136(1), 249-286, 2017, doi:10.1007/s00211-016-0839-5 (**published**).

2. Stefan Karpinski, Iuliu Sorin Pop, Florin Adrian Radu *Analysis of a linearization scheme for an interior penalty discontinuous Galerkin method for two phase flow in porous media with dynamic capillarity effects*, International Journal for Numerical Methods in Engineering, 2017, doi:10.1002/nme.5526 (**published**).

3. Stefan Karpinski, Iuliu Sorin Pop, Florin Adrian Radu *An interior penalty discontinuous Galerkin scheme for two phase flow in heterogeneous porous media with discontinuous dynamic capillary pressure effects*, (**in preparation**).

The main results of Article 1 can be found in Chapter 3 (Sections 3.1, 3.2, and 3.3) and Chapter 4. The main results of Article 2 can be found in Chapter 5 (Sections 5.1, 5.3, and 5.4). Results of Article 3 can be found in Chapter 2 (Section 2.7), Chapter 3 (Section 3.4), Chapter 5 (Section 5.2), and Chapter 6.

Chapter 2

Mathematical model

In this chapter, we introduce our mathematical model for an isothermal two phase flow in porous media with dynamic capillarity effects. We first describe the model for homogeneous media, and then extend it to heterogeneous domains by defining appropriate interface conditions at the material interfaces.

2.1 Model assumptions

We let $\Omega \subset \mathbb{R}^d$ ($d = 2$ or 3) be an open bounded polygonal domain (the porous medium) with boundary Γ and $T > 0$ a maximal, finite time. Both Γ and T are considered dimensionless. We consider a Darcy scale model for the flow of two incompressible and immiscible fluids (one wetting, and one non-wetting) through a porous medium. This is based on the following assumptions:

- *All physical processes are isothermal.*
  Extension to the non-isothermal case would require solving an additional governing equation for the temperature. This is done in e.g. [Acosta et al., 2006; Gupta et al., 2015]. The temperature, however, only negligibly affects the capillary pressure and the associated dynamic effects. Therefore, in our model, we ignore the temperature.

- *Flow velocities lie well within the Darcy regime.*
  For some special applications, like highly fractured media, where the flow at micro-scale is possibly turbulent in nature, the Forchheimer's law can be used instead of the Darcy's law. Some examples of such models can be found in [Hornung, 2012].

- *Porous matrix is rigid.*
  For those porous media applications where the deformations of the porous matrix are large and cannot be ignored, the model can be extended using concepts of poro-elasticity or poro-plasticity. Some examples can be found in [Bause et al., 2017; Both et al., 2017; Gupta et al., 2015].

2.2 Governing equations

Under the assumptions stated above, the mathematical model [Helmig, 1997; Nordbotten and Celia, 2011] includes the mass conservation laws for each phase (the wetting and non-wetting, denoted by $\alpha = w$ and n, respectively):

$$\partial_t(s_\alpha \phi \rho_\alpha) + \nabla \cdot (\rho_\alpha \mathbf{u}_\alpha) = q_\alpha \ . \tag{2.1}$$

Here, ϕ denotes the porosity of the medium, ρ_α the fluid phase densities, s_α the saturation of phase α, and q_α the volumetric sources or sinks. It is assumed that the densities are constant and that system (2.1) can be divided by the densities. Further, $\mathbf{u}_\alpha$ is the Darcy velocity of the phase α, given by

$$\mathbf{u}_\alpha = -\lambda_\alpha(s_w) K \nabla(p_\alpha - gz\rho_\alpha) \ . \tag{2.2}$$

Here, p_α is the pressure of the phase α, K the intrinsic permeability tensor, g the gravitational constant with the gravitational potential z, and $\lambda_\alpha = \dfrac{k_{r,\alpha}}{\mu_\alpha}$ is the mobility function for phase α, with relative permeability $k_{r,\alpha}$ and dynamic viscosity μ_α.

Remark 1 Note that in general the intrinsic permeability tensor K can be non-symmetric. In this thesis, however, we assume K as a symmetric positive definite tensor.

2.3 Closure relationships

The four governing equations presented above contain six unknown quantities, viz. phase saturations, pressures and velocities of both phases. To close the system we consider two more conditions:

1. We assume that at any given point only two phases are present in the system, such that,

$$s_w + s_n = 1. \tag{2.3}$$

2. We parameterize the phase pressure difference as a function of saturation similar to the standard models [Helmig, 1997], and extend this relationship with a term involving the time derivative of the saturation [Hassanizadeh and Gray, 1993] to include the non-standard dynamic capillarity effects,

$$p_c := p_n - p_w = p_c(s_w, \partial_t s_w) \ . \tag{2.4}$$

2.4 Primary variables

We chose three primary unknowns, viz. wetting phase saturation s_w, non-wetting phase pressure p_n, and phase pressure difference p_c, and rewrite the above model as a system of three equations:

$$\begin{aligned} &-\partial_t s_w \phi - \nabla \cdot (\lambda_n(s_w) K \nabla(p_n - gz\rho_n)) = q_n, \\ &\partial_t s_w \phi - \nabla \cdot (\lambda_w(s_w) K \nabla (p_n - p_c - gz\rho_w)) = q_w, \\ &p_c = p_c(s_w, \partial_t s_w). \end{aligned} \tag{2.5}$$

Note: For readability of the proofs in the subsequent sections, we use $p_w = p_n - p_c$, although p_w is a secondary variable.

2.5 Constitutive relationships

The constitutive models for the properties of the fluid-matrix interaction, viz. phase pressure difference (or capillary pressure) p_c and relative permeabilities $k_{r,\alpha}$ are described below.

2.5.1 Dynamic effects in the phase pressure difference

The pressure difference across the wetting and non-wetting phase interface is called the capillary pressure. This pressure difference arises due to balancing of cohesive forces between the fluids and the adhesive forces between the fluid-matrix interfaces. On a pore scale, the capillary pressure is inversely related to the radius of the pore-throat. A common assumption in the modelling of two phase flow in porous media is that the distribution of the two phases inside the pores of the medium is *static*, and the phase pressure difference depends only on the properties of the medium and the volumetric distribution of the phases. The models which are built on this assumption are called the *standard*, equilibrium-based models. These models relate the phase pressure difference p_c and saturation (commonly, the wetting phase saturation s_w) through nonlinear, algebraic functions which are uniquely invertible. Several parameterizations relating p_c and s_w using medium specific parameters have been proposed in the literature. Most prominent examples of such parameterizations include the Brooks-Corey model [Brooks, 1964], and the van Genuchten model [Mualem, 1976; van Genuchten, 1980]. These standard models are valid whenever the processes are slow enough, so that the dynamics of the flow, and in particular the redistribution of the phases inside the pores before achieving equilibrium, can be ignored.

In the recent years, experiments have brought forth some limitations of the equilibrium-based models. For example, the experiments in [Di Carlo, 2004] showed that non-monotonic saturation profiles (over-shoots) can be obtained during infiltration processes in a dry porous medium, and that the amplitude of such over-shoots depends on the flow velocity. Such results lie beyond the scope of the equilibrium-based models, which would predict monotonic profiles regardless of the chosen parameterization. Therefore, alternative modelling theories were required.

To model non-monotonic profiles, several approaches were proposed where the assumption of a uniquely invertible representation of the capillary pressure relationship was dropped, and non-equilibrium or dynamic models were introduced to capture the additional effects observed in the experiments. These models are called the *non-standard* models. Many non-standard models have been proposed, amongst others [Barenblatt et al., 2003; Bourgeat and Panfilov, 1998; Hassanizadeh and Gray, 1993]. An extensive review of these and some other models can be found in [Manthey, 2006], where also a more detailed explanation of each model is included.

In this thesis, we focus on the model developed by Hassanizadeh and Gray in [Hassanizadeh and Gray, 1979a,b, 1993], which was analyzed from a thermodynamical perspective in [Hassanizadeh and Beliaev, 2001]. In this model, the equilibrium-based p_c-s_w relationship was extended by introducing a dynamic damping parameter $\tau(s_w) > 0$, which can depend on the wetting phase saturation, but is often assumed constant. This parameter accounts for the dynamic change of the capillary pressure, leading the a non-equilibrium

(non-standard) model. The capillary pressure is then defined as:

$$p_c = p_{c,eq}(s_w) - \tau \partial_t s_w \ , \tag{2.6}$$

involving the time derivative of the saturation. Here, $p_{c,eq}$ is the capillary pressure at equilibrium, and τ accounts for the dynamic effects. We assume τ to be a positive constant. The additional dynamic term, i.e. $\tau \partial_t s_w$, delays the flow of the wetting phase and forces it first to build up before the capillary pressure can be overcome. This leads to a non-monotonic flow behaviour and a droplet formation (over-shoot) at the tip of an infiltration finger.

Other non-standard effects in the capillary pressure relationship, like terms of even higher order or hysteresis effects, are not accounted for in this thesis, but can be found in e.g. [Cao and Pop, 2015; Jha et al., 2011; Rätz and Schweizer, 2014].

2.5.2 Relative permeabilities

In this work, we study the dynamic effects only in the phase pressure difference. For relative permeabilities, we assume that the dynamic effects are negligible, and use the equilibrium-based models like Brooks-Corey [Brooks, 1964] or van Genuchten [van Genuchten, 1980] in conjunction with the Mualem and Burdine relations [Burdine, 1953; Mualem, 1976] to parameterize relative permeabilities as functions of wetting phase saturation.

2.6 Initial and boundary conditions

To complete the system, we use the following initial and boundary conditions:

$$\begin{aligned} &\text{For all } x \in \Omega \text{ and at } t = 0, \\ &\quad s_w(x,0) = s^0(x) \qquad \text{with, } s^0 \in H^1(\Omega). \qquad (2.7) \\ &\text{For all } x \in \Gamma \text{ and all } t \in [0,T], \\ &\quad p_c(x,t) = p_c^D(x) \ , \quad p_n(x,t) = p_n^D(x) \qquad (2.8) \\ &\quad \text{with } p_n^D \in H^{\frac{1}{2}}(\Gamma) \ , \ p_c^D \in H^{\frac{1}{2}}(\Gamma) \end{aligned}$$

where, s^0, p_n^D, and p_c^D are given functions. $H^1(\Omega)$ and $H^{\frac{1}{2}}(\Gamma)$ are Sobolev spaces, on Ω or Γ respectively. A definition and introduction to Sobolev spaces can be found in [Adams and Fournier, 2003] or [Evans, 1998]. Note that the boundary value of s_w is defined implicitly by the Dirichlet conditions for p_c.

Remark 2 For simplicity, here only Dirichlet boundary conditions are considered. Also, the boundary values are assumed constant in time.

2.7 Interface Conditions

The model presented above is valid only in homogeneous domains. To extend this model to heterogeneous domains, consider a very simple heterogeneous porous media consisting of two distinct homogeneous domains Ω_h, and Ω_l, separated by a material interface Γ. The

subscript l and h refer to a **l**ower and a **h**igher equilibrium capillary pressure, i.e. for each $s_w \in (0, 1]$ holds $p_{c,eq,l}(s_w) \leq p_{c,eq,h}(s_w)$, respectively. (See figure 2.1.) The lower and higher capillary pressures correspond to higher and lower absolute intrinsic permeability respectively. At the material interface, due to the different properties, additional conditions need to be considered.

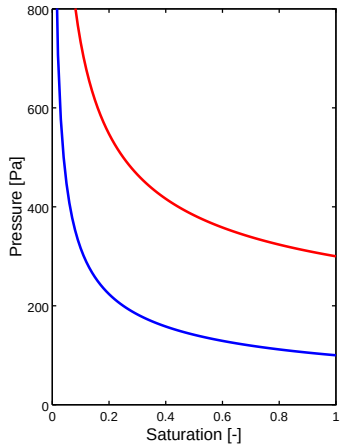

Figure 2.1: Equilibrium capillary pressure, with Brooks Correy parameterization. In red $p_{c,eq,h}(\cdot)$ and blue $p_{c,eq,l}(\cdot)$

.

For the standard models, the interface conditions have been studied extensively in e.g. [Bertsch et al., 2003; Buzzi et al., 2009; Cancès, 2008; van Duijn and de Neef, 1998] as well as [Kueper and Frind, 1991a,b]. In [van Duijn and de Neef, 1998], an analytical solution was derived and analyzed. (Note that in [van Duijn and de Neef, 1998] lower and higher refers to the absolute permeability.) An important aspect of flow in heterogeneous media is that, the flow from the high capillary pressure domain Ω_h to the low capillary pressure domain Ω_l is possible only if the capillary pressure on Ω_l exceeds the entry pressure on Ω_h. This behaviour is commonly known as a capillary barrier. Numerical methods for modelling capillary barriers/standard models have been studied by [Arzanfudi et al., 2014; Cancès et al., 2009; Enchéry et al., 2006; Hoteit and Firoozabadi, 2008]

For the non-standard models, the interface conditions were first studied and extended in [Helmig et al., 2007, 2009] and [Peszynska and Yi, 2008]. Recently, these interface conditions were analyzed rigorously in [van Duijn et al., 2016]. It was shown that if $\tau > 0$, under certain conditions, flow of the non-wetting phase from Ω_l to Ω_h is possible even if the capillary pressure on Ω_l has not exceeded the capillary barrier.

To connect the models on each homogeneous subdomain, the following two conditions must be satisfied for any flow across the interface:

- continuity of the normal component of the fluxes across the interface, and

- continuity of the pressures across the interface.

The first condition ensures the conservation of mass flux over the interface and leads to the following condition:

$$\lambda_{\alpha,h}(s_{w,h})K_h\nabla(p_{\alpha,h} - gz\rho_\alpha)\cdot\vec{n} = \lambda_{\alpha,l}(s_{w,l})K_l\nabla(p_{\alpha,l} - gz\rho_\alpha)\cdot\vec{n}, \tag{2.9}$$

where, $\vec{n}$ is the unit-normal vector pointing into Ω_l. The second condition assumes continuity of the pressures over the interfaces and implies a continuity of the capillary pressure. This may lead to a discontinuity in the saturations across the interface.

Two distinct values of saturation and capillary pressure may exist at each side of the interface. We denote the values at the interface associated with the domain Ω_h as $s_{n,h}$ and $p_{c,h}$, and the values at the interface associated with the domain Ω_l as $s_{n,l}$ and $p_{c,l}$. We define the pressures

$$p_{c,e,l} := p_{c,eq,l}(1) \text{ and } p_{c,e,h} := p_{c,eq,h}(1), \tag{2.10}$$

which will denote the entry pressures. Further, we define the capillary pressure difference $\delta_{p_c,\Gamma}$ over the interface Γ by:

$$\delta_{p_c,\Gamma} := p_{c,h}(s_w) - p_{c,l}(s_w) \tag{2.11}$$

This definition translates directly to the capillary pressure potential p_c:

$$p_{c,h} - p_{c,l} = \delta_{p_c,\Gamma}\ . \tag{2.12}$$

Depending on the chosen parameterization of the capillary pressure, the condition of pressure continuity is not always valid.

In the case of van Genuchten like parameterization, the pressure continuity has to be always fulfilled.

In the case of Brooks Correy like parameterization, the pressure continuity holds true only if both phases are present on both sides of the interface. Otherwise, a capillary barrier exists across the interface, preventing flow from the domain with low capillary pressure to that with high capillary pressure. The discontinuity in capillary pressure leads to a discontinuity in the non-wetting phase pressure, whereas the wetting phase pressure remains continuous across the interface. Physically this can be attributed to the fact, that a phase pressure has no meaning when the phase is not present. Therefore the phase pressure differences, i.e. the capillary pressure becomes meaningless. In the standard model an extension of the capillary pressure from $(0, 1)$ to $[0, 1]$ is possible due to a continuous extension. In the non standard model this is not possible, as no unique extension can be chosen due to the dynamic capillary effect as presented in [van Duijn et al., 2013].

Following [van Duijn et al., 2016], whenever $s_{w,h} < 1$ and $s_{w,l} < 1$, the non-wetting phase is present on both sides of the interface and the following holds on Γ:

$$p_{c,eq,l}(s_w) - \tau_l(s_w)\partial_t s_w = p_{c,eq,h}(s_w) - \tau_h(s_w)\partial_t s_w\ . \tag{2.13}$$

If instead no non-wetting phase is present on Ω_h and $p_{c,l} < p_{c,e,h}$, i.e. not enough non-wetting fluid is present to overcome the capillary barrier, (2.13) is replaced by

$$s_{w,h} = 1 \ . \tag{2.14}$$

Combining (2.13) and (2.14) this leads to:

$$(1 - s_{w,h}) \cdot (p_{c,h} - p_{c,l}) = 0 \ . \tag{2.15}$$

Note that, the dynamic capillary pressure effect results in an ordinary differential equation over the interface.

We elaborate on the behaviour of the pressures in the following three cases:

A. non-wetting phase is absent on the Ω_h side of Γ,

B. non-wetting phase is absent on the Ω_l side of Γ,

C. non-wetting phase is present on both sides of Γ.

The behaviour is described only from the perspective of the non-wetting phase.

Case A: In this case, $s_{w,h} = 1$ and $\partial_t s_{w,h} = 0$, which implies $p_{c,h} = p_{c,e,h}$. As long as $p_{c,l}(s_{w,l}) < p_{c,e,h}$, no flow is possible across the interface. This means that the non-wetting phase has to accumulate until the capillary pressures are balanced, i.e. $p_{c,l}(s_{w,l}) = p_{c,h}(s_{w,h})$. Only after this, the non-wetting fluid can flow into Ω_h. This is the capillary barrier in the standard case, which leads to a jump in the capillary potential p_c denoted by $\delta_{p_c,\Gamma}$ in (2.12).

In the standard case $s_{w,l}$ decreases towards the threshold value s_w^* for which the condition $p_{c,eq,l}(s_w^*) = p_{c,e,h}$ holds. In the non-standard case however the entry pressure may be reached at values $s_{w,l} > s_w^*$, due to the dynamic effects of $\tau > 0$. This leads to scenarios, where flow is possible which can not be observed in the standard case. This is also described in detail in [van Duijn et al., 2016].

In this case, the wetting phase is always present on both sides of the interface. This implies continuity of the wetting pressure potential and leads to the following additional condition on the non-wetting pressure potential :

$$p_{n,h} - p_{n,l} = p_{c,h} - p_{c,l} = \delta_{p_c,\Gamma} \ . \tag{2.16}$$

This condition will be used in Section 3.4 when constructing the discontinuous Galerkin scheme.

Case B: Analogously to case A, here $s_{w,l} = 1$ and $\partial_t s_{w,l} = 1$, leading to $p_{c,l} = p_{c,e,l}$. In this case, $p_{c,h}(s_{w,h}) \geq p_{c,e,l}$ always holds. Therefore, no capillary barrier occurs and flow across the interface is directly possible. The pressures are always continuous.

Case C: In this case, the pressure continuity and capillary pressure continuity always hold, and flow across the interface is always possible.

Summarizing Cases A, B and C, as well as (2.15) and (2.9), we obtain the following relations over the interface Γ:

$$\lambda_{\alpha,h}(s_{w,h})K_h\nabla(p_{\alpha,h} - gz\rho_\alpha)\cdot\vec{n} = \lambda_{\alpha,l}(s_{w,l})K_l\nabla(p_{\alpha,l} - gz\rho_\alpha)\cdot\vec{n} \tag{2.17}$$

$$(1 - s_{w,h})\cdot(p_{c,h} - p_{c,l}) = 0 \tag{2.18}$$

where, $\vec{n}$ defines the vector normal to the interface. Note that, the condition $p_{c,h}(s_{w,h}) = p_{c,e,h}$ corresponds to $s_{w,h} = 1$.

2.8 Notation

The notations below are common in functional analysis [Adams and Fournier, 2003] and will be used throughout this thesis. Whenever values on Γ are involved, these should be understood in the sense of traces, recalling the definitions of the traces in [Evans, 1998, p. 270]. The following notation will be used in this thesis:

- $L^p(\Omega)$ $(1 \leq p < \infty)$ is the usual space of functions that are p-Lebesgue integrable and $L^\infty(\Omega)$ is the space of functions that are essentially bounded in Ω. The elements of $W^{k,p}(\Omega)$ are the functions admitting weak derivatives up to order k that are again in L^p. For simplicity, we use the notation $H^k(\Omega)$ for $W^{k,2}(\Omega)$.

- For $1 \leq p \leq \infty$, $\|\cdot\|_{L^p(\Omega)}$ and $\|\cdot\|_{W^{k,p}(\Omega)}$ are the standard norms in $L^p(\Omega)$, respectively $W^{k,p}(\Omega)$. A simplified notation will be used for the norm in $W^{k,2}(\Omega)$, namely $\|\cdot\|_{\Omega,k}$.

- $H_0^k(\Omega)$ denotes the subspace of $H^k(\Omega)$ taking the value 0 on the boundary (in the sense of traces).

- $L^q(0,T;W^{k,p}(\Omega))$ denotes the Bochner space of vector spaced valued functions $f : [0,T] \to W^{k,p}(\Omega)$ that are q-Bochner integrable on $[0,T]$.

- $H^1(0,T;L^2(\Omega))$ denotes the Bochner space of $L^2(\Omega)$ valued functions admitting a weak time-derivative in $L^2(0,T;L^2(\Omega))$.

As for the domain Ω, the traces on Γ will lie in spaces like $L^p(\Gamma)$, $H^k(\Gamma)$, etc. In particular, by $H^{\frac{1}{2}}(\Gamma)$ we mean the traces on Γ of $H^1(\Omega)$ functions.

2.9 Weak formulation

We now state the weak formulation for our model (2.5) together with the constitutive relationship (2.6) and the initial and boundary conditions (2.7) and (2.8). We multiply the equations with test-functions in $H_0^1(\Omega))$ and partially integrate to obtain:

Problem 1 [**Weak formulation**] Find the triple (s_w, p_n, p_c) s.t. $s_w \in H^1(0,T;H^1(\Omega))$, $s_w = s^0$ at $t = 0$, $p_n - p_n^D \in L^2(0,T;H_0^1(\Omega))$, $p_c - p_c^D \in L^2(0,T;H_0^1(\Omega))$, and for all

$\psi_p \in H_0^1(\Omega)$, $\psi_s \in H_0^1(\Omega)$, and almost every $t \in [0,T]$ it holds

$$
\begin{aligned}
&-\int_\Omega \partial_t s_w \phi \psi_p + \int_\Omega \lambda_n(s_w) K \nabla \left(p_n - gz\rho_n\right) \cdot \nabla \psi_p = \int_\Omega q_n \psi_p, \\
&\int_\Omega \partial_t s_w \phi \psi_p + \int_\Omega \lambda_w(s_w) K \nabla \left(p_n - p_c - gz\rho_w\right) \cdot \nabla \psi_p = \int_\Omega q_w \psi_p, \\
&\int_\Omega p_c \psi_s = \int_\Omega p_{c,eq}(s_w) \psi_s - \int_\Omega \tau \partial_t s_w \psi_s.
\end{aligned}
\tag{2.19}
$$

Existence and uniqueness results for Problem 1 are obtained in [Cao and Pop, 2015, 2016; Fan and Pop, 2011; Koch et al., 2013; Mikelic, 2010].

Chapter 3

Numerical scheme

In this chapter, we develop a numerical discretization scheme for our mathematical model given by Problem 1. The discretization in space is based on an interior penalty discontinuous Galerkin method, while the discretization in time is based on an implicit Euler method. A particular focus is laid on the numerical treatment of the interface conditions for heterogeneous domains.

Preliminaries

Let $\mathcal{T}$ be a decomposition of the domain Ω into N non-degenerate elements T_i. We assume that $\mathcal{T}$ is admissible in the sense of the Definition 2.1 in [Di Pietro and Ern, 2010]. Let $\mathcal{F}$ denote the union of all faces F_j, and let h be the maximal diameter of the elements.

Given $T_i \in \mathcal{T}$ and $F_i \in \mathcal{F}$, we define a set $F(T_i)$ of all the faces associated with the element T_i, s.t.,

$$F(T_i) := \left\{ \bigcup_{F_j \in \mathcal{F}} F_j : F_j \subset T_i \right\},$$

and, a set $T(F_i)$ of all the elements sharing the face F_i, s.t.,

$$T(F_i) := \left\{ \bigcup_{T_j \in \mathcal{T}} T_j : F_i \subset T_j \right\}.$$

In the conforming case, $T(F_i)$ consists of exactly two elements.

With each face $F \in \mathcal{F}$ connecting element T_i and T_j, we associate a normal-vector $\vec{n}$ directed from T_i to T_j ($j > i$).

Following Sec. 1.2.4 in [Di Pietro and Ern, 2012], let $\Pi^k(T)$ denote the space of polynomials on T with degree $\leq k$. For the approximation of saturation S_w, we consider the broken polynomial space with polynomials of order k_s as,

$$V_h^s(\Omega) := \{v \in L^2(\Omega) : v|_T \in \Pi^{k_s}(T) \text{ for all } T \in \mathcal{T}\} , \tag{3.1}$$

and, for the approximation of the pressures p_n and p_c, we consider the broken polynomial space with polynomials of order k_p as,

$$V_h^p(\Omega) := \{v \in L^2(\Omega) : v|_T \in \Pi^{k_p}(T) \text{ for all } T \in \mathcal{T}\} . \tag{3.2}$$

Note that we represent a general broken polynomial space with $V_h(\Omega)$ without specifying the polynomial order.

For $\psi^i, \psi^j \in V_h(\Omega)$, where, $\psi^i = (\psi|_{T^i})|_F$ is the trace of F on the side of the element T_i, and similarly, $\psi^j = (\psi|_{T^j})|_F$ is the trace of F on the side of the element T_j, we define the jump $[\![\cdot]\!]$ and the average $\{\cdot\}$ over the face F as,

$$\text{when } F \text{ is an interior face} \quad : \quad [\![\psi]\!] = \left(\psi^i - \psi^j\right) \quad \text{and} \quad \{\psi\} = \frac{1}{2}\left(\psi^i + \psi^j\right) , \tag{3.3}$$

$$\text{when } F \text{ is a boundary face} \quad : \quad [\![\psi]\!] = \psi^i \quad \text{and} \quad \{\psi\} = \psi^i, \tag{3.4}$$

where, the interior face connects elements T^i and T^j with $i < j$, and the boundary face has no element adjacent to T_i.

Next, we define the following norm on the broken polynomial space,

$$\|v\|_{\Omega,DG}^2 := \sum_{T_i \in \mathcal{T}} \|\nabla v\|_{T_i,0}^2 + \sum_{F_i \in \mathcal{F}} \frac{1}{|F_i|} \|[\![v]\!]\|_{F_i,0}^2 \tag{3.5}$$

and use the following lemma [Di Pietro and Ern, 2010]:

Lemma 1 Given a broken polynomial space $V_h(\Omega)$, for any q such that,

$$1 \leq q \leq \frac{2d}{d-2}, \text{ if } d \geq 3$$
$$1 \leq q < \infty, \text{ if } d = 2 ,$$

there exists a constant $\hat{C}$ depending on the polynomial degree, mesh-parameters and $|\Omega|$, but independent of the mesh size h, such that, for all $v \in V_h(\Omega)$, the following inequality holds:

$$\|v\|_{L^q(\Omega)} \leq \hat{C} \|v\|_{\Omega,DG} . \tag{3.6}$$

Additionally, we use the following trace inequalities, which can be found in [Warburton and Hesthaven, 2003], [Riviere et al., 2001], or [Di Pietro and Ern, 2012]:

Lemma 2 Let γ_0 denote the trace operator. There exists a constant C_t independent of the mesh size h, such that, for any $T \in \mathcal{T}$ with $F \in F(T)$ and for all $v \in H^k(T)$, the following holds:

$$\|\gamma_0 v\|_{0,F} \leq C_t \sqrt{\frac{1}{|F|}} (\|v\|_{0,T} + |F| \|\nabla v\|_{0,T}) \tag{3.7}$$

For $v \in \Pi^k(T)$ and a positive function $f(k)$ depending on the polynomial degree k, the following holds:

$$\|\gamma_0 v\|_{0,F} \leq C_t \sqrt{\frac{f(k)}{|F|}} \|v\|_{0,T} \tag{3.8}$$

We also use the following elementary lemma [Epshteyn and Riviere, 2009]:

Lemma 3 Let $\tilde{C}$ be the maximal number of elements sharing one face, and let $A : \mathcal{T} \to [0, \infty)$ be a function defined on the triangularization $\mathcal{T}$. Then, the following inequality holds:

$$\sum_{F_i} \sum_{T(F_i)} A(T) \leq \tilde{C} \sum_{T_i} A(T_i)$$

Finally, we state the following well known (in-)equalities for $a, b \in \mathbb{R}$ and $\epsilon \in \mathbb{R}^+$, which are used throughout the paper:

$$(a - b) \cdot a = \frac{1}{2}(a - b)^2 + \frac{1}{2}(a^2 - b^2) \tag{3.9}$$

$$ab \leq \frac{\epsilon}{2} a^2 + \frac{1}{2\epsilon} b^2. \tag{3.10}$$

3.1 Discretization in space

The weak form (2.19) of the mathematical model governed by system (2.5) is discretized in space using an interior penalty discontinuous Galerkin numerical scheme.

Problem 2 [**Spatial discretization**] Given the penalty parameters $\sigma_n, \sigma_w \in \mathbb{R}^+$, the parameter $\theta \in \{-1, 0, 1\}$ and the function $f(\cdot)$ introduced in Lemma 2 depending on the polynomial order k_p, find $s_w \in V_h^s(\Omega)$, $p_n \in V_h^p(\Omega)$ and $p_c \in V_h^p(\Omega)$, s.t., for all $\psi_s \in V_h^s(\Omega)$,

$\psi_n \in V_h^p(\Omega)$ and $\psi_w \in V_h^p(\Omega)$ the following holds:

$$
\begin{aligned}
\textbf{PDE-1}\colon & \sum_{T_i\in\mathcal{T}} \int_{T_i} -\partial_t s_w \phi \psi_n + \sum_{T_i\in\mathcal{T}} \int_{T_i} \lambda_n(s_w) K \nabla \left(p_n - gz\rho_n\right) \nabla \psi_n \\
& - \sum_{F_i\in\mathcal{F}} \int_{F_i} \{\lambda_n(s_w) K \nabla \left(p_n - gz\rho_n\right) \cdot \vec{n}\} [\![\psi_n]\!] \\
& + \theta \sum_{F_i\in\mathcal{F}} \int_{F_i} [\![p_n]\!] \{\lambda_n(s_w) K \nabla \psi_n \cdot \vec{n}\} + \sigma_n \sum_{F_i\in\mathcal{F}} \int_{F_i} \frac{f(k_p)}{|F_i|} [\![p_n]\!][\![\psi_n]\!] \\
& = \theta \sum_{F_i\in\Gamma} \int_{F_i} [\![p_n^D]\!] \{\lambda_n(s^D) K \nabla \psi_n \cdot \vec{n}\} + \sigma_n \sum_{F_i\in\Gamma} \int_{F_i} \frac{f(k_p)}{|F_i|} [\![p_n^D]\!][\![\psi_n]\!]
\end{aligned}
\tag{3.11}
$$

$$
\begin{aligned}
\textbf{PDE-2}\colon & \sum_{T_i\in\mathcal{T}} \int_{T_i} \partial_t s_w \phi \psi_w + \sum_{T_i\in\mathcal{T}} \int_{T_i} \lambda_w(s_w) K \nabla (p_n - p_c - gz\rho_w) \nabla \psi_w \\
& - \sum_{F_i\in\mathcal{F}} \int_{F_i} \{\lambda_w(s_w) K \nabla (p_n - p_c - gz\rho_w) \cdot \vec{n}\} [\![\psi_w]\!] \\
& + \theta \sum_{F_i\in\mathcal{F}} \int_{F_i} \{\lambda_w(s_w) K \nabla \psi_w \cdot \vec{n}\} [\![p_n - p_c]\!] + \sigma_w \sum_{F_i\in\mathcal{F}} \int_{F_i} \frac{f(k_p)}{|F_i|} [\![p_n - p_c]\!][\![\psi_w]\!] \\
& = \theta \sum_{F_i\in\Gamma} \int_{F_i} \{\lambda_w(s^D) K \nabla \psi_w \cdot \vec{n}\} [\![p_n^D - p_c^D]\!] + \sigma_w \sum_{F_i\in\Gamma} \int_{F_i} \frac{f(k_p)}{|F_i|} [\![p_n^D - p_c^D]\!][\![\psi_w]\!]
\end{aligned}
\tag{3.12}
$$

$$
\textbf{ODE-Pc}\colon \sum_{T_i\in\mathcal{T}} \int_{T_i} p_c \psi_s = \sum_{T_i\in\mathcal{T}} \int_{T_i} p_{c,eq}(s_w) \psi_s - \sum_{T_i\in\mathcal{T}} \int_{T_i} \tau \partial_t s_w \psi_s \tag{3.13}
$$

The parameters σ_n and σ_w penalize discontinuities in the solutions (i.e., jumps) over the faces. The choice of $\theta = 1$ gives the non-symmetric-interior-penalty (NIP) dG-scheme, $\theta = 0$ gives the incomplete-interior-penalty (IIP) dG-scheme, and $\theta = -1$ gives the symmetric-interior-penalty (SIP) dG-scheme.

3.2 Discretization in time

For the discretization in time, we use an implicit Euler scheme. We subdivide the time domain $[0, T]$ into N intervals of size $\Delta t > 0$ with $T = N \cdot \Delta t$. The i-th discrete time-step is denoted by t_i, s.t., $t_i = i \cdot \Delta t$.

Given a sufficiently smooth function $g(x, t)$, the time derivative of g is approximated by:

$$
\partial^- g^{n+1} := \frac{g(t^{n+1}, x) - g(t^n, x)}{\Delta t} \tag{3.14}
$$

3.3 Discrete system

Using Problem 2 and (3.14), the fully-discrete scheme can be written as:

Problem 3 [Discrete problem at t^{n+1}] Let $P_n^n \in V_h^p(\Omega)$, $P_c^n \in V_h^p(\Omega)$ and $S_w^n \in V_h^s(\Omega)$, find $P_n^{n+1} \in V_h^p(\Omega)$, $P_c^{n+1} \in V_h^p(\Omega)$ and $S_w^{n+1} \in V_h^s(\Omega)$, s.t., for all $\psi_s \in V_h^s(\Omega)$, $\psi_n \in V_h^p(\Omega)$ and $\psi_w \in V_h^p(\Omega)$, the following holds:

$$
\begin{aligned}
\textbf{PDE-1}\colon & \sum_{T_i\in\mathcal{T}}\int_{T_i} -\partial^- S_w^{n+1}\phi\psi_n + \sum_{T_i\in\mathcal{T}}\int_{T_i}\lambda_n(S_w^{n+1})K\nabla\left(P_n^{n+1}-gz\rho_n\right)\nabla\psi_n \\
& - \sum_{F_i\in\mathcal{F}}\int_{F_i}\{\lambda_n(S_w^{n+1})K\nabla\left(P_n^{n+1}-gz\rho_n\right)\cdot\vec{n}\}[\![\psi_n]\!] \\
& + \theta\sum_{F_i\in\mathcal{F}}\int_{F_i}[\![P_n^{n+1}]\!]\{\lambda_n(S_w^{n+1})K\nabla\psi_n\cdot\vec{n}\} + \sigma_n\sum_{F_i\in\mathcal{F}}\int_{F_i}\frac{f(k_p)}{|F_i|}[\![P_n^{n+1}]\!][\![\psi_n]\!] \\
& = \theta\sum_{F_i\in\Gamma}\int_{F_i}[\![p_n^D]\!]\{\lambda_n(s^D)K\nabla\psi_n\cdot\vec{n}\} + \sigma_n\sum_{F_i\in\Gamma}\int_{F_i}\frac{f(k_p)}{|F_i|}[\![p_n^D]\!][\![\psi_n]\!]
\end{aligned}
\tag{3.15}
$$

$$
\begin{aligned}
\textbf{PDE-2}\colon & \sum_{T_i\in\mathcal{T}}\int_{T_i}\partial^- S_w^{n+1}\phi\psi_w + \sum_{T_i\in\mathcal{T}}\int_{T_i}\lambda_w(S_w^{n+1})K\nabla(P_n^{n+1}-P_c^{n+1}-gz\rho_w)\nabla\psi_w \\
& - \sum_{F_i\in\mathcal{F}}\int_{F_i}\{\lambda_w(S_w^{n+1})K\nabla(P_n^{n+1}-P_c^{n+1}-gz\rho_w)\cdot\vec{n}\}[\![\psi_w]\!] \\
& + \theta\sum_{F_i\in\mathcal{F}}\int_{F_i}\{\lambda_w(S_w^{n+1})K\nabla\psi_w\cdot\vec{n}\}[\![P_n^{n+1}-P_c^{n+1}]\!] \\
& + \sigma_w\sum_{F_i\in\mathcal{F}}\int_{F_i}\frac{f(k_p)}{|F_i|}[\![P_n^{n+1}-P_c^{n+1}]\!][\![\psi_w]\!] \\
& = \theta\sum_{F_i\in\Gamma}\int_{F_i}\{\lambda_w(s^D)K\nabla\psi_w\cdot\vec{n}\}[\![p_n^D-p_c^D]\!] \\
& + \sigma_w\sum_{F_i\in\Gamma}\int_{F_i}\frac{f(k_p)}{|F_i|}[\![p_n^D-p_c^D]\!][\![\psi_w]\!]
\end{aligned}
\tag{3.16}
$$

$$
\textbf{ODE-Pc}\colon \sum_{T_i\in\mathcal{T}}\int_{T_i}P_c^{n+1}\psi_s = \sum_{T_i\in\mathcal{T}}\int_{T_i}p_{c,eq}(S_w^{n+1})\psi_s - \sum_{T_i\in\mathcal{T}}\int_{T_i}\tau\partial^- S_w^{n+1}\psi_s \tag{3.17}
$$

3.4 Numerical treatment of the heterogeneities

In Section 2.7, we discussed the additional conditions that must be considered at the material interfaces separating homogeneous blocks in a heterogeneous porous medium, which include flux continuity (2.17) and pressure continuity (2.18) across the interface. In this section, we present the numerical realization of these conditions in our solution scheme. We use the ideas proposed by [Ern et al., 2010] and used further in [Bastian, 2014] for a fully

implicit coupled scheme. In both, [Ern et al., 2010] and [Bastian, 2014], stationary capillary pressure conditions were assumed. We extend the ideas and incorporate non-standard capillary pressure effects.

3.4.1 Pressure condition

We exploit the structure of the dG-scheme and extend the penalty terms to realize the pressure-continuity condition at the interface. This is possible because each element is an *independent* entity by itself; the communication between the elements occurs only through the interfacial terms, i.e., average terms and penalty terms. When the mesh-interfaces and the material-interfaces are aligned, the penalty terms can be naturally extended to incorporate the physical behaviour at the material interfaces. This gives us the possibility to deal with edge aligned heterogeneities without additional numerical constructs.

The dynamic capillary pressure effects for flow in heterogeneous porous media were first rigorously addressed by Weiss et al. in [Helmig et al., 2009] and [Helmig et al., 2007]. They used finite volume scheme for spatial discretization, and described the interface conditions using variational inequalities, which were incorporated in the numerical scheme through a mortar technique. In addition, they used an active-set strategy together with an inexact Newton strategy to solve the non-linear system.

To describe the numerical approximation, we use the same notation as in Section 2.7. To incorporate the jumps in the saturation, we introduce an additional penalty parameter to (3.17), which penalizes jumps over the interface, such that the pressure continuity is fulfilled. For a face $F \in \mathcal{F}$ with $F \subset \Gamma$, we use the capillary pressure condition (2.18) and define the the modified jump term:

$$[\![p_c(S_w^{n+1})]\!]' = \begin{cases} p_{c,e,h} - p_{c,h}(S_{w,h}^{n+1}) & \text{if } p_{c,l}(S_{w,l}^{n+1}) < p_{c,e,h} \text{ and } S_{w,h}^{n+1} = 1 \\ p_{c,h}(S_{w,h}^{n+1}) - p_{c,l}(S_{w,l}^{n+1}) & \text{otherwise} \end{cases} . \tag{3.18}$$

Whether case A, B, or C from Section 2.7 is applicable, is decided by the condition:

$$p_{c,l}(S_{w,l}^{n+1}) < p_{c,e,h} \text{ and } S_{w,h}^{n+1} = 1 \ ,$$

which guarantees that if case A applies, non-wetting fluid accumulates until $p_{c,l}$ reaches the entry pressure $p_{c,e,h}$. As long as the capillary pressure is less than the entry pressure and no non-wetting phase is present on Ω_h , case A is active and saturation will accumulate. Additionally, the capillary pressure potential and non-wetting pressure potential are discontinuous. To ensure that in case B no capillary barrier inhibits the flow, the condition $S_{w,h}^{n+1} = 1$ is checked. In all other cases we ensure continuity of the pressure potentials, i.e. case C is active.

In the present context for edges over the interface Γ one obtains

$$[\![p_c(S_w^{n+1})]\!]' = 0,$$

which ensures the condition

$$p_{c,e,h} = p_{c,h}(S_{w,h}^{n+1}) \quad \text{or} \quad p_{c,h}(S_{w,h}^{n+1}) = p_{c,l}(S_{w,l}^{n+1}).$$

Depending on the currently active case, this leads to continuous or discontinuous capillary pressure respectively. On the other edges we obtain pressure continuity.

The additional condition (2.16) in case A will lead to a discontinuity in the non-wetting pressure potential. In the spirit of (3.18) we extend the continuity condition, i.e. the jump terms, in the non-wetting phase mass balance equation (3.15). Using (2.16) we define:

$$[\![P_n^{n+1}]\!]' = \begin{cases} P_{n,h}^{n+1} - P_{n,l}^{n+1} - \delta_{p_c,F}^n & \text{if } p_{c,l}(S_{w,l}^{n+1}) < p_{c,e,h} \text{ and } S_{w,h}^{n+1} = 1 \\ P_{n,h}^{n+1} - P_{n,l}^{n+1} & \text{otherwise} \end{cases}, \tag{3.19}$$

where, we use $\delta_{p_c,F}^n$ as defined in (2.12) with the additional superscript denoting the timestep at which the evaluation takes place. Also in this case, we have either pressure continuity or $[\![P_n^{n+1}]\!]$ matches the jump in the capillary pressure.

3.4.2 Discrete scheme with interface conditions

Using (3.19) and (3.18) we get the following scheme:

Problem 4 [Discrete problem at t^{n+1} with interface conditions] Let $P_n^n \in V_h^p(\Omega)$, $P_c^n \in V_h^p(\Omega)$, and $S_w^n \in V_h^s(\Omega)$. Find $P_n^{n+1} \in V_h^p(\Omega)$, $P_c^{n+1} \in V_h^p(\Omega)$, and $S_w^{n+1} \in V_h^s(\Omega)$, s.t., for all $\psi_s \in V_h^s(\Omega)$, $\psi_n \in V_h^p(\Omega)$, and $\psi_w \in V_h^p(\Omega)$, the following holds:

$$\begin{aligned}
\textbf{PDE-1}: & \sum_{T_i \in \mathcal{T}} \int_{T_i} -\partial^- S_w^{n+1} \phi \psi_n + \sum_{T_i \in \mathcal{T}} \int_{T_i} \lambda_n(S_w^{n+1}) K \nabla (P_n^{n+1} - gz\rho_n) \nabla \psi_n \\
& - \sum_{F_i \in \mathcal{F}} \int_{F_i} \{\lambda_n(S_w^{n+1}) K \nabla (P_n^{n+1} - gz\rho_n) \cdot \vec{n}\} [\![\psi_n]\!] \\
& + \theta \sum_{F_i \in \mathcal{F}} \int_{F_i} [\![P_n^{n+1}]\!]' \{\lambda_n(S_w^{n+1}) K \nabla \psi_n \cdot \vec{n}\} + \sigma_n \sum_{F_i \in \mathcal{F}} \int_{F_i} \frac{f(k_p)}{|F_i|} [\![P_n^{n+1}]\!]' [\![\psi_n]\!] \\
& = \theta \sum_{F_i \in \Gamma_D} \int_{F_i} [\![P_n^D]\!] \{\lambda_n(s^D) K \nabla \psi_n \cdot \vec{n}\} + \sigma_n \sum_{F_i \in \Gamma_D} \int_{F_i} \frac{f(k_p)}{|F_i|} [\![P_n^D]\!] [\![\psi_n]\!]
\end{aligned} \tag{3.20}$$

$$\begin{aligned}
\textbf{PDE-2}: & \sum_{T_i \in \mathcal{T}} \int_{T_i} \partial^- S_w^{n+1} \phi \psi_w + \sum_{T_i \in \mathcal{T}} \int_{T_i} \lambda_w(S_w^{n+1}) K \nabla (P_n^{n+1} - P_c^{n+1} - gz\rho_w) \nabla \psi_w \\
& - \sum_{F_i \in \mathcal{F}} \int_{F_i} \{\lambda_w(S_w^{n+1}) K \nabla (P_n^{n+1} - P_c^{n+1} - gz\rho_w) \cdot \vec{n}\} [\![\psi_w]\!] \\
& + \theta \sum_{F_i \in \mathcal{F}} \int_{F_i} \{\lambda_w(S_w^{n+1}) K \nabla \psi_w \cdot \vec{n}\} [\![P_n^{n+1} - P_c^{n+1}]\!] \\
& + \sigma_w \sum_{F_i \in \mathcal{F}} \int_{F_i} \frac{f(k_p)}{|F_i|} [\![P_n^{n+1} - P_c^{n+1}]\!] [\![\psi_w]\!]
\end{aligned}$$

$$= \theta \sum_{F_i \in \Gamma_D} \int_{F_i} \{\lambda_w(s^D) K \nabla \psi_w \cdot \vec{n}\} [\![P_n^D - P_c^D]\!]$$
$$+ \sigma_w \sum_{F_i \in \Gamma_D} \int_{F_i} \frac{f(k_p)}{|F_i|} [\![P_n^D - P_c^D]\!] [\![\psi_w]\!] \tag{3.21}$$

ODE-Pc: $$\sum_{T_i \in \mathcal{T}} \int_{T_i} P_c^{n+1} \psi_s = \sum_{T_i \in \mathcal{T}} \int_{T_i} p_{c,eq}(S_w^{n+1}) \psi_s - \sum_{T_i \in \mathcal{T}} \int_{T_i} \partial^- T(S_w^{n+1}) \psi_s$$
$$+ \sigma_s \sum_{F_i \in \mathcal{F}} \int_{F_i} \frac{f(k_s)}{|F_i|} [\![p_{c,eq}(S_w^{n+1}) - \partial^- T(S_w^{n+1})]\!]' [\![\psi_w]\!] \tag{3.22}$$

3.4.3 Flux continuity

The flux continuity is implicitly enforced by the proposed scheme 4. To show this we proceed the same way as in [Ern et al., 2010]. For a solution of the scheme the following condition holds due to (3.20):

$$\sum_{T_i \in \mathcal{T}} \int_{T_i} -\partial^- S_w^{n+1} \phi \psi_n + \sum_{T_i \in \mathcal{T}} \int_{T_i} \lambda_n(S_w^{n+1}) K \nabla (P_n^{n+1} - g z \rho_n) \nabla \psi_n$$
$$- \sum_{F_i \in \mathcal{F}} \int_{F_i} \{\lambda_n(S_w^{n+1}) K \nabla (P_n^{n+1} - g z \rho_n) \cdot \vec{n}\} [\![\psi_n]\!]$$
$$+ \theta \sum_{F_i \in \mathcal{F}} \int_{F_i} [\![P_n^{n+1}]\!]' \{\lambda_n(S_w^{n+1}) K \nabla \psi_n \cdot \vec{n}\} + \sigma_n \sum_{F_i \in \mathcal{F}} \int_{F_i} \frac{f(k_p)}{|F_i|} [\![P_n^{n+1}]\!]' [\![\psi_n]\!]$$
$$= 0$$

By partial integration and using the relationship,

$$[\![uv]\!] = \{u\} [\![v]\!] + \{v\} [\![u]\!] \,,$$

for the interior edges we obtain:

$$\sum_{T_i \in \mathcal{T}} \int_{T_i} \left(-\partial^- S_w^{n+1} \phi - \nabla \cdot \left(\lambda_n(S_w^{n+1}) K \nabla (P_n^{n+1} - g z \rho_n) \right) \right) \psi_n$$
$$+ \sum_{F_i \in \mathcal{F}} \int_{F_i} \{\psi_n\} [\![\lambda_n(S_w^{n+1}) K \nabla (P_n^{n+1} - g z \rho_n) \cdot \vec{n}]\!]$$
$$+ \theta \sum_{F_i \in \mathcal{F}} \int_{F_i} [\![P_n^{n+1}]\!]' \{\lambda_n(S_w^{n+1}) K \nabla \psi_n \cdot \vec{n}\}$$
$$+ \sigma_n \sum_{F_i \in \mathcal{F}} \int_{F_i} \frac{f(k_p)}{|F_i|} [\![P_n^{n+1}]\!]' [\![\psi_n]\!] = 0$$

The first term is the weak residual of the conservation law for the non-wetting phase. The second term enforces the normal flux continuity across the interface, and the third and the fourth terms ensure the continuity of the pressure. Note that we are using the extended jump

definition (3.19), leading to either a continuous or discontinuous pressure across the interface respectively. In either cases, due to the construction of the jump terms, for a convergent solution

$$[\![P_n^{n+1}]\!]' = 0$$

holds true.

In a similar way, we partially integrate the wetting phase equation (3.21) and get:

$$\begin{aligned}
&\sum_{T_i \in \mathcal{T}} \int_{T_i} \left(\partial^- S_w^{n+1} \phi - \nabla \cdot \left(\lambda_w(S_w^{n+1}) K \nabla (P_n^{n+1} - P_c^{n+1} - gz\rho_w)\right)\right) \psi_w \\
&+ \sum_{F_i \in \mathcal{F}} \int_{F_i} \{\psi_w\} [\![\lambda_w(S_w^{n+1}) K \nabla (P_n^{n+1} - P_c^{n+1} - gz\rho_w) \cdot \vec{n}]\!] \\
&+ \theta \sum_{F_i \in \mathcal{F}} \int_{F_i} [\![P_n^{n+1} - P_c^{n+1}]\!] \{\lambda_w(S_w^{n+1}) K \nabla \psi_w \cdot \vec{n}\} \\
&+ \sigma_w \sum_{F_i \in \mathcal{F}} \int_{F_i} \frac{f(k_p)}{|F_i|} [\![P_n^{n+1} - P_c^{n+1}]\!] [\![\psi_w]\!] = 0 \, .
\end{aligned}$$

Again, the first term represents the weak residual of the conservation law for the wetting phase. The second term gives the normal flux continuity across the interface, and the third and the fourth terms ensure the continuity of the pressure.

Chapter 4

Convergence Analysis of the Numerical Scheme

In this chapter, we prove that the numerical scheme is well-posed and convergent. We first show the existence of a discrete solution using a fixed-point argument, followed by the energy estimates for the discrete solutions. Finally, we show the convergence of the scheme by proving some error estimates.

Preliminaries We make the following assumptions to prove existence and convergence of the numerical scheme:

(A4.1) The initial and boundary conditions in (2.7) and (2.8) are sufficiently smooth. Additionally, the initial condition is compatible with the boundary condition, i.e. the initial condition fulfills the boundary condition at $t = 0$.

(A4.2) The permeability matrix $K \in \mathbb{R}^{d\times d}$ is symmetric and positive definite, i.e. there exist two constants $\overline{\kappa}$ and $\underline{\kappa}$, s.t., for any vector $x \in \mathbb{R}^d$, the following holds:

$$\underline{\kappa}\|x\|^2 \leq x^T K x \leq \overline{\kappa}\|x\|^2$$

(A4.3) The equilibrium capillary pressure function $p_{c,eq}(\cdot)$ is in $C^2(\mathbb{R})$, and is assumed to be positive, bounded and decreasing. Let $P_{c,eq}(\cdot)$ define the primitive, i.e.:

$$P_{c,eq}(S) := \begin{cases} \int_1^S p_{c,eq}(\xi)d\xi = \int_0^S p_{c,eq}(\xi)d\xi - \int_0^1 p_{c,eq}(\xi)d\xi & \text{for } S \leq 1 \\ 0 & \text{otherwise} \end{cases}. \tag{4.1}$$

It can be inferred that $P_{c,eq}(S)$ is concave and non-positive.

(A4.4) The functions $\lambda_w(\cdot)$ and $\lambda_n(\cdot)$ are Lipschitz-continuous and bounded from above and below by the constants $0 < \overline{\lambda_\alpha} < \underline{\lambda_\alpha} < \infty$.

For the error analysis, let $s_w(t,x)$, $p_n(t,x)$, and $p_c(t,x)$ be the exact solutions of the problem. For simplicity, we will use $s_w^i = s_w(t_i,x)$, $p_n^i = p_n(t_i,x)$, and $p_c^i = p_c(t_i,x)$. For all $t \in [0,T]$ we denote the projection of $p_n(t)$, $p_c(t)$, and $s_w(t)$ onto the space $V_h^p(\Omega)$ or $V_h^s(\Omega)$ with, $\tilde{p}_n(t) \in V_h^p(\Omega)$, $\tilde{p}_c(t) \in V_h^p(\Omega)$, and $\tilde{s}_w(t) \in V_h^s(\Omega)$, respectively. Further, we assume for all $t \in [0,T]$ that $\tilde{p}_n(t) \in W^{1,\infty}(\Omega)$, $\tilde{p}_c(t) \in W^{1,\infty}(\Omega)$ and $\tilde{s}_w(t) \in W^{1,\infty}(\Omega)$. We also assume that the solutions possess enough regularity such that the the following approximation properties are fulfilled:

For all $t \in [0,T]$, $l_{p_n} \in \mathbb{R}^+$, $l_{p_c} \in \mathbb{R}^+$, $l_s \in \mathbb{R}^+$, and $T \in \mathcal{T}$, for $\tilde{p}_n(t) \in W^{1,\infty}$, $\tilde{p}_c(t) \in W^{1,\infty}$ and $\tilde{s}_w(t) \in W^{1,\infty}$ there exists a constant C independent of h, k_s, k_p and Δt s.t.,

$$\text{for } 0 < q \le l_{p_n}\ , \quad \|p_n(t) - \tilde{p}_n(t)\|_{T,q} \le C \frac{h^{\min(k_p+1,l_{p_n})-q}}{k_p^{l_{p_n}-q}} \|p_n(t)\|_{T,l_{p_n}} \tag{4.2}$$

$$\text{for } 0 < q \le l_{p_c}\ , \quad \|p_c(t) - \tilde{p}_c(t)\|_{T,q} \le C \frac{h^{\min(k_p+1,l_{p_c})-q}}{k_p^{l_{p_c}-q}} \|p_c(t)\|_{T,l_{p_c}} \tag{4.3}$$

$$\text{for } 0 < q \le l_s\ , \quad \|s_n(t) - \tilde{s}_n(t)\|_{T,q} \le C \frac{h^{\min(k_s+1,l_s)-q}}{k_s^{l_s-q}} \|s_n(t)\|_{T,l_s} \tag{4.4}$$

The proof for the results (4.2), (4.3) and (4.4) can be found in [Babuska and Suri, 1987]. Recall that the norm $\|\cdot\|_{T,q}$ is defined as $\|\cdot\|_{W^{q,2}(T)}$, see also Section 2.8.

Further, we write the numerical errors for $i = 1, \ldots, N$ as,

$$e_{s,h}^i = S^i - \tilde{s}_w^i\ , \quad e_s^i = \tilde{s}_w^i - s^i\ , \quad e_{p_\alpha,h}^i = P_\alpha^i - \tilde{p}_\alpha^i\ , \quad e_{p_\alpha}^i = \tilde{p}_\alpha^i - p_\alpha^i\ .$$

4.1 Existence of a discrete solution

We now prove the existence of a discrete solution for the Problem 3.

For given real numbers $P_{n,l} \in \mathbb{R}$, $P_{c,l} \in \mathbb{R}$ and $S_{w,k} \in \mathbb{R}$, we define $\tilde{P}_n, \tilde{P}_c \in V_h^p(\Omega)$ and $\tilde{S}_w \in V_h^s(\Omega)$ by,

$$\tilde{P}_n = \sum_{l=0}^{d_p} P_{n,l}\varphi_l^p \quad \tilde{P}_c = \sum_{l=0}^{d_p} P_{c,l}\varphi_l^p \quad \tilde{S}_w = \sum_{k=0}^{d_s} S_{w,k}\varphi_k^s\ , \tag{4.5}$$

where φ_i^p and φ_k^s are elements of a basis for $V_h^p(\Omega)$ and $V_h^s(\Omega)$ and $d_p \in \mathbb{N}$ and $d_s \in \mathbb{N}$ denote the dimension. We define the coefficient vectors $\hat{P}_n, \hat{P}_c \in \mathbb{R}^{d_p}$ and $\hat{S}_w \in \mathbb{R}^{d_s}$ by:

$$\begin{aligned} \hat{P}_n &= \begin{pmatrix} P_{n,1}, & P_{n,2}, & \ldots, P_{n,d_p} \end{pmatrix}^T \\ \hat{P}_c &= \begin{pmatrix} P_{c,1}, & P_{c,2}, & \ldots, P_{c,d_p} \end{pmatrix}^T \\ \hat{S}_w &= \begin{pmatrix} S_{w,1}, & S_{w,2}, & \ldots, S_{w,d_s} \end{pmatrix}^T\ . \end{aligned} \tag{4.6}$$

Furthermore, for given real numbers $S^n_{w,k} \in \mathbb{R}$, we define $P_{w,l} \in \mathbb{R}$ for $l = 0, \dots, d_p$ and $dS_{w,k} \in \mathbb{R}$ for $k = 0, \dots, d_s$, with,

$$\begin{aligned} P_{w,l} &:= P_{n,l} - P_{c,l} \ , \\ \text{and} \quad dS_{w,k} &= \frac{1}{\Delta t}(S_{w,k} - S^n_{w,k}) \ , \end{aligned} \tag{4.7}$$

which gives us $\tilde{P}_w \in V^p_h(\Omega)$, $S^n_w \in V^s_h(\Omega)$ and $\tilde{dS}_w \in V^s_h(\Omega)$, s.t.,

$$\begin{aligned} \tilde{P}_w &:= \tilde{P}_n - \tilde{P}_c = \sum_{i=0}^{d_p} P_{w,i}\varphi^p_i \ , \\ \text{and} \quad \tilde{dS}_w &:= \frac{1}{\Delta t}(\tilde{S}_w - S^n_w) = \sum_{k=0}^{d_s} dS_{w,k}\varphi^s_k \ . \end{aligned} \tag{4.8}$$

The coefficient vectors $\hat{P}_w \in \mathbb{R}^{d_p}$ and $\hat{dS}_w \in \mathbb{R}^{d_s}$ are defined analogous to (4.6).

Next, we define $\langle \cdot, \cdot \rangle_{\ell^2}$ as the ℓ^2-scalar product on $\mathbb{R}^{2d_p+d_s}$, and $\| \cdot \|_{\ell^2}$ as the induced ℓ^2-norm on $\mathbb{R}^{2d_p+d_s}$.

Note that for a coefficient vector $\hat{X} \in \mathbb{R}^{2d_p+d_s}$ and the induced vector $\tilde{X} \in V^p_h(\Omega) \times V^p_h(\Omega) \times V^s_h(\Omega)$ there exists constants $c > 0, c \in \mathbb{R}$ and $C > 0, C \in \mathbb{R}$, such that the following inequality holds:

$$c\|\tilde{X}\|_{\Omega,0} \leq \|\hat{X}\|^2_{\ell^2} = \langle \hat{X}, \hat{X} \rangle_{\ell^2} \leq C\|\tilde{X}\|_{\Omega,0} \ . \tag{4.9}$$

Note that the constants c and C may depend on the mesh size h.

Using the definitions (4.5), (4.7) and (4.8) in (3.15)-(3.17), we define $F^{P_n}_i, F^{P_c}_i, F^S_k \in \mathbb{R}$ for $i = 0, 1, \dots, d_p$ and $k = 0, 1, \dots, d_s$, s.t.,

$$\begin{aligned} F^{P_n}_l := &\sum_{T_i \in \mathcal{T}} \int_{T_i} -\frac{1}{\Delta t}(\tilde{S}_w - S^n_w)\phi\varphi^p_l + \sum_{T_i \in \mathcal{T}} \int_{T_i} \lambda_n(\tilde{S}_w)K\nabla\tilde{P}_n\nabla\varphi^p_l \\ &- \sum_{F_i \in \mathcal{F}} \int_{F_i} \{\lambda_n(\tilde{S}_w)K\nabla\tilde{P}_n \cdot \vec{n}\}[\![\varphi^p_l]\!] \\ &+ \theta \sum_{F_i \in \mathcal{F}} \int_{F_i} [\![\tilde{P}_n]\!]\{\lambda_n(\tilde{S}_w)K\nabla\varphi^p_l \cdot \vec{n}\} + \sigma_n \sum_{F_i \in \mathcal{F}} \int_{F_i} \frac{f(k_p)}{|F_i|}[\![\tilde{P}_n]\!][\![\varphi^p_l]\!] \\ &- \theta \sum_{F_i \in \Gamma} \int_{F_i} [\![p^D_n]\!]\{\lambda_n(s^D)K\nabla\varphi^p_l \cdot \vec{n}\} - \sigma_n \sum_{F_i \in \Gamma} \int_{F_i} \frac{f(k_p)}{|F_i|}[\![p^D_n]\!][\![\varphi^p_l]\!] \end{aligned} \tag{4.10}$$

$$\begin{aligned} F^{P_c}_l := &\sum_{T_i \in \mathcal{T}} \int_{T_i} \frac{1}{\Delta t}(\tilde{S}_w - S^n_w)\phi\varphi^p_l + \sum_{T_i \in \mathcal{T}} \int_{T_i} \lambda_w(\tilde{S}_w)K\nabla(\tilde{P}_n - \tilde{P}_c)\nabla\varphi^p_l \\ &- \sum_{F_i \in \mathcal{F}} \int_{F_i} \{\lambda_w(\tilde{S}_w)K\nabla(\tilde{P}_n - \tilde{P}_c) \cdot \vec{n}\}[\![\varphi^p_l]\!] \end{aligned}$$

$$
\begin{aligned}
&+\theta \sum_{F_i\in\mathcal{F}} \int_{F_i} \{\lambda_w(\tilde{S}_w) K\nabla\varphi_l^p \cdot \vec{n}\} [\![\tilde{P}_n - \tilde{P}_c]\!] \\
&+\sigma_w \sum_{F_i\in\mathcal{F}} \int_{F_i} \frac{f(k_p)}{|F_i|} [\![\tilde{P}_n - \tilde{P}_c]\!][\![\varphi_l^p]\!] \\
&-\theta \sum_{F_i\in\Gamma} \int_{F_i} \{\lambda_w(s^D) K\nabla\varphi_l^p \cdot \vec{n}\} [\![p_n^D - p_c^D]\!] \\
&-\sigma_w \sum_{F_i\in\Gamma} \int_{F_i} \frac{f(k_p)}{|F_i|} [\![p_n^D - p_c^D]\!][\![\varphi_l^p]\!] \,,
\end{aligned}
\tag{4.11}
$$

$$
\begin{aligned}
F_k^S :=& \sum_{T_i\in\mathcal{T}} \int_{T_i} \phi \tilde{P}_c \varphi_k^s - \sum_{T_i\in\mathcal{T}} \int_{T_i} \phi p_{c,eq}(\tilde{S}_w)\varphi_k^s \\
&- \sum_{T_i\in\mathcal{T}} \int_{T_i} \phi\tau \frac{1}{\Delta t}(\tilde{S}_w - S_w^n)\varphi_k^s \,.
\end{aligned}
\tag{4.12}
$$

As before, we define analogous to (4.6) the coefficient vectors $\hat{F}^{P_n}, \hat{F}^{P_c} \in \mathbb{R}^{d_p}$ and $\hat{F}^S \in \mathbb{R}^{d_s}$. Observe that, if $F_i^{P_n} = F_i^{P_c} = F_k^S = 0$ for all $i = 0, 1, \ldots, d_p$ and $k = 0, 1, \ldots, d_s$, then $\tilde{P}_n$, $\tilde{P}_c$ and $\tilde{S}_w$ are a solution to the Problem 3.

The definitions (4.5)-(4.12) define a continuous mapping $\mathcal{P} : \mathbb{R}^{2d_p+d_s} \to \mathbb{R}^{2d_p+d_s}$ by,

$$\mathcal{P}(\hat{P}_n, \hat{P}_w, d\hat{S}_w) = (\hat{F}^{P_n}, \hat{F}^{P_c}, \hat{F}^S) \,.$$

Existence To prove existence of a solution to our system, we use Lemma 1.4 in [Temam, 2001, p. 164]:

Lemma 4 Let X be a finite dimensional Hilbert space with scalar product $\langle\cdot,\cdot\rangle$ and norm $\|\cdot\|$ and let $\mathcal{P}$ be a continuous mapping from X into itself such that,

$$\langle \mathcal{P}(\xi), \xi\rangle > 0 \text{ for } \|\xi\| = k > 0 \,.$$

Then, there exists a $\xi \in X$, $\|\xi\| \le k$ s.t.,

$$\mathcal{P}(\xi) = 0 \,.$$

Another version of this lemma can be found in Chapter IV of [Girault and Raviart, 1986].

To apply Lemma 4 we chose $\mathbb{R}^{2d_p+d_s}$ as the Hilbert space X and we use the scalar product $\langle\cdot,\cdot\rangle_{\ell^2}$ and the norm $\|\cdot\|_{\ell^2}$. Further, let $\begin{pmatrix}\hat{P}_n & \hat{P}_c & \hat{S}_w\end{pmatrix} \in \mathbb{R}^{2d_p+d_s}$ and define $R > 0$ as

$$R := \langle \begin{pmatrix}\hat{P}_n & \hat{P}_c & \hat{S}_w\end{pmatrix}, \begin{pmatrix}\hat{P}_n & \hat{P}_c & \hat{S}_w\end{pmatrix}\rangle = \langle \hat{P}_n, \hat{P}_n\rangle + \langle \hat{P}_w, \hat{P}_w\rangle + \langle d\hat{S}_w, d\hat{S}_w\rangle.$$

Specifically, we show that whenever

$$R > \sum_{T_i\in\mathcal{T}} \int_{T_i} \phi \frac{1}{\Delta t} |P_{c,eq}(S_w^n)| + \left(\frac{\sigma_n}{2} + \frac{\overline{\lambda_n}^2 \theta^2 C_t^2 \tilde{C}}{\underline{\lambda_n}} \right) \sum_{F_i\in\Gamma} \frac{f(k_p)}{|F_i|} \|p_n^D\|_{F_i,0}^2$$
$$+ \left(\frac{\sigma_w}{2} + \frac{\overline{\lambda_w}^2 \theta^2 C_t^2 \tilde{C}}{\underline{\lambda_w}} \right) \sum_{F_i\in\Gamma} \frac{f(k_p)}{|F_i|} \|p_w^D\|_{F_i,0}^2,$$

then one gets

$$\begin{aligned} &\langle \hat{F}^{P_n}, \hat{P}_n \rangle + \langle \hat{F}^{P_c}, \hat{P}_w \rangle + \langle \hat{F}^S, \hat{dS}_w \rangle \\ &= \sum_{i=0}^{d_p} P_{n,i} F_i^{P_n} + \sum_{i=0}^{d_p} (P_{n,i} - P_{c,i}) F_i^{P_c} + \sum_{k=0}^{d_s} dS_{w,k} F_k^S \\ &> 0 \,, \end{aligned} \tag{4.13}$$

which gives the following existence result:

Lemma 5 For sufficiently large σ_n, σ_w , the Problem 3 has a solution.

Proof 1 We estimate the terms $(I) := \sum_{i=0}^{d_p} P_{n,i} F_i^{P_n}$, $(II) := \sum_{i=0}^{d_p} P_{w,i} F_i^{P_c}$, and $(III) := \sum_{k=0}^{d_s} dS_{w,k} F_k^S$ separately.

Estimate for (I) We start with:

$$\begin{aligned} (I) = &\sum_{T_i\in\mathcal{T}} \int_{T_i} \lambda_n(\tilde{S}_w) \left| K^{\frac{1}{2}} \nabla \tilde{P}_n \right|^2 + \sigma_n \sum_{F_i\in\mathcal{F}} \int_{F_i} \frac{f(k_p)}{|F_i|} [\![\tilde{P}_n]\!]^2 \\ &- (1-\theta) \sum_{F_i\in\mathcal{F}} \int_{F_i} \{\lambda_n(\tilde{S}_w) K \nabla \tilde{P}_n \cdot \vec{n}\} [\![\tilde{P}_n]\!] - \sum_{T_i\in\mathcal{T}} \int_{T_i} \frac{1}{\Delta t} (\tilde{S}_w - S_w^n) \phi \tilde{P}_n \\ &- \theta \sum_{F_i\in\Gamma} \int_{F_i} [\![p_n^D]\!] \{\lambda_n(s^D) K \nabla \tilde{P}_n \cdot \vec{n}\} - \sigma_n \sum_{F_i\in\Gamma} \int_{F_i} \frac{f(k_p)}{|F_i|} [\![p_n^D]\!] [\![\tilde{P}_n]\!] \\ &= P_1 + P_2 - P_3 - P_4 - P_5 - P_6 \,. \end{aligned}$$

Using the assumption (A4.4) for $P_1 + P_2$, we get:

$$P_1 + P_2 \ \geq \underline{\lambda_n} \sum_{T_i\in\mathcal{T}} \left\| K^{\frac{1}{2}} \nabla \tilde{P}_n \right\|_{T_i,0}^2 + \sigma_n \sum_{F_i\in\mathcal{F}} \frac{f(k_p)}{|F_i|} \|[\![\tilde{P}_n]\!]\|_{F_i,0}^2 \,. \tag{4.14}$$

Using Cauchy-Schwarz inequality together with the assumption (A4.4), we get:

$$P_3 \leq \overline{\lambda_n}(1-\theta) \sum_{F_i\in\mathcal{F}} \|\{K^{\frac{1}{2}} \nabla \tilde{P}_n\}\|_{F_i,0} \|[\![\tilde{P}_n]\!]\|_{F_i,0} \,.$$

For a fixed face F_i, let $T_\pm$ be the adjacent elements. By the trace inequality (3.8), the following holds:

$$\overline{\lambda_n}(1-\theta)\sum_{F_i\in\mathcal{F}}\|\{K^{\frac{1}{2}}\nabla\tilde{P}_n\}\|_{F_i,0}\|[\![\tilde{P}_n]\!]\|_{F_i,0}$$
$$\leq\overline{\lambda_n}(1-\theta)C_t\sqrt{\frac{f(k_p)}{|F_i|}}\frac{1}{2}\sum_{F_i\mathcal{F}}\left(\left\|K^{\frac{1}{2}}\nabla\tilde{P}_n\right\|_{T_+,0}+\left\|K^{\frac{1}{2}}\nabla\tilde{P}_n\right\|_{T_-,0}\right)\|[\![\tilde{P}_n]\!]\|_{F_i,0}\,.$$

Further, with Lemma 3 and Cauchy-Schwarz inequality we obtain:

$$\overline{\lambda_n}(1-\theta)C_t\sqrt{\frac{f(k_p)}{|F_i|}}\frac{1}{2}\sum_{F_i\in\mathcal{F}}\left(\left\|K^{\frac{1}{2}}\nabla\tilde{P}_n\right\|_{T_+,0}+\left\|K^{\frac{1}{2}}\nabla\tilde{P}_n\right\|_{T_-,0}\right)\|[\![\tilde{P}_n]\!]\|_{F_i,0}$$
$$\leq\left(\sum_{T_i\in\mathcal{T}}\left\|K^{\frac{1}{2}}\nabla\tilde{P}_n\right\|^2_{T_i,0}\right)^{\frac{1}{2}}\left(\overline{\lambda_n}^2(1-\theta)^2C_t^2\tilde{C}\frac{f(k_p)}{|F_i|}\sum_{F_i\in\mathcal{F}}\|[\![\tilde{P}_n]\!]\|^2_{F_i,0}\right)^{\frac{1}{2}},$$

which, on using the scaled Young's inequality, leads to:

$$P_3\leq\frac{\epsilon_1}{2}\sum_{T_i\in\mathcal{T}}\left\|K^{\frac{1}{2}}\nabla\tilde{P}_n\right\|^2_{T_i,0}+\frac{1}{2\epsilon_1}\overline{\lambda_n}^2(1-\theta)^2C_t^2\tilde{C}\sum_{F_i\in\mathcal{F}}\frac{f(k_p)}{|F_i|}\|[\![\tilde{P}_n]\!]\|^2_{F_i,0}\,. \tag{4.15}$$

The term P_5 is estimated in a similar way as P_3 leading to:

$$P_5\leq\frac{\epsilon_2}{2}\sum_{T_i\in\mathcal{T}}\left\|K^{\frac{1}{2}}\nabla\tilde{P}_n\right\|^2_{T_i,0}+\frac{1}{2\epsilon_2}\overline{\lambda_n}^2\theta^2C_t^2\tilde{C}\sum_{F_i\in\Gamma}\frac{f(k_p)}{|F_i|}\|p_n^D\|^2_{F_i,0}\,, \tag{4.16}$$

and, the term P_6 is estimated as:

$$P_6\leq\frac{\epsilon_3}{2}\sum_{F_i\in\Gamma}\frac{f(k_p)}{|F_i|}\|\tilde{P}_n\|^2_{F_i,0}+\frac{\sigma_n^2}{2\epsilon_3}\sum_{F_i\in\Gamma}\frac{f(k_p)}{|F_i|}\|p_n^D\|^2_{F_i,0}\,. \tag{4.17}$$

Choosing $\epsilon_1=\epsilon_2=\frac{\underline{\lambda_n}}{2}$, and $\epsilon_3=\sigma_n$ in (4.14), (4.15), (4.16) and (4.17), we get the following estimate for the term (I):

$$\begin{aligned}(I)\geq&\sum_{T_i\in\mathcal{T}}\int_{T_i}-\frac{1}{\Delta t}(\tilde{S}_w-S_w^n)\phi\tilde{P}_n+\sum_{T_i\in\mathcal{T}}\frac{\underline{\lambda_n}}{2}\|K^{\frac{1}{2}}\nabla\tilde{P}_n\|^2_{T_i,0}\\&+\left(\frac{\sigma_n}{2}-\frac{(1-\theta)^2\overline{\lambda_n}^2C_t^2\tilde{C}}{2\underline{\lambda_n}}\right)\sum_{F_i\in\mathcal{F}}\frac{f(k_p)}{|F_i|}\|[\![\tilde{P}_n]\!]\|^2_{F_i,0}\\&-\left(\frac{\sigma_n}{2}+\frac{\overline{\lambda_n}^2\theta^2C_t^2\tilde{C}}{\underline{\lambda_n}}\right)\sum_{F_i\in\Gamma}\frac{f(k_p)}{|F_i|}\|p_n^D\|^2_{F_i,0}\end{aligned} \tag{4.18}$$

Estimate for (II) To estimate term (II), we follow the same steps as for term (I). We use the assumption (A4.4), trace inequalities from Lemma 2, Lemma 3, Cauchy-Schwarz and

scaled Young's inequality, in that order, and with $\epsilon_4 = \epsilon_5 = \frac{\lambda_w}{2}$ and $\epsilon_6 = \sigma_w$, we arrive at the following estimate:

$$
\begin{aligned}
(II) \geq & \sum_{T_i \in \mathcal{T}} \int_{T_i} \frac{1}{\Delta t}(\tilde{S}_w - S_w^n)\phi \tilde{P}_w + \sum_{T_i \in \mathcal{T}} \frac{\lambda_w}{2} \|K^{\frac{1}{2}} \nabla \tilde{P}_w\|^2_{T_i,0} \\
& + \left(\frac{\sigma_w}{2} - \frac{(1-\theta)^2 \overline{\lambda_w}^2 C_t^2 \tilde{C}}{2\underline{\lambda_w}} \right) \sum_{F_i \in \mathcal{F}} \frac{f(k_p)}{|F_i|} \|[\![\tilde{P}_w]\!]\|^2_{F_i,0} \\
& - \left(\frac{\sigma_w}{2} + \frac{\overline{\lambda_w}^2 \theta^2 C_t^2 \tilde{C}}{\underline{\lambda_w}} \right) \sum_{F_i \in \Gamma} \frac{f(k_p)}{|F_i|} \|p_w^D\|^2_{F_i,0} \, .
\end{aligned} \tag{4.19}
$$

Estimate for (III) We start with:

$$
\begin{aligned}
(III) = & \sum_{T_i \in \mathcal{T}} \int_{T_i} \phi \tilde{P}_c \frac{1}{\Delta t}(\tilde{S}_w - S_w^n) - \sum_{T_i \in \mathcal{T}} \int_{T_i} \phi p_{c,eq}(\tilde{S}_w) \frac{1}{\Delta t}(\tilde{S}_w - S_w^n) \\
& + \sum_{T_i \in \mathcal{T}} \int_{T_i} \phi \tau \frac{1}{\Delta t^2}(\tilde{S}_w - S_w^n)^2 \, .
\end{aligned}
$$

Using the primitive defined in (4.1), we get the following estimate:

$$
\begin{aligned}
(III) \geq & \sum_{T_i \in \mathcal{T}} \int_{T_i} \phi \tilde{P}_c \frac{1}{\Delta t}(\tilde{S}_w - S_w^n) + \sum_{T_i \in \mathcal{T}} \int_{T_i} \phi \frac{1}{\Delta t} \left(|P_{c,eq}(\tilde{S}_w)| - |P_{c,eq}(S_w^n)| \right) \\
& + \sum_{T_i \in \mathcal{T}} \int_{T_i} \phi \tau \frac{1}{\Delta t^2}(\tilde{S}_w - S_w^n)^2 \, .
\end{aligned} \tag{4.20}
$$

Combined estimate For sufficiently large σ_n and σ_w, using (3.6) from Lemma 1 with $q = 2$, and summing the estimates (4.18), (4.19) and (4.20), we obtain:

$$
\begin{aligned}
& \sum_{i=0}^{d_{p_n}} P_{n,i} F_i^{P_n} + \sum_{j=0}^{d_{p_c}} P_{w,j} F_j^{P_c} + \sum_{k=0}^{d_s} dS_{w,k} F_k^S \\
& \geq \; C\|\tilde{P}_n\|^2_{\Omega,0} + C\|\tilde{P}_w\|^2_{\Omega,0} + C\|d\tilde{S}_w\|^2_{\Omega,0} \\
& + \sum_{T_i \in \mathcal{T}} \int_{T_i} \phi \frac{1}{\Delta t} |P_{c,eq}(\tilde{S}_w)| - \sum_{T_i \in \mathcal{T}} \int_{T_i} \phi \frac{1}{\Delta t} |P_{c,eq}(S_w^n)| \\
& - \left(\frac{\sigma_n}{2} + \frac{\overline{\lambda_n}^2 \theta^2 C_t^2 \tilde{C}}{\underline{\lambda_n}} \right) \sum_{F_i \in \Gamma} \frac{f(k_p)}{|F_i|} \|p_n^D\|^2_{F_i,0} \\
& - \left(\frac{\sigma_w}{2} + \frac{\overline{\lambda_w}^2 \theta^2 C_t^2 \tilde{C}}{\underline{\lambda_w}} \right) \sum_{F_i \in \Gamma} \frac{f(k_p)}{|F_i|} \|p_w^D\|^2_{F_i,0} \, .
\end{aligned} \tag{4.21}
$$

Observe that the positivity of the last but one terms in (4.18) and (4.19) is only guaranteed under restrictions on σ_n and σ_w. However, these restrictions do not depend on the time step or the argument in the mapping $\mathcal{P}$. Now, one can choose the radius R as announced above to

guarantee that the right hand side in (4.21) is positive, and using (4.9) leads to the estimate (4.13), and the existence of a zero for $\mathcal{P}$ and hence of a solution to Problem 3 follows directly by Lemma 4.

4.2 Discrete energy estimate

Lemma 6 For sufficiently large σ_n and σ_w, there exists a constant C independent of Δt, h and the polynomial degrees k_p and k_s, s.t., the following energy estimate holds:

$$\begin{aligned}
&\Delta t \sum_{n=0}^{N} \sum_{T_i \in \mathcal{T}} \left\| \partial^- S_w^{n+1} \right\|_{T_i,0}^2 + \Delta t \sum_{n=0}^{N} \sum_{T_i \in \mathcal{T}} \left\| K^{\frac{1}{2}} \nabla P_n^{n+1} \right\|_{T_i,0}^2 \\
&+ \Delta t \sum_{n=0}^{N} \sum_{F_i \in \mathcal{F}} \frac{f(k_p)}{|F_i|} \| [\![P_n^{n+1}]\!] \|_{F_i,0}^2 + \Delta t \sum_{n=0}^{N} \sum_{T_i \in \mathcal{T}} \| K^{\frac{1}{2}} \nabla P_w^{n+1} \|_{T_i,0}^2 \\
&+ \Delta t \sum_{n=0}^{N} \sum_{F_i \in \mathcal{F}} \frac{f(k_p)}{|F_i|} \| [\![P_w^{n+1}]\!] \|_{F_i,0}^2 + \sum_{T_i \in \mathcal{T}} \int_{T_i} |P_{c,eq}(S_w^{N+1})| \\
&\leq C \sum_{T_i \in \mathcal{T}} \int_{T_i} |P_{c,eq}(S_w^0)| + C \Delta t \sum_{n=0}^{N} \sum_{F_i \in \Gamma} \frac{f(k_p)}{|F_i|} \| p_n^D \|_{F_i,0}^2 \\
&+ C \Delta t \sum_{n=0}^{N} \sum_{F_i \in \Gamma} \frac{f(k_p)}{|F_i|} \| p_w^D \|_{F_i,0}^2 \qquad (4.22)
\end{aligned}$$

Proof 2 Starting with the discrete system at t^{n+1} (i.e. Problem 3), we test in (3.15) with P_n^{n+1}, in (3.16) with $P_w^{n+1} = P_n^{n+1} - P_c^{n+1}$ and in (3.17) with $\partial^- S_w^{n+1}$.

Note that we define a generic constant $C = C(\tau, \sigma_\alpha, \underline{\lambda_\alpha}, \overline{\lambda_\alpha}, \theta, C_t, \tilde{C})$ for $\alpha = w, n$. We proceed with the same steps as in the proof of Lemma 5 and obtain:

$$\begin{aligned}
&\sum_{T_i \in \mathcal{T}} \phi \tau \left\| \partial^- S_w^{n+1} \right\|_{T_i,0}^2 + \frac{\underline{\lambda_n}}{2} \sum_{T_i \in \mathcal{T}} \left\| K^{\frac{1}{2}} \nabla P_n^{n+1} \right\|_{T_i,0}^2 + \frac{\underline{\lambda_w}}{2} \sum_{T_i \in \mathcal{T}} \| K^{\frac{1}{2}} \nabla P_w^{n+1} \|_{T_i,0}^2 \\
&+ \left(\sigma_n - \frac{1}{2\underline{\lambda_n}} \overline{\lambda_n}^2 (1-\theta)^2 C_t^2 \tilde{C}^2 \right) \sum_{F_i \in \mathcal{F}} \frac{f(k_p)}{|F_i|} \| [\![P_n^{n+1}]\!] \|_{F_i,0}^2 \\
&+ \left(\sigma_w - \frac{1}{2\underline{\lambda_w}} \overline{\lambda_w}^2 (1-\theta)^2 C_t^2 \tilde{C}^2 \right) \sum_{F_i \in \mathcal{F}} \frac{f(k_p)}{|F_i|} \| [\![P_w^{n+1}]\!] \|_{F_i,0}^2 \\
&\leq \sum_{T_i \in \mathcal{T}} \int_{T_i} \frac{1}{\Delta t} \left(P_{c,eq}(S_w^{n+1}) - P_{c,eq}(S_w^n) \right) \\
&+ \left(\frac{\sigma_n}{2} + \frac{\overline{\lambda_n}^2 \theta^2 C_t^2 \tilde{C}^2}{\underline{\lambda_n}} \right) \sum_{F_i \in \Gamma} \frac{f(k_p)}{|F_i|} \| p_n^D \|_{F_i,0}^2
\end{aligned}$$

$$+\left(\frac{\sigma_w}{2}+\frac{\overline{\lambda_w}^2\theta^2C_t^2\tilde{C}^2}{\underline{\lambda_w}}\right)\sum_{F_i\in\Gamma}\frac{f(k_p)}{|F_i|}\|p_w^D\|^2_{F_i,0}$$

The final estimate (4.22) is obtained by multiplying the above inequality by Δt and summing over all $n = 0 \dots N$.

4.3 Error Estimates

After showing the existence of a discrete solution and deriving the general energy estimates, we now show a convergence result for the scheme.

4.3.1 Estimate for the non-wetting phase

Lemma 7 For a sufficiently large σ_n there exists a constant C independent of h, Δt, k_p and k_s such that the following estimate holds:

$$\begin{aligned}
&\sum_{T_i\in\mathcal{T}}\int_{T_i}\left[-\partial^- S_w^{n+1}+\partial_t s_w\right]\phi e^{n+1}_{p_n,h}+\sum_{T_i\in\mathcal{T}}\|K^{\frac{1}{2}}\nabla e^{n+1}_{p_n,h}\|^2_{T_i,0}\\
&+\sum_{F_i\in\mathcal{F}}\frac{f(k_p)}{|F_i|}\|[\![e^{n+1}_{p_n,h}]\!]\|^2_{F_i,0}\\
\le\, & C\left(\frac{5}{2\underline{\lambda_n}}+\frac{3f(k_s)}{2\sigma_n f(k_p)}\right)\overline{\lambda_n'}\|K^{\frac{1}{2}}\nabla\tilde{p}_n^{n+1}\|^2_{\Omega,\infty}\sum_{T_i\in\mathcal{T}}\|e^{n+1}_{s,h}\|^2_{T_i,0}\\
&+C\overline{\lambda_n'}\frac{5}{2\underline{\lambda_n}}\|K^{\frac{1}{2}}\nabla\tilde{p}_n^{n+1}\|^2_{\Omega,\infty}\|e_s^{n+1}\|^2_{\Omega,0}+C\frac{5\overline{\lambda_n}}{2\underline{\lambda_n}}\|K^{\frac{1}{2}}\nabla e^{n+1}_{p_n}\|^2_{\Omega,0}\\
&+\frac{3f(k_s)}{2\sigma_n f(k_p)}\overline{\lambda_n'}\tilde{C}\|K^{\frac{1}{2}}\nabla\tilde{p}_n^{n+1}\|_{\Omega,\infty}(\|e_s^{n+1}\|^2_{\Omega,0}+h^2\|\nabla e_s^{n+1}\|^2_{\Omega,0})\\
&+C\left(\frac{3\sigma_n C_t^2\tilde{C}}{2}+\frac{5\theta\overline{\lambda_n}^2C_t^2\tilde{C}}{\underline{\lambda_n}}\right)(h^{-2}\|e^{n+1}_{p_n}\|^2_{\Omega,0}+\|\nabla e^{n+1}_{p_n}\|^2_{\Omega,0})\\
&+C\frac{3\overline{\lambda_n}^2C_t^2\tilde{C}}{2\sigma_n}\left(\left\|K^{\frac{1}{2}}\nabla e^{n+1}_{p_n}\right\|^2_{\Omega,0}+h^2\left\|K^{\frac{1}{2}}\nabla^2 e^{n+1}_{p_n}\right\|^2_{\Omega,0}\right)
\end{aligned}$$

Proof 3 We subtract (3.11) and (3.15) and test with $e^{n+1}_{p_n,h}$ to get:

$$\begin{aligned}
&\sum_{T_i\in\mathcal{T}}\int_{T_i}\left[-\partial^- S_w^{n+1}+\partial_t s_w\right]\phi e^{n+1}_{p_n,h}\\
+&\sum_{T_i\in\mathcal{T}}\int_{T_i}\left[\lambda_n(S_w^{n+1})K\nabla P_n^{n+1}-\lambda_n(s_w)K\nabla p_n\right]\nabla e^{n+1}_{p_n,h}
\end{aligned}$$

$$
\begin{aligned}
&+ \sigma_n \sum_{F_i \in \mathcal{F}} \int_{F_i} \frac{f(k_p)}{|F_i|} \left[[\![P_n^{n+1}]\!] - [\![p_n]\!] \right] [\![e_{p_n,h}^{n+1}]\!] \\
&= \sum_{F_i \in \mathcal{F}} \int_{F_i} \left[\{ \lambda_n(S_w^{n+1}) K \nabla P_n^{n+1} \cdot \vec{n} \} - \{ \lambda_n(s_w) K \nabla p_n \cdot \vec{n} \} \right] [\![e_{p_n,h}^{n+1}]\!] \\
&- \theta \sum_{F_i \in \mathcal{F}} \int_{F_i} \left[[\![P_n^{n+1}]\!] \{ \lambda_n(S_w^{n+1}) K \nabla e_{p_n,h}^{n+1} \cdot \vec{n} \} - [\![p_n]\!] \{ \lambda_n(s_w) K \nabla e_{p_n,h}^{n+1} \cdot \vec{n} \} \right]
\end{aligned}
$$

We rewrite this equation termwise as:

$$
P_1 + P_2 + P_3 = P_4 \ ,
$$

and estimate each term individually.

We expand each term P_1 to P_4 by adding and subtracting $\tilde{p}_n$.

Estimate for P_2

$$
\begin{aligned}
P_2 = &\sum_{T_i \in \mathcal{T}} \int_{T_i} \lambda_n(S_w^{n+1}) K \nabla e_{p_n,h}^{n+1} \nabla e_{p_n,h}^{n+1} \\
&+ \sum_{T_i \in \mathcal{T}} \int_{T_i} \Big(\lambda_n(S_w^{n+1}) - \lambda_n(s_w) \Big) K \nabla \tilde{p}_n^{n+1} \nabla e_{p_n,h}^{n+1} \\
&+ \sum_{T_i \in \mathcal{T}} \int_{T_i} \lambda_n(s_w) K \nabla e_{p_n}^{n+1} \nabla e_{p_n,h}^{n+1} \\
=: &\, P_{2,1} + P_{2,2} + P_{2,3}
\end{aligned}
$$

where, we estimate $P_{2,1}$, $P_{2,2}$ and $P_{2,3}$ as:

$$
P_{2,1} \geq \sum_{T_i \in \mathcal{T}} \underline{\lambda_n} \| K^{\frac{1}{2}} \nabla e_{p_n,h}^{n+1} \|_{T_i,0}^2 \tag{4.23}
$$

$$
\begin{aligned}
P_{2,2} \leq &\sum_{T_i \in \mathcal{T}} \int_{T_i} \overline{\lambda_n'} (S_w^{n+1} - s_w^{n+1}) K \nabla \tilde{p}_n^{n+1} \cdot \nabla e_{p_n,h}^{n+1} \\
\leq &\sum_{T_i \in \mathcal{T}} \int_{T_i} \overline{\lambda_n'} (e_{s,h}^{n+1} + e_s^{n+1}) K \nabla \tilde{p}_n^{n+1} \cdot \nabla e_{p_n,h}^{n+1} \\
\leq &\frac{\epsilon_{2,2}}{2} \sum_{T_i \in \mathcal{T}} \| K^{\frac{1}{2}} \nabla e_{p_n,h}^{n+1} \|_{T_i,0}^2 \\
&+ \overline{\lambda_n'}^2 \frac{1}{2\epsilon_{2,2}} \| K^{\frac{1}{2}} \nabla \tilde{p}_n^{n+1} \|_{\Omega,\infty}^2 \sum_{T_i \in \mathcal{T}} \left(\| e_{s,h}^{n+1} \|_{T_i,0}^2 + \| e_s^{n+1} \|_{T_i,0}^2 \right)
\end{aligned} \tag{4.24}
$$

$$
P_{2,3} \leq \frac{\epsilon_{2,3}}{2} \sum_{T_i \in \mathcal{T}} \| K^{\frac{1}{2}} \nabla e_{p_n,h}^{n+1} \|_{T_i,0}^2 + \frac{\overline{\lambda_n}^2}{2\epsilon_{2,3}} \sum_{T_i \in \mathcal{T}} \| K^{\frac{1}{2}} \nabla e_{p_n}^{n+1} \|_{T_i,0}^2 \tag{4.25}
$$

Estimate for P_3

$$P_3 = \sigma_n \sum_{F_i \in \mathcal{F}} \int_{F_i} \frac{f(k_p)}{|F_i|} \left[[\![e_{p_n,h}^{n+1}]\!] + [\![e_{p_n}^{n+1}]\!] \right] [\![e_{p_n,h}^{n+1}]\!] = P_{3,1} + P_{3,2}$$

where,

$$P_{3,1} = \sigma_n \sum_{F_i \in \mathcal{F}} \frac{f(k_p)}{|F_i|} \| [\![e_{p_n,h}^{n+1}]\!] \|_{F_i,0}^2 \,, \tag{4.26}$$

and,

$$\begin{aligned} P_{3,2} \leq & \frac{\epsilon_{3,2}}{2} \sum_{F_i \in \mathcal{F}} \frac{f(k_p)}{|F_i|} \| [\![e_{p_n,h}^{n+1}]\!] \|_{F_i,0}^2 \\ & + \frac{1}{2\epsilon_{3,2}} \sigma_n^2 C_t^2 \tilde{C} (h^{-2} \| e_{p_n}^{n+1} \|_{\Omega,0}^2 + \| \nabla e_{p_n}^{n+1} \|_{\Omega,0}^2) \end{aligned} \tag{4.27}$$

Estimate for P_4

$$\begin{aligned} P_4 = & (1-\theta) \sum_{F_i \in \mathcal{F}} \int_{F_i} \left[\{ \lambda_n(S_w^{n+1}) K \nabla e_{p_n,h}^{n+1} \cdot \vec{n} \} \right] [\![e_{p_n,h}^{n+1}]\!] \\ & + \sum_{F_i \in \mathcal{F}} \int_{F_i} \left\{ (\lambda_n(S_w^{n+1}) - \lambda_n(s_w)) K \nabla \tilde{p}_n^{n+1} \cdot \vec{n} \right\} [\![e_{p_n,h}^{n+1}]\!] \\ & + \sum_{F_i \in \mathcal{F}} \int_{F_i} \{ \lambda_n(s_w) K \nabla e_{p_n}^{n+1} \cdot \vec{n} \} [\![e_{p_n,h}^{n+1}]\!] \\ & - \theta \sum_{F_i \in \mathcal{F}} \int_{F_i} [\![e_{p_n}^{n+1}]\!] \{ \lambda_n(s_w) K \nabla e_{p_n,h}^{n+1} \cdot \vec{n} \} \\ & - \theta \sum_{F_i \in \mathcal{F}} \int_{F_i} [\![\tilde{p}_n^{n+1}]\!] \{ (\lambda_n(S_w^{n+1}) - \lambda_n(s_w)) K \nabla e_{p_n,h}^{n+1} \cdot \vec{n} \} \\ = & P_{4,1} + \cdots + P_{4,5} \end{aligned}$$

where, we estimate $P_{4,1}$ to $P_{4,4}$ separately, in the same way as (4.15) in Lemma 5:

$$\begin{aligned} P_{4,1} \leq & \frac{\epsilon_{4,1}}{2} \sum_{T_i \in \mathcal{T}} \left\| K^{\frac{1}{2}} \nabla e_{p_n,h}^{n+1} \right\|_{T_i,0}^2 \\ & + (1-\theta)^2 \frac{1}{2\epsilon_{4,1}} \overline{\lambda_n}^2 C_t^2 \tilde{C} \sum_{F_i} \frac{f(k_p)}{|F_i|} \| [\![e_{p_n,h}^{n+1}]\!] \|_{F_i,0}^2 \end{aligned} \tag{4.28}$$

$$\begin{aligned} P_{4,2} \leq & \overline{\lambda_n'} \tilde{C} \| K^{\frac{1}{2}} \nabla \tilde{p}_n^{n+1} \|_{\Omega,\infty} \sum_{F_i \in \mathcal{F}} \int_{F_i} \{ (e_{s,h}^{n+1} + e_s^{n+1}) \} [\![e_{p_n,h}^{n+1}]\!] \\ \leq & \frac{\epsilon_{4,2}}{2} \sum_{F_i} \frac{f(k_s)}{|F_i|} \| [\![e_{p_n,h}^{n+1}]\!] \|_{F_i,0}^2 + \frac{1}{2\epsilon_{4,2}} \overline{\lambda_n'}^2 \tilde{C} \| K^{\frac{1}{2}} \nabla \tilde{p}_n^{n+1} \|_{\Omega,\infty}^2 \sum_{T_i \in \mathcal{T}}^{2} \| e_{s,h}^{n+1} \|_{T_i,0}^2 \\ & + \frac{1}{2\epsilon_{4,2}} \overline{\lambda_n'}^2 \tilde{C} \| K^{\frac{1}{2}} \nabla \tilde{p}_n^{n+1} \|_{\Omega,\infty}^2 (\| e_s^{n+1} \|_{\Omega,0}^2 + h^2 \| \nabla e_s^{n+1} \|_{\Omega,0}^2) \end{aligned} \tag{4.29}$$

$$
\begin{aligned}
P_{4,3} \leq & \left(\overline{\lambda_n}^2 C_t^2 \tilde{C} \sum_{T_i \in \mathcal{T}} \left(\left\| K^{\frac{1}{2}} \nabla e_{p_n}^{n+1} \right\|_{T_i,0}^2 + |F_i|^2 \left\| K^{\frac{1}{2}} \nabla^2 e_{p_n}^{n+1} \right\|_{T_i,0}^2 \right) \right)^{\frac{1}{2}} \cdot \\
& \left(\sum_{F_i} \frac{f(k_p)}{|F_i|} \| [\![e_{p_n,h}^{n+1}]\!] \|_{F_i,0}^2 \right)^{\frac{1}{2}} \\
\leq & \overline{\lambda_n}^2 C_t^2 \tilde{C} \frac{1}{2\epsilon_{4,3}} \left(\left\| K^{\frac{1}{2}} \nabla e_{p_n}^{n+1} \right\|_{\Omega,0}^2 + h^2 \left\| K^{\frac{1}{2}} \nabla^2 e_{p_n}^{n+1} \right\|_{\Omega,0}^2 \right) \\
& + \frac{\epsilon_{4,3}}{2} \sum_{F_i} \frac{f(k_p)}{|F_i|} \| [\![e_{p_n,h}^{n+1}]\!] \|_{F_i,0}^2 \qquad (4.30) \\
P_{4,4} \leq & \frac{\epsilon_{4,4}}{2} \sum_{T_i \in \mathcal{T}} \left\| K^{\frac{1}{2}} \nabla e_{p_n,h}^{n+1} \right\|_{T_i,0}^2 \\
& + \frac{1}{2\epsilon_{4,4}} \theta^2 \overline{\lambda_n}^2 C_t^2 \tilde{C} (h^{-2} \| e_{p_n}^{n+1} \|_{\Omega,0}^2 + \| \nabla e_{p_n}^{n+1} \|_{\Omega,0}^2) \qquad (4.31)
\end{aligned}
$$

If $\tilde{p}_n^{n+1}$ is continuous, the jump term in $P_{4,5}$ vanishes making $P_{4,5} = 0$. Otherwise, we proceed with the same steps as for $P_{4,4}$. We use the continuity of p_n to replace $[\![\tilde{p}_n^{n+1}]\!]$ by $[\![e_{p_n}^{n+1}]\!]$ and get the following estimate for $P_{4,5}$:

$$
\begin{aligned}
P_{4,5} \leq & \frac{\epsilon_{4,5}}{2} \sum_{T_i \in \mathcal{T}} \left\| K^{\frac{1}{2}} \nabla e_{p_n,h}^{n+1} \right\|_{T_i,0}^2 \\
& + \frac{1}{2\epsilon_{4,5}} \theta^2 \overline{\lambda_n}^2 C_t^2 \tilde{C} (h^{-2} \| e_{p_n}^{n+1} \|_{\Omega,0}^2 + \| \nabla e_{p_n}^{n+1} \|_{\Omega,0}^2) \qquad (4.32)
\end{aligned}
$$

Combined estimate Putting the estimates (4.23) to (4.32) together, we get:

$$
\begin{aligned}
& \sum_{T_i \in \mathcal{T}} \int_{T_i} \left[-\partial^- S_w^{n+1} + \partial_t s_w \right] \phi e_{p_n,h}^{n+1} \\
& + \left(\underline{\lambda_n} - \frac{\epsilon_{2,2}}{2} - \frac{\epsilon_{2,3}}{2} - \frac{\epsilon_{4,1}}{2} - \frac{\epsilon_{4,4}}{2} - \frac{\epsilon_{4,5}}{2} \right) \sum_{T_i \in \mathcal{T}} \| K^{\frac{1}{2}} \nabla e_{p_n,h}^{n+1} \|_{T_i,0}^2 \\
& + \left(\sigma_n - \frac{f(k_p)}{2} \left(\epsilon_{3,2} + \epsilon_{4,3} + \frac{(1-\theta)^2 \overline{\lambda_n} C_t \tilde{C}}{\epsilon_{4,1}} \right) - \frac{f(k_s)\epsilon_{4,2}}{2} \right) \sum_{F_i \in \mathcal{F}} \frac{1}{|F_i|} \| [\![e_{p_n,h}^{n+1}]\!] \|_{F_i,0}^2 \\
& \leq \left(\frac{1}{2\epsilon_{2,2}} + \frac{1}{2\epsilon_{4,2}} \right) \overline{\lambda_n'}^2 \| K^{\frac{1}{2}} \nabla \tilde{p}_n^{n+1} \|_{\Omega,\infty}^2 \sum_{T_i \in \mathcal{T}} \| e_{s,h}^{n+1} \|_{T_i,0}^2 \\
& + \overline{\lambda_n'}^2 \frac{1}{2\epsilon_{2,2}} \| K^{\frac{1}{2}} \nabla \tilde{p}_n^{n+1} \|_{\Omega,\infty}^2 \| e_s^{n+1} \|_{\Omega,0}^2 + \frac{\overline{\lambda_n}^2}{2\epsilon_{2,3}} \sum_{T_i \in \mathcal{T}} \| K^{\frac{1}{2}} \nabla e_{p_n}^{n+1} \|_{T_i,0}^2 \\
& + \frac{1}{2\epsilon_{4,2}} \overline{\lambda_n'}^2 \tilde{C} \| K^{\frac{1}{2}} \nabla \tilde{p}_n^{n+1} \|_{\Omega,\infty}^2 (\| e_s^{n+1} \|_{\Omega,0}^2 + h^2 \| \nabla e_s^{n+1} \|_{\Omega,0}^2) \\
& + \frac{1}{2\epsilon_{3,2}} \sigma_n^2 C_t^2 \tilde{C} \sum_{T_i \in \mathcal{T}} (|F_i|^{-2} \| e_{p_n}^{n+1} \|_{T_i,0}^2 + \| \nabla e_{p_n}^{n+1} \|_{T_i,0}^2)
\end{aligned}
$$

$$+\overline{\lambda_n}^2 C_t^2 \tilde{C} \frac{1}{2\epsilon_{4,3}} \left(\left\| K^{\frac{1}{2}} \nabla e_{p_n}^{n+1} \right\|_{\Omega,0}^2 + h^2 \left\| K^{\frac{1}{2}} \nabla^2 e_{p_n}^{n+1} \right\|_{\Omega,0}^2 \right)$$
$$+ \left(\frac{1}{2\epsilon_{4,4}} + \frac{1}{2\epsilon_{4,5}} \right) \theta^2 \overline{\lambda_n}^2 C_t^2 \tilde{C} (h^{-2} \|e_{p_n}^{n+1}\|_{\Omega,0}^2 + \|\nabla e_{p_n}^{n+1}\|_{\Omega,0}^2) \tag{4.33}$$

Choosing $\epsilon_{2,2} = \epsilon_{2,3} = \epsilon_{4,1} = \epsilon_{4,4} = \epsilon_{4,5} = \frac{\lambda_n}{5}$, and $\epsilon_{3,2} = \frac{f(k_s)}{f(k_p)} \epsilon_{4,2} = \epsilon_{4,3} = \frac{\sigma_n}{3}$, we arrive at the desired estimate for the non-wetting phase.

4.3.2 Estimate for the wetting phase

Lemma 8 For a sufficiently large σ_w there exists a constant C independent of h, Δt, k_p and k_s such that the following estimate holds:

$$\sum_{T_i \in \mathcal{T}} \int_{T_i} \left[-\partial^- S_w^{n+1} + \partial_t s_w \right] \phi e_{p_w,h}^{n+1} + \sum_{T_i \in \mathcal{T}} \|K^{\frac{1}{2}} \nabla e_{p_w,h}^{n+1}\|_{T_i,0}^2$$
$$+ \sum_{F_i \in \mathcal{F}} \frac{f(k_p)}{|F_i|} \|[\![e_{p_w,h}^{n+1}]\!]\|_{F_i,0}^2$$
$$\leq C \left(\frac{5}{2\underline{\lambda_w}} + \frac{3f(k_s)}{2\sigma_w f(k_p)} \right) \overline{\lambda_w'} \|K^{\frac{1}{2}} \nabla \tilde{p}_w^{n+1}\|_{\Omega,\infty}^2 \sum_{T_i \in \mathcal{T}} \|e_{s,h}^{n+1}\|_{T_i,0}^2$$
$$+ C \overline{\lambda_w'} \frac{5}{2\underline{\lambda_w}} \|K^{\frac{1}{2}} \nabla \tilde{p}_w^{n+1}\|_{\Omega,\infty}^2 \|e_s^{n+1}\|_{\Omega,0}^2 + C \frac{5\overline{\lambda_w}}{2\underline{\lambda_w}} \|K^{\frac{1}{2}} \nabla e_{p_w}^{n+1}\|_{\Omega,0}^2$$
$$+ \frac{3f(k_s)}{2\sigma_w f(k_p)} \overline{\lambda_w'} \tilde{C} \|K^{\frac{1}{2}} \nabla \tilde{p}_w^{n+1}\|_{\Omega,\infty} (\|e_s^{n+1}\|_{\Omega,0}^2 + h^2 \|\nabla e_s^{n+1}\|_{\Omega,0}^2)$$
$$+ C \left(\frac{3\sigma_w C_t^2 \tilde{C}}{2} + \frac{5\theta \overline{\lambda_w}^2 C_t^2 \tilde{C}}{\underline{\lambda_w}} \right) (h^{-2} \|e_{p_w}^{n+1}\|_{\Omega,0}^2 + \|\nabla e_{p_w}^{n+1}\|_{\Omega,0}^2)$$
$$+ C \frac{3\overline{\lambda_w}^2 C_t^2 \tilde{C}}{2\sigma_w} \left(\left\| K^{\frac{1}{2}} \nabla e_{p_w}^{n+1} \right\|_{\Omega,0}^2 + h^2 \left\| K^{\frac{1}{2}} \nabla^2 e_{p_w}^{n+1} \right\|_{\Omega,0}^2 \right)$$

Proof 4 The proof is the same as for the non-wetting phase (Section 4.3.1) and is therefore left out.

4.3.3 Estimate for the capillary pressure

Lemma 9 There exists a constant C independent of h, Δt, k_p and k_s such that the following estimate holds:

$$\begin{aligned}
&\phi \sum_{T_i\in\mathfrak{T}} \int_{T_i} e_{p_c,h}^{n+1}\partial^- e_{s,h}^{n+1} + \frac{|\underline{p'_{c,eq}}|\phi}{2} \sum_{T_i\in\mathfrak{T}} \partial^- \|e_{s,h}^{n+1}\|_{T_i,0}^2 \\
&+\frac{|\underline{p'_{c,eq}}|\phi}{2} \sum_{T_i\in\mathfrak{T}} \frac{1}{\Delta t}\|e_{s,h}^{n+1} - e_{s,h}^{n}\|_{T_i,0}^2 + \phi\tau \sum_{T_i\in\mathfrak{T}} \|\partial^- e_{s,h}^{n+1}\|_{T_i,0}^2 \\
&\leq \frac{3\phi}{2\tau} \sum_{T_i\in\mathfrak{T}} \int_{T_i} \|e_{p_c}^{n+1}\|_{T_i,0}^2 + \frac{|\underline{p'_{c,eq}}|\phi}{4} \sum_{T_i\in\mathfrak{T}} \|e_{s,h}^{n+1}\|_{T_i,0}^2 + \frac{L_{p_c}^2\phi}{|\underline{p'_{c,eq}}|} \sum_{T_i\in\mathfrak{T}} \|e_{s}^{n+1}\|_{T_i,0}^2 \\
&+\frac{\tau\phi}{2}\Delta t \sum_{T_i\in\mathfrak{T}} \int_{t_n}^{t_{n+1}} \|\partial_{tt}\tilde{s}_w^{n+1}\|_{T_i,0}^2\, dt + \frac{3\tau\phi}{2} \sum_{T_i\in\mathfrak{T}} \|\partial_t e_s^{n+1}\|_{T_i,0}^2
\end{aligned} \tag{4.34}$$

Proof 5 We subtract (3.17) in Problem 3 from (3.13) in Problem 2, and use $\psi_{p_c} = \phi\partial^- e_{s,h}^{n+1}$ to get

$$\begin{aligned}
&\phi \sum_{T_i\in\mathfrak{T}} \int_{T_i} e_{p_c,h}^{n+1}\partial^- e_{s,h}^{n+1} + \phi \sum_{T_i\in\mathfrak{T}} \int_{T_i} e_{p_c}^{n+1}\partial^- e_{s,h}^{n+1} \\
&- \phi \sum_{T_i\in\mathfrak{T}} \int_{T_i} (p_{c,eq}(S_w^{n+1}) - p_{c,eq}(\tilde{s}_w^{n+1}) + p_{c,eq}(\tilde{s}_w^{n+1}) - p_{c,eq}(s_w))\partial^- e_{s,h}^{n+1} \\
&+ \phi \sum_{T_i\in\mathfrak{T}} \int_{T_i} \tau(\partial^- e_{s,h}^{n+1} + (\partial^- - \partial_t)\tilde{s}_w^{n+1} + \partial_t e_s^{n+1})\partial^- e_{s,h}^{n+1} \\
&= \phi \sum_{T_i\in\mathfrak{T}} \int_{T_i} e_{p_c,h}^{n+1}\partial^- e_{s,h}^{n+1} + Pc_1 + Pc_2 + Pc_3 \\
&= 0\,.
\end{aligned} \tag{4.35}$$

Estimate for Pc_1 We use Hölder's and Young's inequality to obtain

$$Pc_1 \leq \frac{\phi^2}{2\epsilon_{pc1}} \sum_{T_i\in\mathfrak{T}} \int_{T_i} \|e_{p_c}^{n+1}\|_{T_i,0}^2 + \frac{\epsilon_{pc1}}{2} \sum_{T_i\in\mathfrak{T}} \int_{T_i} \|\partial^- e_{s,h}^{n+1}\|_{T_i,0}^2 \tag{4.36}$$

Estimate for Pc_2

$$\begin{aligned}
Pc_2 = &- \phi \sum_{T_i\in\mathfrak{T}} \int_{T_i} (p_{c,eq}(S_w^{n+1}) - p_{c,eq}(\tilde{s}_w^{n+1}))\partial^- e_{s,h}^{n+1} \\
&- \phi \sum_{T_i\in\mathfrak{T}} \int_{T_i} (p_{c,eq}(\tilde{s}_w^{n+1}) - p_{c,eq}(s_w))\partial^- e_{s,h}^{n+1}
\end{aligned}$$

$$=Pc_{2,1} + Pc_{2,2}. \tag{4.37}$$

Here $Pc_{2,1}$ is estimated as

$$\begin{aligned} Pc_{2,1} =&\phi \sum_{T_i\in\mathcal{T}} \int_{T_i} |p'_{c,eq}(\xi)| e_{s,h}^{n+1}\partial^- e_{s,h}^{n+1} \geq \phi |\underline{p'_{c,eq}}| \sum_{T_i\in\mathcal{T}} \int_{T_i} e_{s,h}^{n+1}\partial^- e_{s,h}^{n+1} \\ =&\frac{|\underline{p'_{c,eq}}|\phi}{2} \sum_{T_i\in\mathcal{T}} \partial^- \|e_{s,h}^{n+1}\|_{T_i,0}^2 + \frac{|\underline{p'_{c,eq}}|\phi}{2} \sum_{T_i\in\mathcal{T}} \frac{1}{\Delta t}\|e_{s,h}^{n+1} - e_{s,h}^{n}\|_{T_i,0}^2. \end{aligned}$$

For $Pc_{2,2}$, using Young's Inequality and the Lipschitz continuity one has

$$Pc_{2,2} \leq \phi \sum_{T_i\in\mathcal{T}} \int_{T_i} L_{p_c} e_s^{n+1} e_{s,h}^{n+1} \leq \frac{\epsilon_{pc22}}{2} \sum_{T_i\in\mathcal{T}} \|e_{s,h}^{n+1}\|_{T_i,0}^2 + \frac{L_{p_c}^2\phi^2}{2\epsilon_{pc22}} \sum_{T_i\in\mathcal{T}} \|e_s^{n+1}\|_{T_i,0}^2$$

Estimate for Pc_3

$$\begin{aligned} Pc_3 =&\phi\tau \sum_{T_i\in\mathcal{T}} \|\partial^- e_{s,h}^{n+1}\|_{T_i,0}^2 + \phi\tau \sum_{T_i\in\mathcal{T}} \int_{T_i} (\partial^- - \partial_t)\tilde{s}_w^{n+1}\partial^- e_{s,h}^{n+1} \\ &+ \phi\tau \sum_{T_i\in\mathcal{T}} \int_{T_i} \partial_t e_s^{n+1}\partial^- e_{s,h}^{n+1} \\ =&Pc_{3,1} + Pc_{3,2} + Pc_{3,3} \end{aligned} \tag{4.38}$$

We approximate the consistency error in $Pc_{3,2}$ using a Taylor expansion

$$\frac{1}{\Delta t}(\tilde{s}_w^{n+1} - \tilde{s}_w^{n}) - \partial_t \tilde{s}_w^{n+1} = \frac{1}{\Delta t}\int_{t_n}^{t_{n+1}} (t - t_n)\partial_{tt}\tilde{s}_w^{n+1}\, dt\ ,$$

which leads to the following estimate for $Pc_{3,2}$

$$\begin{aligned} Pc_{3,2} \leq& \frac{\tau^2\phi^2}{2\epsilon_{pc32}} \sum_{T_i\in\mathcal{T}} \|(\partial^- - \partial_t)\tilde{s}_w^{n+1}\|_{T_i,0}^2 + \frac{\epsilon_{pc32}}{2} \sum_{T_i\in\mathcal{T}} \|\partial^- e_{s,h}^{n+1}\|_{T_i,0}^2 \\ \leq& \frac{\epsilon_{pc32}}{2} \sum_{T_i\in\mathcal{T}} \|\partial^- e_{s,h}^{n+1}\|_{T_i,0}^2 + \frac{\tau^2\phi^2}{6\epsilon_{pc32}}\Delta t \sum_{T_i\in\mathcal{T}} \int_{t_n}^{t_{n+1}} \|\partial_{tt}\tilde{s}_w^{n+1}\|_{T_i,0}^2\, dt\ . \end{aligned}$$

To estimate $Pc_{3,3}$, we use Young's inequality:

$$Pc_{3,3} \leq \frac{\epsilon_{pc33}}{2} \sum_{T_i\in\mathcal{T}} \|\partial^- e_{s,h}^{n+1}\|_{T_i,0}^2 + \frac{\tau^2\phi^2}{2\epsilon_{pc33}} \sum_{T_i\in\mathcal{T}} \|\partial_t e_s^{n+1}\|_{T_i,0}^2$$

Combined estimate We substitute the estimates (4.36), (4.37) and (4.38) into (4.35) to get

$$\phi \sum_{T_i\in\mathcal{T}} \int_{T_i} e_{p_c,h}^{n+1}\partial^- e_{s,h}^{n+1} + \frac{|\underline{p'_{c,eq}}|\phi}{2} \sum_{T_i\in\mathcal{T}} \partial^- \|e_{s,h}^{n+1}\|_{T_i,0}^2$$

$$
\begin{aligned}
&+\frac{|p'_{c,eq}|\phi}{2}\sum_{T_i\in\mathcal{T}}\frac{1}{\Delta t}\|e_{s,h}^{n+1}-e_{s,h}^{n}\|_{T_i,0}^2+\phi\tau\sum_{T_i\in\mathcal{T}}\|\partial^- e_{s,h}^{n+1}\|_{T_i,0}^2\\
&\leq\frac{\phi^2}{2\epsilon_{pc1}}\sum_{T_i\in\mathcal{T}}\int_{T_i}\|e_{p_c}^{n+1}\|_{T_i,0}^2+\frac{\epsilon_{pc1}}{2}\sum_{T_i\in\mathcal{T}}\int_{T_i}\|\partial^- e_{s,h}^{n+1}\|_{T_i,0}^2\\
&+\frac{\epsilon_{pc22}}{2}\sum_{T_i\in\mathcal{T}}\|e_{s,h}^{n+1}\|_{T_i,0}^2+\frac{L_{p_c}^2\phi^2}{2\epsilon_{pc22}}\sum_{T_i\in\mathcal{T}}\|e_{s}^{n+1}\|_{T_i,0}^2\\
&+\frac{\epsilon_{pc32}}{2}\sum_{T_i\in\mathcal{T}}\|\partial^- e_{s,h}^{n+1}\|_{T_i,0}^2+\frac{\tau^2\phi^2}{6\epsilon_{pc32}}\Delta t\sum_{T_i\in\mathcal{T}}\int_{t_n}^{t_{n+1}}\|\partial_{tt}\tilde{s}_w^{n+1}\|_{T_i,0}^2\,dt\\
&+\frac{\epsilon_{pc33}}{2}\sum_{T_i\in\mathcal{T}}\|\partial^- e_{s,h}^{n+1}\|_{T_i,0}^2+\frac{\tau^2\phi^2}{2\epsilon_{pc33}}\sum_{T_i\in\mathcal{T}}\|\partial_t e_{s}^{n+1}\|_{T_i,0}^2
\end{aligned}
$$

Setting $\epsilon_{pc1}=\epsilon_{pc32}=\epsilon_{pc33}=\dfrac{\phi\tau}{3}$ and, $\epsilon_{pc22}=\dfrac{|p'_{c,eq}|\phi}{2}$, we get the desired estimate.

4.3.4 Convergence result

We are now in a position to deduce the following theorem about the convergence of the scheme:

Theorem 1 For sufficiently large σ_n and σ_w, there exists a constant C independent of h and Δt, s.t., the following estimate holds:

$$
\begin{aligned}
&\sum_{T_i\in\mathcal{T}}\|e_{s,h}^{N+1}\|_{T_i,0}^2+\sum_{n=0}^{N}\sum_{T_i\in\mathcal{T}}\|e_{s,h}^{n+1}-e_{s,h}^{n}\|_{T_i,0}^2+\Delta t\sum_{n=0}^{N}\sum_{T_i\in\mathcal{T}}\|\partial^- e_{s,h}^{n+1}\|_{T_i,0}^2\\
&+\Delta t\sum_{n=0}^{N}\sum_{T_i\in\mathcal{T}}\left(\|\nabla e_{p_w,h}^{n+1}\|_{T_i,0}^2+\|\nabla e_{p_n,h}^{n+1}\|_{T_i,0}^2\right)\\
&+\Delta t\sum_{n=0}^{N}\sum_{F_i\in\mathcal{F}}\frac{f(k_p)}{|F_i|}\left(\|[\![e_{p_w,h}^{n+1}]\!]\|_{F_i,0}^2+\|[\![e_{p_n,h}^{n+1}]\!]\|_{F_i,0}^2\right)\\
&\leq C\sum_{T_i\in\mathcal{T}}\|e_{s,h}^{0}\|_{T_i,0}^2+C\frac{h^{2\min(k_s+1,l_s)}}{k_s^{2l_s-2}}\left(1+\frac{1}{k_s^2}\right)\Delta t\sum_{n=0}^{N}\|s_w(t)\|_{\Omega,l_s}^2+C\Delta t^2\\
&+C\frac{h^{2\min(k_s+1,l_s)}}{k_s^{2l_s}}\Delta t\sum_{n=0}^{N}\|\partial_t s_w(t)\|_{\Omega,l_s}^2\\
&+C\frac{h^{2\min(k_p+1,l_{p_n})-2}}{k_p^{2l_{p_n}-2}}\left(1+\frac{1}{k_p^2}+k_p^2\right)\Delta t\sum_{n=0}^{N}\|p_n(t)\|_{\Omega,l_{p_n}}^2\\
&+C\frac{h^{2\min(k_p+1,l_{p_c})-2}}{k_p^{2l_{p_c}-2}}\left(1+\frac{1}{k_p^2}+k_p^2\right)\Delta t\sum_{n=0}^{N}\|p_c(t)\|_{\Omega,l_{p_c}}^2
\end{aligned}
$$

Proof 6 We add the results of Lemma 7, 8, and 9, and rearrange them to get:

$$
\begin{aligned}
&\sum_{T_i\in\mathcal{T}}\int_{T_i}\left[-\partial^- S_w^{n+1}+\partial_t s_w\right]\phi e_{p_n,h}^{n+1}+\sum_{T_i\in\mathcal{T}}\int_{T_i}\left[\partial^- S_w^{n+1}-\partial_t s_w\right]\phi e_{p_w,h}^{n+1}\\
&+\phi\sum_{T_i\in\mathcal{T}}\int_{T_i} e_{p_c,h}^{n+1}\partial^- e_{s,h}^{n+1}+\frac{|\underline{p'_{c,eq}}|\phi}{2}\sum_{T_i\in\mathcal{T}}\partial^-\|e_{s,h}^{n+1}\|_{T_i,0}^2\\
&+\frac{|\underline{p'_{c,eq}}|\phi}{2}\sum_{T_i\in\mathcal{T}}\frac{1}{\Delta t}\|e_{s,h}^{n+1}-e_{s,h}^{n}\|_{T_i,0}^2+\phi\tau\sum_{T_i\in\mathcal{T}}\|\partial^- e_{s,h}^{n+1}\|_{T_i,0}^2\\
&+\sum_{T_i\in\mathcal{T}}\left(\|K^{\frac{1}{2}}\nabla e_{p_w,h}^{n+1}\|_{T_i,0}^2+\|K^{\frac{1}{2}}\nabla e_{p_n,h}^{n+1}\|_{T_i,0}^2\right)\\
&+\sum_{F_i\in\mathcal{F}}\frac{f(k_p)}{|F_i|}\left(\|[\![e_{p_w,h}^{n+1}]\!]\|_{F_i,0}^2+\|[\![e_{p_n,h}^{n+1}]\!]\|_{F_i,0}^2\right)\\
&\leq\frac{3\phi}{2\tau}\sum_{T_i\in\mathcal{T}}\int_{T_i}\|e_{p_c}^{n+1}\|_{T_i,0}^2+\frac{|\underline{p'_{c,eq}}|\phi}{4}\sum_{T_i\in\mathcal{T}}\|e_{s,h}^{n+1}\|_{T_i,0}^2+\frac{L_{p_c}^2\phi}{|\underline{p'_{c,eq}}|}\sum_{T_i\in\mathcal{T}}\|e_s^{n+1}\|_{T_i,0}^2\\
&+\frac{\tau\phi}{2}\Delta t\sum_{T_i\in\mathcal{T}}\int_{t_n}^{t_{n+1}}\|\partial_{tt}\tilde{s}_w^{n+1}\|_{T_i,0}^2\,dt+\frac{3\tau\phi}{2}\sum_{T_i\in\mathcal{T}}\|\partial_t e_s^{n+1}\|_{T_i,0}^2\\
&+\sum_{\alpha=w,n}\left[C\left(\frac{5}{2\underline{\lambda_\alpha}}+\frac{3f(k_s)}{2\sigma_\alpha f(k_p)}\right)\overline{\lambda'_\alpha}\|K^{\frac{1}{2}}\nabla\tilde{p}_\alpha^{n+1}\|_{\Omega,\infty}^2\right]\sum_{T_i\in\mathcal{T}}\|e_{s,h}^{n+1}\|_{T_i,0}^2\\
&+\sum_{\alpha=w,n}\Bigg[C\frac{5\overline{\lambda'_\alpha}}{2\underline{\lambda_\alpha}}\|K^{\frac{1}{2}}\nabla\tilde{p}_\alpha^{n+1}\|_{\Omega,\infty}^2\|e_s^{n+1}\|_{\Omega,0}^2+C\frac{5\overline{\lambda_\alpha}}{2\underline{\lambda_\alpha}}\sum_{T_i\in\mathcal{T}}\|K^{\frac{1}{2}}\nabla e_{p_\alpha}^{n+1}\|_{T_i,0}^2\\
&\qquad+\frac{3f(k_s)\overline{\lambda'_\alpha}\tilde{C}}{2\sigma_\alpha f(k_p)}\|K^{\frac{1}{2}}\nabla\tilde{p}_\alpha^{n+1}\|_{\Omega,\infty}(\|e_s^{n+1}\|_{\Omega,0}^2+h^2\|\nabla e_s^{n+1}\|_{\Omega,0}^2)\\
&\qquad+C\left(\frac{3\sigma_\alpha C_t^2\tilde{C}}{2}+\frac{5\theta^2\overline{\lambda_\alpha}^2C_t^2\tilde{C}}{\underline{\lambda_\alpha}}\right)(h^{-2}\|e_{p_\alpha}^{n+1}\|_{\Omega,0}^2+\|\nabla e_{p_\alpha}^{n+1}\|_{\Omega,0}^2)\\
&\qquad+C\frac{3\overline{\lambda_\alpha}^2C_t^2\tilde{C}}{2\sigma_\alpha}\left(\left\|K^{\frac{1}{2}}\nabla e_{p_\alpha}^{n+1}\right\|_{\Omega,0}^2+h^2\left\|K^{\frac{1}{2}}\nabla^2 e_{p_\alpha}^{n+1}\right\|_{\Omega,0}^2\right)\Bigg]
\end{aligned}
\tag{4.39}
$$

We combine the first three summation terms of (4.39) to get:

$$
\begin{aligned}
&\sum_{T_i\in\mathcal{T}}\int_{T_i}\left[-\partial^- S_w^{n+1}+\partial_t s_w\right]\phi e_{p_n,h}^{n+1}+\sum_{T_i\in\mathcal{T}}\int_{T_i}\left[\partial^- S_w^{n+1}-\partial_t s_w\right]\phi e_{p_w,h}^{n+1}\\
&+\phi\sum_{T_i\in\mathcal{T}}\int_{T_i} e_{p_c,h}^{n+1}\partial^- e_{s,h}^{n+1}\\
=&\sum_{T_i\in\mathcal{T}}\int_{T_i}\phi\left[\partial^- e_{s,h}^{n+1}+(\partial^- -\partial_t)\tilde{s}_w^{n+1}+\partial_t e_s^{n+1}\right](e_{p_n,h}^{n+1}-e_{p_c,h}^{n+1}-e_{p_n,h}^{n+1})
\end{aligned}
$$

$$
\begin{aligned}
&+ \phi \sum_{T_i \in \mathcal{T}} \int_{T_i} e_{p_c,h}^{n+1} \partial^- e_{s,h}^{n+1} \\
&= - \sum_{T_i \in \mathcal{T}} \int_{T_i} \phi (\partial^- - \partial_t) \tilde{s}_w^{n+1} e_{p_c,h}^{n+1} - \sum_{T_i \in \mathcal{T}} \int_{T_i} \phi \partial_t e_s^{n+1} e_{p_c,h}^{n+1} \\
&=: Ps_1 + Ps_2
\end{aligned}
$$

Estimate for Ps_1

$$
Ps_1 \leq \frac{\epsilon_{ps1}}{2} \sum_{T_i \in \mathcal{T}} \|e_{p_c,h}^{n+1}\|_{T_i,0}^2 + \frac{\phi^2}{6\epsilon_{ps1}} \Delta t \sum_{T_i \in \mathcal{T}} \int_{t_n}^{t_{n+1}} \|\partial_{tt} \tilde{s}_w^{n+1}\|_{T_i,0}^2 \, dt \ . \tag{4.40}
$$

Estimate for Ps_2

$$
Ps_2 \leq \frac{\epsilon_{ps2}}{2} \sum_{T_i \in \mathcal{T}} \|e_{p_c,h}^{n+1}\|_{T_i,0}^2 + \frac{\phi^2}{2\epsilon_{ps2}} \sum_{T_i \in \mathcal{T}} \|\partial_t e_s^{n+1}\|_{T_i,0}^2 \tag{4.41}
$$

To absorb the error $\|e_{p_c,h}^{n+1}\|_{T_i,0}^2$, we use the triangle inequality together with Lemma 1 to get the following estimate:

$$
\begin{aligned}
\sum_{T_i \in \mathcal{T}} \|e_{p_c,h}^{n+1}\|_{T_i,0}^2 \leq & \sum_{T_i \in \mathcal{T}} \|\nabla e_{p_n,h}^{n+1}\|_{T_i,0}^2 + \sum_{F_i \in \mathcal{F}} \frac{f(k_p)}{|F_i|} \|[\![e_{p_n,h}^{n+1}]\!]\|_{F_i,0}^2 \\
& + \sum_{T_i \in \mathcal{T}} \|\nabla e_{p_w,h}^{n+1}\|_{T_i,0}^2 + \sum_{F_i \in \mathcal{F}} \frac{f(k_p)}{|F_i|} \|[\![e_{p_w,h}^{n+1}]\!]\|_{F_i,0}^2 \ .
\end{aligned} \tag{4.42}
$$

After substituting the estimates (4.40) and (4.41) together with the estimate (4.42) into the estimate (4.39), and choosing $\epsilon_{ps1} = \epsilon_{ps2} = \dfrac{1}{2}$ we get:

$$
\begin{aligned}
& \frac{|\underline{p'_{c,eq}}|\phi}{2} \sum_{T_i \in \mathcal{T}} \partial^- \|e_{s,h}^{n+1}\|_{T_i,0}^2 + \frac{|\underline{p'_{c,eq}}|\phi}{2} \sum_{T_i \in \mathcal{T}} \frac{1}{\Delta t} \|e_{s,h}^{n+1} - e_{s,h}^n\|_{T_i,0}^2 \\
& + \frac{\phi\tau}{2} \sum_{T_i \in \mathcal{T}} \|\partial^- e_{s,h}^{n+1}\|_{T_i,0}^2 + \frac{1}{2} \sum_{T_i \in \mathcal{T}} \left(\|K^{\frac{1}{2}} \nabla e_{p_w,h}^{n+1}\|_{T_i,0}^2 + \|K^{\frac{1}{2}} \nabla e_{p_n,h}^{n+1}\|_{T_i,0}^2 \right) \\
& + \frac{1}{2} \sum_{F_i \in \mathcal{F}} \frac{f(k_p)}{|F_i|} \left(\|[\![e_{p_w,h}^{n+1}]\!]\|_{F_i,0}^2 + \|[\![e_{p_n,h}^{n+1}]\!]\|_{F_i,0}^2 \right) \\
& \leq \sum_{\alpha = w,n} \left[C \left(\frac{5}{2\underline{\lambda_\alpha}} + \frac{3f(k_s)}{2\sigma_\alpha f(k_p)} \right) \overline{\lambda'_\alpha} \|K^{\frac{1}{2}} \nabla \tilde{p}_\alpha^{n+1}\|_{\Omega,\infty}^2 + \frac{|\underline{p'_{c,eq}}|\phi}{4} \right] \sum_{T_i \in \mathcal{T}} \|e_{s,h}^{n+1}\|_{T_i,0}^2 \\
& + \frac{L_{p_c}^2 \phi}{|\underline{p'_{c,eq}}|} \|e_s^{n+1}\|_{\Omega,0}^2 + \frac{3\phi}{2\tau} \|e_{p_c}^{n+1}\|_{\Omega,0}^2 + \left(\frac{3\tau\phi}{2} + \phi^2 \right) \|\partial_t e_s^{n+1}\|_{\Omega,0}^2 \\
& + \left(\frac{\tau\phi}{2} + \frac{\phi^2}{3} \right) \Delta t \int_{t_n}^{t_{n+1}} \|\partial_{tt} \tilde{s}_w^{n+1}\|_{\Omega,0}^2 \, dt
\end{aligned}
$$

$$
\begin{aligned}
&+\sum_{\alpha=w,n}\Bigg[C\frac{\overline{\lambda'_\alpha}5}{2\underline{\lambda_\alpha}}\|K^{\frac{1}{2}}\nabla\tilde{p}_\alpha^{n+1}\|^2_{\Omega,\infty}\|e_s^{n+1}\|^2_{\Omega,0}+C\frac{5\overline{\lambda_\alpha}}{2\underline{\lambda_\alpha}}\|K^{\frac{1}{2}}\nabla e_{p_\alpha}^{n+1}\|^2_{\Omega,0}\\
&\qquad+\frac{3f(k_s)\overline{\lambda'_\alpha}\tilde{C}}{2\sigma_\alpha f(k_p)}\|K^{\frac{1}{2}}\nabla\tilde{p}_\alpha^{n+1}\|_{\Omega,\infty}(\|e_s^{n+1}\|^2_{\Omega,0}+h^2\|\nabla e_s^{n+1}\|^2_{\Omega,0})\\
&\qquad+C\left(\frac{3\sigma_\alpha C_t^2\tilde{C}}{2}+C\frac{5\theta^2\overline{\lambda_\alpha}^2C_t^2\tilde{C}}{\underline{\lambda_\alpha}}\right)(h^{-2}\|e_{p_\alpha}^{n+1}\|^2_{\Omega,0}+\|\nabla e_{p_\alpha}^{n+1}\|^2_{\Omega,0})\\
&\qquad+C\overline{\lambda_\alpha}^2C_t^2\tilde{C}\frac{3}{2\sigma_\alpha}\left(\left\|K^{\frac{1}{2}}\nabla e_{p_\alpha}^{n+1}\right\|^2_{\Omega,0}+h^2\left\|K^{\frac{1}{2}}\nabla^2 e_{p_\alpha}^{n+1}\right\|^2_{\Omega,0}\right)\Bigg]
\end{aligned}
\tag{4.43}
$$

Using a generic constant C, we rewrite (4.43) as:

$$
\begin{aligned}
&\frac{|\underline{p'_{c,eq}}|\phi}{2}\sum_{T_i\in\mathcal{T}}\partial^-\|e_{s,h}^{n+1}\|^2_{T_i,0}+\frac{|\underline{p'_{c,eq}}|\phi}{2}\sum_{T_i\in\mathcal{T}}\frac{1}{\Delta t}\|e_{s,h}^{n+1}-e_{s,h}^{n}\|^2_{T_i,0}\\
&+\frac{\phi\tau}{2}\sum_{T_i\in\mathcal{T}}\|\partial^-e_{s,h}^{n+1}\|^2_{T_i,0}+\frac{1}{2}\sum_{T_i\in\mathcal{T}}\left(\|K^{\frac{1}{2}}\nabla e_{p_w,h}^{n+1}\|^2_{T_i,0}+\|K^{\frac{1}{2}}\nabla e_{p_n,h}^{n+1}\|^2_{T_i,0}\right)\\
&+\frac{1}{2}\sum_{F_i\in\mathcal{F}}\frac{f(k_p)}{|F_i|}\left(\|[\![e_{p_w,h}^{n+1}]\!]\|^2_{F_i,0}+\|[\![e_{p_n,h}^{n+1}]\!]\|^2_{F_i,0}\right)\\
&\le\left(C+\frac{|\underline{p'_{c,eq}}|\phi}{4}\right)\sum_{T_i\in\mathcal{T}}C\|e_{s,h}^{n+1}\|^2_{T_i,0}+C\|e_s^{n+1}\|^2_{\Omega,0}+C\|e_{p_c}^{n+1}\|^2_{\Omega,0}\\
&+C\Delta t\int_{t_n}^{t_{n+1}}\|\partial_{tt}\tilde{s}_w^{n+1}\|^2_{\Omega,0}\,dt+C\|\partial_t e_s^{n+1}\|^2_{\Omega,0}+Ch^2\|\nabla e_s^{n+1}\|^2_{\Omega,0}\\
&+\sum_{\alpha=w,n}\left[C\|\nabla e_{p_\alpha}^{n+1}\|^2_{\Omega,0}+Ch^{-2}\|e_{p_\alpha}^{n+1}\|^2_{\Omega,0}+Ch^2\left\|\nabla^2 e_{p_\alpha}^{n+1}\right\|^2_{\Omega,0}\right]
\end{aligned}
$$

Multiplying the above inequality by Δt, summing over $n=0,\dots,N$, and absorbing $\|e_{s,h}^{N+1}\|^2_{\Omega,0}$, we get:

$$
\begin{aligned}
&\left(\frac{|\underline{p'_{c,eq}}|\phi}{2}-C\Delta t\right)\sum_{T_i\in\mathcal{T}}\|e_{s,h}^{N+1}\|^2_{T_i,0}+\frac{|\underline{p'_{c,eq}}|\phi}{2}\sum_{n=0}^{N}\sum_{T_i\in\mathcal{T}}\|e_{s,h}^{n+1}-e_{s,h}^{n}\|^2_{T_i,0}\\
&+\frac{\Delta t}{2}\sum_{n=0}^{N}\sum_{F_i\in\mathcal{F}}\frac{f(k_p)}{|F_i|}\left(\|[\![e_{p_w,h}^{n+1}]\!]\|^2_{F_i,0}+\|[\![e_{p_n,h}^{n+1}]\!]\|^2_{F_i,0}\right)\\
&+\frac{\Delta t}{2}\sum_{n=0}^{N}\sum_{T_i\in\mathcal{T}}\left(\|K^{\frac{1}{2}}\nabla e_{p_w,h}^{n+1}\|^2_{T_i,0}+\|K^{\frac{1}{2}}\nabla e_{p_n,h}^{n+1}\|^2_{T_i,0}\right)\\
&+\frac{\phi\tau}{2}\Delta t\sum_{n=0}^{N}\sum_{T_i\in\mathcal{T}}\|\partial^-e_{s,h}^{n+1}\|^2_{T_i,0}\\
&\le\frac{|\underline{p'_{c,eq}}|\phi}{2}\sum_{T_i\in\mathcal{T}}\|e_{s,h}^{0}\|^2_{T_i,0}+\left(C+\frac{|\underline{p'_{c,eq}}|\phi}{4}\right)\Delta t\sum_{n=0}^{N-1}\sum_{T_i\in\mathcal{T}}C\|e_{s,h}^{n+1}\|^2_{T_i,0}
\end{aligned}
$$

$$+C\Delta t\sum_{n=0}^{N}\|e_s^{n+1}\|_{\Omega,0}^2+C\Delta t\sum_{n=0}^{N}\|e_{p_c}^{n+1}\|_{\Omega,0}^2+C\Delta t\sum_{n=0}^{N}\|\partial_t e_s^{n+1}\|_{\Omega,0}^2$$
$$+C\Delta t^2\int_0^T\|\partial_{tt}\tilde{s}_w^{n+1}\|_{\Omega,0}^2\,dt+Ch^2\Delta t\sum_{n=0}^{N}\|\nabla e_s^{n+1}\|_{\Omega,0}^2$$
$$+\sum_{\alpha=w,n}\Delta t\left[C\sum_{n=0}^{N}\|\nabla e_{p_\alpha}^{n+1}\|_{\Omega,0}^2+Ch^{-2}\sum_{n=0}^{N}\|e_{p_\alpha}^{n+1}\|_{\Omega,0}^2+Ch^2\sum_{n=0}^{N}\left\|\nabla^2 e_{p_\alpha}^{n+1}\right\|_{\Omega,0}^2\right]$$

For a sufficiently small Δt, we use Grönwall's inequality, and postulate that there exists a constant independent of Δt, h, $k_p$or k_s, s.t.:

$$\left(\frac{|p'_{c,eq}|\phi}{2}-C\Delta t\right)\sum_{T_i\in\mathcal{T}}\|e_{s,h}^{N+1}\|_{T_i,0}^2+\frac{|p'_{c,eq}|\phi}{2}\sum_{n=0}^{N}\sum_{T_i\in\mathcal{T}}\|e_{s,h}^{n+1}-e_{s,h}^{n}\|_{T_i,0}^2$$
$$+\frac{\Delta t}{2}\sum_{n=0}^{N}\sum_{T_i\in\mathcal{T}}\left(\|K^{\frac{1}{2}}\nabla e_{p_w,h}^{n+1}\|_{T_i,0}^2+\|K^{\frac{1}{2}}\nabla e_{p_n,h}^{n+1}\|_{T_i,0}^2\right)$$
$$+\frac{\Delta t}{2}\sum_{n=0}^{N}\sum_{F_i\in\mathcal{F}}\frac{f(k_p)}{|F_i|}\left(\|[\![e_{p_w,h}^{n+1}]\!]\|_{F_i,0}^2+\|[\![e_{p_n,h}^{n+1}]\!]\|_{F_i,0}^2\right)$$
$$+\frac{\phi\tau}{2}\Delta t\sum_{n=0}^{N}\sum_{T_i\in\mathcal{T}}\|\partial^- e_{s,h}^{n+1}\|_{T_i,0}^2$$
$$\leq\frac{|p'_{c,eq}|\phi}{2}\sum_{T_i\in\mathcal{T}}\|e_{s,h}^{0}\|_{T_i,0}^2+C\Delta t\sum_{n=0}^{N}\|e_s^{n+1}\|_{\Omega,0}^2+C\Delta t\sum_{n=0}^{N}\|e_{p_c}^{n+1}\|_{\Omega,0}^2$$
$$+C\Delta t^2\int_0^T\|\partial_{tt}\tilde{s}_w^{n+1}\|_{\Omega,0}^2\,dt+C\Delta t\sum_{n=0}^{N}\|\partial_t e_s^{n+1}\|_{\Omega,0}^2+Ch^2\Delta t\sum_{n=0}^{N}\|\nabla e_s^{n+1}\|_{\Omega,0}^2$$
$$+C\Delta t\sum_{n=0}^{N}\|\nabla e_{p_n}^{n+1}\|_{\Omega,0}^2+Ch^{-2}\Delta t\sum_{n=0}^{N}\|e_{p_n}^{n+1}\|_{\Omega,0}^2+Ch^2\Delta t\sum_{n=0}^{N}\left\|\nabla^2 e_{p_n}^{n+1}\right\|_{\Omega,0}^2$$
$$+C\Delta t\sum_{n=0}^{N}\|\nabla e_{p_w}^{n+1}\|_{\Omega,0}^2+Ch^{-2}\Delta t\sum_{n=0}^{N}\|e_{p_w}^{n+1}\|_{\Omega,0}^2+Ch^2\Delta t\sum_{n=0}^{N}\left\|\nabla^2 e_{p_w}^{n+1}\right\|_{\Omega,0}^2$$

Using the error estimates (4.2), (4.3) and (4.4), and the triangle inequality for the error terms in $p_w=p_n-p_c$, we can write:

$$\left(\frac{|p'_{c,eq}|\phi}{2}-C\Delta t\right)\sum_{T_i\in\mathcal{T}}\|e_{s,h}^{N+1}\|_{T_i,0}^2+\frac{|p'_{c,eq}|\phi}{2}\sum_{n=0}^{N}\sum_{T_i\in\mathcal{T}}\|e_{s,h}^{n+1}-e_{s,h}^{n}\|_{T_i,0}^2$$
$$+\frac{\Delta t}{2}\sum_{n=0}^{N}\sum_{T_i\in\mathcal{T}}\left(\|K^{\frac{1}{2}}\nabla e_{p_w,h}^{n+1}\|_{T_i,0}^2+\|K^{\frac{1}{2}}\nabla e_{p_n,h}^{n+1}\|_{T_i,0}^2\right)$$
$$+\frac{\Delta t}{2}\sum_{n=0}^{N}\sum_{F_i\in\mathcal{F}}\frac{f(k_p)}{|F_i|}\left(\|[\![e_{p_w,h}^{n+1}]\!]\|_{F_i,0}^2+\|[\![e_{p_n,h}^{n+1}]\!]\|_{F_i,0}^2\right)$$

$$
\begin{aligned}
&+\frac{\phi\tau}{2}\Delta t\sum_{n=0}^{N}\sum_{T_i\in\mathcal{T}}\|\partial^- e_{s,h}^{n+1}\|_{T_i,0}^2\\
&\leq C\sum_{T_i\in\mathcal{T}}\|e_{s,h}^0\|_{T_i,0}^2+C\Delta t\sum_{n=0}^{N}\frac{h^{2\min(k_s+1,l_s)}}{k_s^{2l_s}}\|s_w(t)\|_{\Omega,l_s}^2+C\Delta t^2\\
&+C\Delta t\sum_{n=0}^{N}\frac{h^{2\min(k_s+1,l_s)}}{k_s^{2l_s}}\|\partial_t s_w(t)\|_{\Omega,l_s}^2+Ch^2\Delta t\sum_{n=0}^{N}\frac{h^{2\min(k_s+1,l_s)-2}}{k_s^{2l_s-2}}\|s_w(t)\|_{\Omega,l_s}^2\\
&+C\Delta t\sum_{n=0}^{N}\frac{h^{2\min(k_p+1,l_{p_n})-2}}{k_p^{2l_{p_n}-2}}\|p_n(t)\|_{\Omega,l_{p_n}}^2+Ch^{-2}\Delta t\sum_{n=0}^{N}\frac{h^{2\min(k_p+1,l_{p_n})}}{k_p^{2l_{p_n}}}\|p_n(t)\|_{\Omega,l_{p_n}}^2\\
&+Ch^2\Delta t\sum_{n=0}^{N}\frac{h^{2\min(k_p+1,l_{p_n})-4}}{k_p^{2l_{p_n}-4}}\|p_n(t)\|_{\Omega,l_{p_n}}^2+C\Delta t\sum_{n=0}^{N}\frac{h^{2\min(k_p+1,l_{p_c})-2}}{k_p^{2l_{p_c}-2}}\|p_c(t)\|_{\Omega,l_{p_c}}^2\\
&+Ch^{-2}\Delta t\sum_{n=0}^{N}\frac{h^{2\min(k_p+1,l_{p_c})}}{k_p^{2l_{p_c}}}\|p_c(t)\|_{\Omega,l_{p_c}}^2+Ch^2\Delta t\sum_{n=0}^{N}\frac{h^{2\min(k_p+1,l_{p_c})-4}}{k_p^{2l_{p_c}-4}}\|p_c(t)\|_{\Omega,l_{p_c}}^2
\end{aligned}
$$

from where, the stated estimate follows.

From the Theorem we can directly deduce the following Corollary:

Corollary 1 For sufficiently smooth solutions $p_n \in L^2(0,T;H^{k_p+1}(\Omega))$, $p_c \in L^2(0,T;H^{k_p+1}(\Omega))$ and $s_w \in H^2(0,T;H^{k_s+1}(\Omega))$ and sufficiently large σ_n and σ_w, there exists a constant C independent of h and Δt, s.t., the following estimate holds:

$$
\begin{aligned}
&\|e_{s,h}^{N+1}\|_{\Omega,0}^2+\Delta t\sum_{n=0}^{N}\|\partial^- e_{s,h}^{n+1}\|_{\Omega,0}^2+\Delta t\sum_{n=0}^{N}\left(\|e_{p_c,h}^{n+1}\|_{\Omega,DG}^2+\|e_{p_n,h}^{n+1}\|_{\Omega,DG}^2\right)\\
&\leq C\Delta t^2+C\frac{h^{2k_s}}{k_s^{2k_s}}+C\frac{h^{2k_p}}{k_p^{2k_p-2}}
\end{aligned}
$$

4.4 Numerical Experiments

In this section, we verify the convergence rates derived in Theorem 1 through numerical experiments. We consider an analytical solution to compute the L^2- and H^1-errors. We show the h and Δt dependence through successive refinement of the spatial mesh, respectively of the time step.

Problem definition We consider the domain $\Omega = (0,1)\times(0,1)\subset\mathbb{R}^2$ and $t\in[0,1]$. The properties of the phases and the porous medium are listed in Table 4.1.

Table 4.1: Properties for Test problem 1

Phase Properties		
wetting phase dynamic viscosity	$\mu_w \left[\frac{kg}{ms}\right]$	1
non-wetting phase dynamic viscosity	$\mu_n \left[\frac{kg}{ms}\right]$	1
wetting phase density	$\rho_w \left[\frac{kg}{m^3}\right]$	1
non-wetting phase density	$\rho_n \left[\frac{kg}{m^3}\right]$	1
Hydraulic Properties		
absolute permeability	$K \ [m^2]$	1
residual wetting phase saturation	S_{rw}	0
residual non-wetting phase saturation	S_{rn}	0
porosity	φ	0.4
damping coefficient	$\tau \ [Pa \cdot s]$	1
Brooks-Correy Parameters		
entry pressure	$p_d \ [Pa]$	1
pore size distribution index	λ	2

The right hand side in the equations are chosen such that the exact solution for $t \geq 0$ equals:

$$
\begin{aligned}
p_n(t,x,y) &= \frac{1}{4}\cos((x+y)\pi - t) + \frac{1}{2} \\
s_w(t,x,y) &= \frac{1}{4}\sin((x+y)\pi - t) + \frac{1}{2} \\
p_c(t,x,y) &= p_{c,eq}(s_w(t,x,y)) - \tau\partial_t s_w(t,x,y)
\end{aligned}
$$

Implementation We chose $\theta = 1$, which gives a NIP dG-scheme, and the penalty parameters as $\sigma_w = \sigma_n = 10$. We implement the numerical scheme in the C++ based DUNE-PDELab framework [Bastian et al., 2007, 2010, 2011]. For linearization, we use the Newton-Raphson scheme with a line-search strategy [Deuflhard, 2004]. We solve the resulting linear system with SuperLU solver [Demmel et al., September 1999].

Simulation To show the spatial convergence rates, we consider two cases: Case 1 with polynomials of order 1, and Case 2 with polynomials of order 2. We make five simulations each with the following mesh and time step refinements:

		p-order=1	p-order=2
	no. of elements	time step size	time step size
Run-1:	2×2	$\Delta t = 1$	$\Delta t = 1$,
Run-2:	4×4	$\Delta t = 1/2$	$\Delta t = 1/4$,
Run-3:	8×8	$\Delta t = 1/4$	$\Delta t = 1/16$,
Run-4:	16×16	$\Delta t = 1/8$	$\Delta t = 1/64$,
Run-5:	32×32	$\Delta t = 1/16$	$\Delta t = 1/256$.

In Case 1, a linear convergence rate is expected. In Case 2, we use quadratic polynomials, and let the time step size Δt depend quadratically on the size of the elements h. This prevents the errors due to the time discretization from becoming dominating and thus affecting the convergence rates. Here, we expect a quadratic convergence rate.

In case 3, to show the time convergence rates, we make five simulations with polynomial order 2 and the following mesh and time step refinements:

		p-order=2
	no. of elements	time step size
Run-1:	2×2	$\Delta t = 1$,
Run-2:	4×4	$\Delta t = 1/2$,
Run-3:	8×8	$\Delta t = 1/4$,
Run-4:	16×16	$\Delta t = 1/8$,
Run-5:	32×32	$\Delta t = 1/16$.

In this case, the time steps are chosen such that the error due to time discretization is ultimately dominating.

Results The solution of the problem at time $t = 1$ and with a refinement of 32×32 is shown in Figures 4.1a, 4.1b and 4.1c.

In Figure 4.2, we show the spatial convergence rates for the test problem. Figures 4.2a and 4.2b show the calculated error for piecewise linear polynomials for the non-wetting pressure p_n, capillary pressure p_c, and wetting saturation s_w. Figures 4.2c and 4.2d show the calculated error for piecewise quadratic polynomials for p_n, p_c, and s_w. In Figure 4.3, we show the temporal convergence rates for the test problem, with piecewise quadratic polynomials for p_n, p_c, and s_w.

Observe the agreement with the theoretical convergence rates obtained in Theorem 1. For Case 1, we observe a linear convergence order, and for Case 2 a quadratic convergence order. In Case 3 we see a linear convergence order due to the time discretization. The expected convergence rates for each of the cases are plotted in green for reference in Figures 4.2 and 4.3.

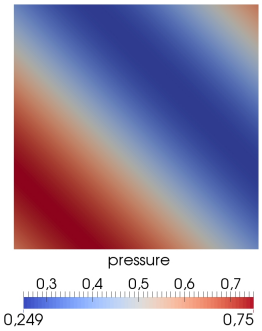

(a) p_n

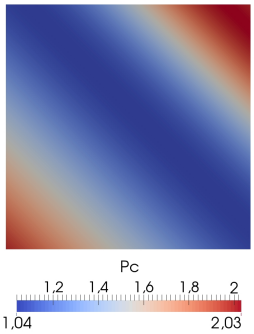

(b) p_c

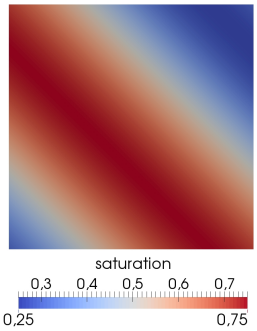

(c) s_w

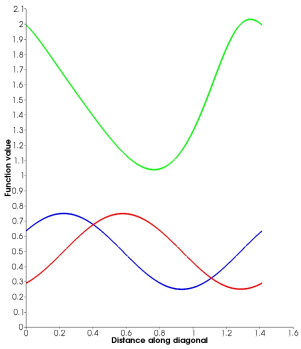

(d) Plot over the diagonal $Y = X$,
legend: s_w,p_n and p_c

Figure 4.1: Simulation results at $t = 1$.

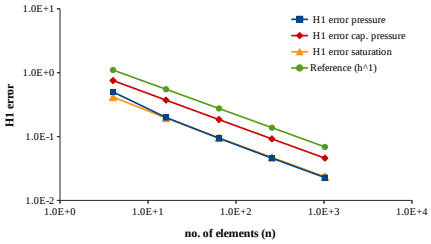

(a) H^1 error for piecewise linear polynomials

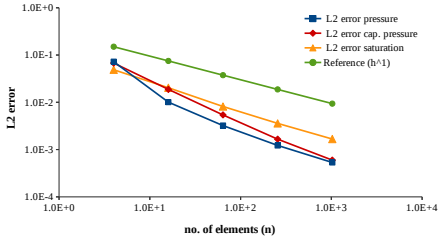

(b) L^2 error for piecewise linear polynomials

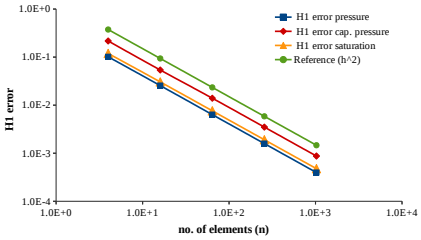

(c) H^1 error for piecewise quadratic polynomials

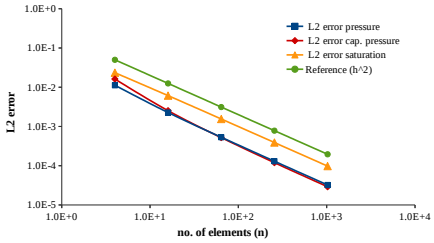

(d) L^2 error for piecewise quadratic polynomials

Figure 4.2: hp-convergence rates.

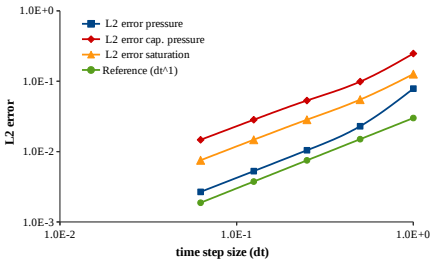

Figure 4.3: Temporal convergence rates
L^2 error for piecewise quadratic polynomials.

Chapter 5

Linearization scheme

The non-linearities in Problem 4 can be resolved in different ways. The basic idea is to approximate the nonlinearities such, that a linear problem remains to solve. The L-scheme is an alternative linearization method similar to a fixed point iteration.

The main trait of the scheme is, that an additional term involving the scaling parameter "L" is used, to enhance the convergence properties. The parameter L represents a generalized approximation of the first derivative with respect to the unknown nonlinear variables, which is used in a Newton method. The choice of this parameter is restricted with respect to the non-linearity, which come from the convergence analysis of the scheme [Karpinski et al., 2017]:

$$L_s \geq \sup_s \frac{dp_{c,eq}(s)}{ds}, \tag{5.1}$$

$$L_{s,T} \geq \sup_s \frac{dT(s)}{ds} \tag{5.2}$$

The main benefit of the scheme is, that contrary to the Newton method, only a mild restriction on the timestep-size independent of the spatial discretization is imposed [Karpinski et al., 2017; Radu et al., 2015b].

Assumptions We base the linearization scheme on the following assumptions:

(A5.1) For the initial and boundary data one has $s^0 \in H^1(\Omega)$, $p_n^D(x) \in H^{\frac{1}{2}}(\Gamma)$ and a function $s^D(x) \in H^{\frac{1}{2}}(\Gamma)$ exists s.t. $p_c^D(x) = p_{c,eq}(s^D(x))$. Further, the initial and boundary conditions are compatible.

(A5.2) The permeability matrix $K \in \mathbb{R}^{d\times d}$ is symmetric and positive definite, i.e. there exist two constants $\overline{\kappa}$ and $\underline{\kappa}$, s.t., for any vector $x \in \mathbb{R}^d$, the following holds:

$$\underline{\kappa}\|x\|^2 \leq x^T K x \leq \overline{\kappa}\|x\|^2$$

(A5.3) The equilibrium capillary pressure function $p_{c,eq}(\cdot)$ is in $C^2(\mathbb{R})$, and is assumed positive, bounded and decreasing. Further we assume that there exist $L_{p_{c,eq}}, l_{p_{c,eq}} > 0$ such that for all $S \in \mathbb{R}$ it holds

$$0 < l_{p_{c,eq}} \leq \left|p'_{c,eq}(\cdot)\right| \leq L_{p_{c,eq}} < \infty. \tag{5.3}$$

(A5.4) The functions $\lambda_w(\cdot)$ and $\lambda_n(\cdot)$ are Lipschitz-continuous and two constants $\overline{\lambda_\alpha}, \underline{\lambda_\alpha} > 0$ exist such that for all $S \in \mathbb{R}$,

$$0 < \underline{\lambda_\alpha} < \lambda_\alpha(S) < \overline{\lambda_\alpha} < \infty, \qquad (\alpha \in \{w, n\}). \tag{5.4}$$

(A5.5) The dynamic capillary pressure function $\tau(\cdot)$ is in $C^2(\mathbb{R})$, positive, bounded, and decreasing. Letting $T(\cdot)$ denote its primitive, we assume that there exist $L_T, l_T > 0$ such that for all $S \in \mathbb{R}$ one has

$$0 < l_T \leq \tau(S) \leq L_T < \infty. \tag{5.5}$$

To develop the linearization scheme for the nonlinear Problem 3, we start with the discretization in time (3.14) to obtain a sequence of time-discrete problems ($n = 0, \ldots, N-1$):

Problem 5 [**Time discrete problem**] Given s_w^n, p_n^n and p_c^n, find s_w^{n+1}, p_n^{n+1} and p_c^{n+1}, s.t., the following holds:

$$\begin{aligned}
&\frac{s_w^{n+1} - s_w^n}{\Delta t}\phi + \nabla \cdot \left(\lambda_n(s_w^{n+1}) K \nabla (p_n^{n+1} - gz\rho_n)\right) = 0 \\
&\frac{s_w^{n+1} - s_w^n}{\Delta t}\phi + \nabla \cdot \left(\lambda_w(s_w^{n+1}) K \nabla (p_n^{n+1} - p_c^{n+1} - gz\rho_w)\right) = 0 \\
&p_c^{n+1} = p_{c,eq}(s_w^{n+1}) - \frac{T(s_w^{n+1}) - T(s_w^n)}{\Delta t}
\end{aligned}$$

Observe that, at each time step, this results into a nonlinear problem. For solving it we propose an iteration scheme that builds on the ideas in [List and Radu, 2016; Pop et al., 2004; Radu et al., 2015a,b; Slodička, 2002, 2005a,b; Yong and Pop, 1996] (the "L"-scheme). The idea is to construct a sequence of triplets $(s_w^{n+1,i-1}, p_n^{n+1,i-1}, p_c^{n+1,i-1})$ converging as $i \to \infty$ to the solution $(s_w^{n+1}, p_n^{n+1}, p_c^{n+1})$ of Problem 5. Recalling Assumptions (A5.3) and (A5.5), we let $L_s, L_{s,T} > 0$ be two positive constants satisfying

$$L_s \geq L_{p_{c,eq}} \quad \text{and} \quad L_{s,T} \geq L_T \tag{5.6}$$

and define the following linearization scheme:

Problem 6 [**Linearization scheme**] Let $i > 0$ and $s_w^{n+1,i-1}$, $p_n^{n+1,i-1}$, $p_c^{n+1,i-1}$ be given.

Find $s_w^{n+1,i}$, $p_n^{n+1,i}$, and $p_c^{n+1,i}$ such that

$$
\begin{aligned}
&-\frac{s_w^{n+1,i}-s_w^n}{\Delta t}\phi+\nabla\cdot\left(\lambda_n(s_w^{n+1,i-1})K\nabla(p_n^{n+1,i}-gz\rho_n)\right)=0\\
&\frac{s_w^{n+1,i}-s_w^n}{\Delta t}\phi+\nabla\cdot\left(\lambda_w(s_w^{n+1,i-1})K\nabla(p_n^{n+1,i}-p_c^{n+1,i}-gz\rho_w)\right)=0\\
&p_c^{n+1,i}-p_{c,eq}(s_w^{n+1,i-1})+\frac{T(s_w^{n+1,i-1})-T(s_w^n)}{\Delta t}\\
&+L_s(s_w^{n+1,i}-s_w^{n+1,i-1})+L_{s,T}\left(\frac{s_w^{n+1,i}-s_w^{n+1,i-1}}{\Delta t}\right)=0
\end{aligned}
$$

Remark 3 Observe that the first two equations are nothing but the semi-implicit discretization of the corresponding in Problem 5, whereas the third equation includes two additional terms involving the parameters L_s and $L_{s,T}$. Formally one can see that if the scheme is convergent, these terms are vanishing and the limit solves the nonlinear time discrete problem. In [Karpinski et al., 2017] it is proven that the scheme converges indeed, and that this convergence holds for any initial guess. However, since this is an evolution problem, it is natural to use the solution at the previous time step at starting point, i.e. $s_w^{n+1,0}=s_w^n$, $p_n^{n+1,0}=p_n^n$, and $p_c^{n+1,0}=p_c^n$.

5.1 Discrete system

Starting from Problem 6 and with the parameters $L_s, L_{s,T}$ satisfying (5.6), the fully discrete linearized scheme becomes

Problem 7 [Fully discrete linearization scheme] Let $P_n^n\in V_h^p(\Omega)$, $P_c^n\in V_h^p(\Omega)$, and $S_w^n\in V_h^s(\Omega)$. Given $P_n^{n+1,i-1}\in V_h^p(\Omega)$, $P_c^{n+1,i-1}\in V_h^p(\Omega)$, and $S_w^{n+1,i-1}\in V_h^s(\Omega)$ with $P_n^{n+1,0}=P_n^n$, $P_c^{n+1,0}=P_c^n$, and $S_w^{n+1,0}=S_w^n$, find $P_n^{n+1,i}\in V_h^p(\Omega)$, $P_c^{n+1,i}\in V_h^p(\Omega)$, and $S_w^{n+1,i}\in V_h^s(\Omega)$, s.t., for all $\psi_s\in V_h^s(\Omega)$, $\psi_n\in V_h^p(\Omega)$, and $\psi_w\in V_h^p(\Omega)$, the following holds:

$$
\begin{aligned}
\textbf{PDE-1}:\ &-\sum_{T_r\in\mathcal{T}}\int_{T_r}\partial^- S_w^{n+1,i}\phi\psi_n+\sum_{T_r\in\mathcal{T}}\int_{T_r}\lambda_n(S_w^{n+1,i-1})K\nabla\left(P_n^{n+1,i}-gz\rho_n\right)\nabla\psi_n\\
&-\sum_{F_r\in\mathcal{F}}\int_{F_r}\{\lambda_n(S_w^{n+1,i-1})K\nabla\left(P_n^{n+1,i}-gz\rho_n\right)\cdot\vec{n}\}[\![\psi_n]\!]\\
&+\theta\sum_{F_r\in\mathcal{F}}\int_{F_r}[\![P_n^{n+1,i}]\!]\{\lambda_n(S_w^{n+1,i-1})K\nabla\psi_n\cdot\vec{n}\}\\
&+\sigma_n\sum_{F_r\in\mathcal{F}}\int_{F_r}\frac{f(k_p)}{|F_r|}[\![P_n^{n+1,i}]\!][\![\psi_n]\!]\\
&=\theta\sum_{F_r\in\Gamma}\int_{F_r}[\![p_n^D]\!]\{\lambda_n(s^D)K\nabla\psi_n\cdot\vec{n}\}+\sigma_n\sum_{F_r\in\Gamma}\int_{F_r}\frac{f(k_p)}{|F_r|}[\![p_n^D]\!][\![\psi_n]\!]
\end{aligned}
\tag{5.7}
$$

$$
\textbf{PDE-2}:\ \sum_{T_r\in\mathcal{T}}\int_{T_r}\partial^- S_w^{n+1,i}\phi\psi_w+\sum_{T_r\in\mathcal{T}}\int_{T_r}\lambda_w(S_w^{n+1,i-1})K\nabla\left(P_w^{n+1,i}-gz\rho_w\right)\nabla\psi_w
$$

$$
\begin{aligned}
&- \sum_{F_r \in \mathcal{F}} \int_{F_r} \{\lambda_w(S_w^{n+1,i-1}) K \nabla \left(P_w^{n+1,i} - gz\rho_w\right) \cdot \vec{n}\} [\![\psi_w]\!] \\
&+ \theta \sum_{F_r \in \mathcal{F}} \int_{F_r} \{\lambda_w(S_w^{n+1,i-1}) K \nabla \psi_w \cdot \vec{n}\} [\![P_w^{n+1,i}]\!] \\
&+ \sigma_w \sum_{F_r \in \mathcal{F}} \int_{F_r} \frac{f(k_p)}{|F_r|} [\![P_w^{n+1,i}]\!] [\![\psi_w]\!] \\
&= \theta \sum_{F_r \in \Gamma} \int_{F_r} \{\lambda_w(s^D) K \nabla \psi_w \cdot \vec{n}\} [\![p_n^D - p_c^D]\!] \\
&+ \sigma_w \sum_{F_r \in \Gamma} \int_{F_r} \frac{f(k_p)}{|F_r|} [\![p_n^D - p_c^D]\!] [\![\psi_w]\!] \qquad (5.8)
\end{aligned}
$$

$$
\begin{aligned}
\textbf{ODE-Pc}: &\sum_{T_r \in \mathcal{T}} \int_{T_r} L_s(S_w^{n+1,i} - S_w^{n+1,i-1}) \psi_s + \sum_{T_r \in \mathcal{T}} \int_{T_r} L_{s,T} \left(\frac{S_w^{n+1,i} - S_w^{n+1,i-1}}{\Delta t} \right) \psi_s \\
&+ \sum_{T_r \in \mathcal{T}} \int_{T_r} P_c^{n+1,i} \psi_s - \sum_{T_r \in \mathcal{T}} \int_{T_r} p_{c,eq}(S_w^{n+1,i-1}) \psi_s \\
&+ \sum_{T_r \in \mathcal{T}} \int_{T_r} \frac{T(S_w^{n+1,i-1}) - T(S_w^n)}{\Delta t} \psi_s = 0 \qquad (5.9)
\end{aligned}
$$

In line with Remark 3, the solution at the previous time step is chosen as initial guess for the fully discrete the iteration scheme. However, the convergence result proved in [Karpinski et al., 2017] does not require this starting point.

5.2 Linearization of the interface condition

To linearize the interface condition, we evaluate which of the cases in Section 2.7, i.e. which case of (3.18), has to be considered. This detection is for both linearization schemes evaluated explicitly, i.e. we use the values of the previous time step. In the same way the calculation of the jump for the non-wetting pressure (2.12) is evaluated at the previous time-step. It is possible to also linearize those conditions, as it was done by Weiss et al. in [Helmig et al., 2009]. There, an active and non-active set strategy was proposed and implemented.

A first order Taylor expansion is used to linearize the nonlinear jump condition in (5.9) over the interface, leading to the following scheme:

Problem 8 [Fully discrete linearization scheme] Let $P_n^n \in V_h^p(\Omega)$, $P_c^n \in V_h^p(\Omega)$, and $S_w^n \in V_h^s(\Omega)$. Given $P_n^{n+1,i-1} \in V_h^p(\Omega)$, $P_c^{n+1,i-1} \in V_h^p(\Omega)$, and $S_w^{n+1,i-1} \in V_h^s(\Omega)$ with $P_n^{n+1,0} = P_n^n$, $P_c^{n+1,0} = P_c^n$, and $S_w^{n+1,0} = S_w^n$, find $P_n^{n+1,i} \in V_h^p(\Omega)$, $P_c^{n+1,i} \in V_h^p(\Omega)$, and $S_w^{n+1,i} \in V_h^s(\Omega)$, s.t., for all $\psi_s \in V_h^s(\Omega)$, $\psi_n \in V_h^p(\Omega)$, and $\psi_w \in V_h^p(\Omega)$, the following holds:

$$
\textbf{PDE-1}: \; - \sum_{T_i \in \mathcal{T}} \int_{T_i} \partial^- S_w^{n+1,i} \phi \psi_n + \sum_{T_i \in \mathcal{T}} \int_{T_i} \lambda_n(S_w^{n+1,i-1}) K \nabla \left(P_n^{n+1,i} - gz\rho_n\right) \nabla \psi_n
$$

$$
\begin{aligned}
&- \sum_{F_i \in \mathcal{F}} \int_{F_i} \{\lambda_n(S_w^{n+1,i-1}) K \nabla \left(P_n^{n+1,i} - gz\rho_n\right) \cdot \vec{n}\} [\![\psi_n]\!] \\
&+ \theta \sum_{F_i \in \mathcal{F}} \int_{F_i} [\![P_n^{n+1,i}]\!]' \{\lambda_n(S_w^{n+1,i-1}) K \nabla \psi_n \cdot \vec{n}\} \\
&+ \sigma_n \sum_{F_i \in \mathcal{F}} \int_{F_i} \frac{f(k_p)}{|F_i|} [\![P_n^{n+1,i}]\!]' [\![\psi_n]\!] \\
&= \theta \sum_{F_i \in \Gamma_D} \int_{F_i} [\![P_n^D]\!] \{\lambda_n(s^D) K \nabla \psi_n \cdot \vec{n}\} + \sigma_n \sum_{F_i \in \Gamma_D} \int_{F_i} \frac{f(k_p)}{|F_i|} [\![P_n^D]\!] [\![\psi_n]\!]
\end{aligned}
\tag{5.10}
$$

PDE-2:

$$
\begin{aligned}
&\sum_{T_i \in \mathcal{T}} \int_{T_i} \partial^- S_w^{n+1,i} \phi \psi_w + \sum_{T_i \in \mathcal{T}} \int_{T_i} \lambda_w(S_w^{n+1,i-1}) K \nabla \left(P_w^{n+1,i} - gz\rho_w\right) \nabla \psi_w \\
&- \sum_{F_i \in \mathcal{F}} \int_{F_i} \{\lambda_w(S_w^{n+1,i-1}) K \nabla \left(P_w^{n+1,i} - gz\rho_w\right) \cdot \vec{n}\} [\![\psi_w]\!] \\
&+ \theta \sum_{F_i \in \mathcal{F}} \int_{F_i} \{\lambda_w(S_w^{n+1,i-1}) K \nabla \psi_w \cdot \vec{n}\} [\![P_w^{n+1,i}]\!] \\
&+ \sigma_w \sum_{F_i \in \mathcal{F}} \int_{F_i} \frac{f(k_p)}{|F_i|} [\![P_w^{n+1,i}]\!] [\![\psi_w]\!] \\
&= \theta \sum_{F_i \in \Gamma_D} \int_{F_i} \{\lambda_w(s^D) K \nabla \psi_w \cdot \vec{n}\} [\![P_n^D - P_c^D]\!] \\
&+ \sigma_w \sum_{F_i \in \Gamma_D} \int_{F_i} \frac{f(k_p)}{|F_i|} [\![P_n^D - P_c^D]\!] [\![\psi_w]\!]
\end{aligned}
\tag{5.11}
$$

ODE-Pc:

$$
\begin{aligned}
&\sum_{T_i \in \mathcal{T}} \int_{T_i} L_s(S_w^{n+1,i} - S_w^{n+1,i-1}) \psi_s + \sum_{T_i \in \mathcal{T}} \int_{T_i} L_{s,T} \left(\frac{S_w^{n+1,i} - S_w^{n+1,i-1}}{\Delta t} \right) \psi_s \\
&+ \sum_{T_i \in \mathcal{T}} \int_{T_i} P_c^{n+1,i} \psi_s - \sum_{T_i \in \mathcal{T}} \int_{T_i} p_{c,eq}(S_w^{n+1,i-1}) \psi_s \\
&+ \sum_{T_i \in \mathcal{T}} \int_{T_i} \frac{T(S_w^{n+1,i-1}) - T(S_w^n)}{\Delta t} \psi_s \\
&- \sigma_s \sum_{F_i \in \mathcal{F}} \int_{F_i} \frac{f(k_s)}{|F_i|} \left[\![p_{c,eq}(S_w^n) - p'_{c,eq}(S_w^n) \left(S_w^{n+1,i+1} - S_w^n\right) \right]\!]' [\![\psi_s]\!] \\
&+ \sigma_s \sum_{F_i \in \mathcal{F}} \int_{F_i} \frac{f(k_s)}{|F_i|} \left[\!\!\left[T'(S_w^n) \frac{S_w^{n+1,i+1} - S_w^n}{\Delta t} \right]\!\!\right]' [\![\psi_s]\!] = 0
\end{aligned}
\tag{5.12}
$$

5.3 Convergence Analysis of the Linearization Scheme

In this section, we present a rigorous proof for the convergence of the linear iterative scheme introduced in Section 5.1.

We use the following notations for the errors at the i-th iteration:

$$e_s^i = S_w^{n+1,i} - S_w^{n+1}, \qquad e_{p_\alpha}^i = P_\alpha^{n+1,i} - P_\alpha^{n+1} \tag{5.13}$$

where $\alpha = n, w, c$. To simplify the presentation, we also use the following notation for the errors in $\lambda_n(\cdot)$, $\lambda_w(\cdot)$, $T(\cdot)$, and $p_{c,eq}(\cdot)$, respectively:

$$\begin{aligned} e_{\lambda_n}^i &= \lambda_n(S_w^{n+1,i}) - \lambda_n(S_w^{n+1}) & e_{\lambda_w}^i &= \lambda_w(S_w^{n+1,i}) - \lambda_w(S_w^{n+1}) \\ e_{p_{c,eq}}^i &= p_{c,eq}(S_w^{n+1,i}) - p_{c,eq}(S_w^{n+1}) & e_T^i &= T(S_w^{n+1,i}) - T(S_w^{n+1}) \quad . \end{aligned} \tag{5.14}$$

The following theorem states the convergence of the linear iterative scheme. It is proved under a mild restriction on the time step which is uniform w.r.t. the spatial mesh.

Theorem 2 Convergence L-scheme
Under assumptions (A5.1)-(A5.5) and with a sufficiently small Δt, the iterative scheme (5.7)-(5.9) converges linearly.

To prove the convergence of the scheme, we subtract (5.7), (5.8) and (5.9) from (3.15), (3.16) and (3.17) respectively to get the following system of equations:

$$\begin{aligned} \textbf{PDE-1}: &- \sum_{T_r \in \mathcal{T}} \int_{T_r} (\partial^- S_w^{n+1,i} - \partial^- S_w^{n+1}) \phi \psi_n \\ &+ \sum_{T_r \in \mathcal{T}} \int_{T_r} (\lambda_n(S_w^{n+1,i-1}) K \nabla P_n^{n+1,i} - \lambda_n(S_w^{n+1}) K \nabla P_n^{n+1}) \nabla \psi_n \\ &- \sum_{F_r \in \mathcal{F}} \int_{F_r} \{(\lambda_n(S_w^{n+1,i-1}) K \nabla P_n^{n+1,i} - \lambda_n(S_w^{n+1}) K \nabla P_n^{n+1}) \cdot \vec{n}\} [\![\psi_n]\!] \\ &+ \theta \sum_{F_r \in \mathcal{F}} \int_{F_r} [\![P_n^{n+1,i}]\!] \{\lambda_n(S_w^{n+1,i-1}) K \nabla \psi_n \cdot \vec{n}\} - [\![P_n^{n+1}]\!] \{\lambda_n(S_w^{n+1}) K \nabla \psi_n \cdot \vec{n}\} \\ &+ \sigma_n \sum_{F_r \in \mathcal{F}} \int_{F_r} \frac{f(k_p)}{|F_r|} [\![P_n^{n+1,i} - P_n^{n+1}]\!] [\![\psi_n]\!] = 0 \end{aligned} \tag{5.15}$$

$$\begin{aligned} \textbf{PDE-2}: &\sum_{T_r \in \mathcal{T}} \int_{T_r} (\partial^- S_w^{n+1,i} - \partial^- S_w^{n+1}) \phi \psi_w \\ &+ \sum_{T_r \in \mathcal{T}} \int_{T_r} (\lambda_w(S_w^{n+1,i-1}) K \nabla (P_n^{n+1,i} - P_c^{n+1,i}) \nabla \psi_w \end{aligned}$$

$$
\begin{aligned}
&- \sum_{T_r \in \mathcal{T}} \int_{T_r} (\lambda_w(S_w^{n+1}) K \nabla (P_n^{n+1} - P_c^{n+1}) \nabla \psi_w \\
&- \sum_{F_r \in \mathcal{F}} \int_{F_r} \{(\lambda_w(S_w^{n+1,i-1}) K \nabla (P_n^{n+1,i} - P_c^{n+1,i}) \cdot \vec{n}\} [\![\psi_w]\!] \\
&+ \sum_{F_r \in \mathcal{F}} \int_{F_r} \{(\lambda_w(S_w^{n+1}) K \nabla (P_n^{n+1} - P_c^{n+1})) \cdot \vec{n}\} [\![\psi_w]\!] \\
&+ \theta \sum_{F_r \in \mathcal{F}} \int_{F_r} \{\lambda_w(S_w^{n+1,i-1}) K \nabla \psi_w \cdot \vec{n}\} [\![P_n^{n+1,i} - P_c^{n+1,i}]\!] \\
&- \theta \sum_{F_r \in \mathcal{F}} \int_{F_r} \{\lambda_w(S_w^{n+1}) K \nabla \psi_w \cdot \vec{n}\} [\![P_n^{n+1} - P_c^{n+1}]\!] \\
&+ \sigma_w \sum_{F_r \in \mathcal{F}} \int_{F_r} \frac{f(k_p)}{|F_r|} [\![(P_n^{n+1,i} - P_c^{n+1,i}) - (P_n^{n+1} - P_c^{n+1})]\!] [\![\psi_w]\!] = 0 \quad (5.16)
\end{aligned}
$$

$$
\begin{aligned}
\textbf{ODE-Pc}: &\sum_{T_r \in \mathcal{T}} \int_{T_r} L_s(S_w^{n+1,i} - S_w^{n+1,i-1}) \psi_s + \sum_{T_r \in \mathcal{T}} \int_{T_r} L_{s,T} \left(\frac{S_w^{n+1,i} - S_w^{n+1,i-1}}{\Delta t} \right) \psi_s \\
&+ \sum_{T_r \in \mathcal{T}} \int_{T_r} (P_c^{n+1,i} - P_c^{n+1}) \psi_s - \sum_{T_r \in \mathcal{T}} \int_{T_r} (p_{c,eq}(S_w^{n+1,i-1}) - p_{c,eq}(S_w^{n+1})) \psi_s \\
&+ \sum_{T_r \in \mathcal{T}} \int_{T_r} (\partial^- T(S_w^{n+1,i-1}) - \partial^- T(S_w^{n+1})) \psi_s = 0 \quad (5.17)
\end{aligned}
$$

We proceed by first obtaining error estimates separately for the phase pressures in Sections 5.3.1 and 5.3.2 and for the capillary pressure in Section 5.3.3. These estimates are then combined to prove the convergence of the linearization scheme in Section 5.3.4.

5.3.1 Estimate for the non-wetting phase

Taking $\psi_n = e_{p_n}^i$ in (5.15), we get,

$$
\begin{aligned}
&- \sum_{T_r \in \mathcal{T}} \int_{T_r} \partial^- e_s^i \phi e_{p_n}^i + \sum_{T_r \in \mathcal{T}} \int_{T_r} \lambda_n(S_w^{n+1,i-1}) K |\nabla e_{p_n}^i|^2 + \sigma_n \sum_{F_r \in \mathcal{F}} \int_{F_r} \frac{f(k_p)}{|F_r|} [\![e_{p_n}^i]\!]^2 \\
= &- \sum_{T_r \in \mathcal{T}} \int_{T_r} (\lambda_n(S_w^{n+1,i-1}) - \lambda_n(S_w^{n+1})) K \nabla P_n^{n+1} \nabla e_{p_n}^i \\
&+ (1-\theta) \sum_{F_r \in \mathcal{F}} \int_{F_r} [\![e_{p_n}^i]\!] \{\lambda_n(S_w^{n+1,i-1}) K \nabla e_{p_n}^i \cdot \vec{n}\} \\
&- \sum_{F_r \in \mathcal{F}} \int_{F_r} \{(\lambda_n(S_w^{n+1,i-1}) - \lambda_n(S_w^{n+1})) K \nabla P_n^{n+1}) \cdot \vec{n}\} [\![e_{p_n}^i]\!] \\
&- \sum_{F_r \in \mathcal{F}} \int_{F_r} \theta \{(\lambda_n(S_w^{n+1,i-1}) - \lambda_n(S_w^{n+1})) K \nabla e_{p_n}^i \cdot \vec{n}\} [\![P_n^{n+1}]\!]
\end{aligned}
$$

$=: P_1 + P_2 + P_3 + P_4$

We start with the term P_4:

$$|P_4| \leq \|P_n^{n+1}\|_{\Omega,\infty}\theta \sum_{F_r\in\mathcal{F}} \int_{F_r} |\{(\lambda_n(S_w^{n+1,i-1}) - \lambda_n(S_w^{n+1}))K\nabla e_{p_n}^i \cdot \vec{n}\}| \,.$$

Using the trace inequality (3.8), Lemma 3, Cauchy-Schwarz inequality and Young's inequality (3.10), we get,

$$\begin{aligned}
|P_4| &\leq \|P_n^{n+1}\|_{\Omega,\infty}\theta \sum_{T_r\in\mathcal{T}} \left(\frac{1}{\sqrt{|F_r|}}\tilde{C}C_t\sqrt{\frac{f(k)}{|F_r|}}\left\|e_{\lambda_n}^{i-1}\right\|_{T_r,0} \right. \\
&\qquad\qquad \left. \tilde{C}C_t\sqrt{\frac{f(k)}{|F_r|}}\sqrt{|F_r|}\left\|K^{\frac{1}{2}}\nabla e_{p_n}^i\right\|_{T_r,0}\right) \\
&\leq \sqrt{\sum_{T_r\in\mathcal{T}} \|P_n^{n+1}\|_{\Omega,\infty}^2\theta^2\tilde{C}^4C_t^4\frac{f^2(k)}{|F_r|^2}\left\|e_{\lambda_n}^{i-1}\right\|_{T_r,0}^2}\sqrt{\sum_{T_r\in\mathcal{T}}\left\|K^{\frac{1}{2}}\nabla e_{p_n}^i\right\|_{T_r,0}^2} \\
&\leq \frac{1}{2\epsilon_4}\|P_n^{n+1}\|_{\Omega,\infty}^2\theta^2\tilde{C}^4C_t^4\frac{f^2(k)}{|F_r|^2}\sum_{T_r\in\mathcal{T}}\left\|e_{\lambda_n}^{i-1}\right\|_{T_r,0}^2 + \frac{\epsilon_4}{2}\sum_{T_r\in\mathcal{T}}\left\|K^{\frac{1}{2}}\nabla e_{p_n}^i\right\|_{T_r,0}^2
\end{aligned}$$

for any $\epsilon_4 > 0$.

For the terms P_1, P_2, and P_3, after carrying out steps similar to Section 4.3.1, we obtain for any $\epsilon_1, \epsilon_2, \epsilon_3 > 0$,

$$\begin{aligned}
|P_1| &\leq \frac{\epsilon_1}{2}\sum_{T_r\in\mathcal{T}}\|K^{\frac{1}{2}}\nabla e_{p_n}^i\|_{T_r,0}^2 + \frac{1}{2\epsilon_1}C\|\nabla P_n^{n+1}\|_{\Omega,\infty}\sum_{T_r\in\mathcal{T}}\|e_{\lambda_n}^{i-1}\|_{T_r,0}^2 \\
|P_2| &\leq \frac{\epsilon_2}{2}\sum_{T_r\in\mathcal{T}}\left\|K^{\frac{1}{2}}\nabla e_{p_n}^{n+1}\right\|_{T_r,0}^2 + (1-\theta)^2\frac{1}{2\epsilon_2}\overline{\lambda_n}^2C_t^2\tilde{C}^2\sum_{F_r}\frac{f(k_p)}{|F_r|}\|[\![e_{p_n}^{n+1}]\!]\|_{F_r,0}^2 \\
|P_3| &\leq \frac{\epsilon_3}{2}\sum_{F_r\in\mathcal{F}}\frac{f(k_p)}{|F_r|}\|[\![e_{p_n}^i]\!]\|_{F_r,0}^2 + \frac{1}{2\epsilon_3}\|K\nabla P_n^{n+1}\|_{\Omega,\infty}\tilde{C}^2C_t^2\sum_{T_r\in\mathcal{T}}\|e_{\lambda_n}^{i-1}\|_{T_r,0}^2 \,.
\end{aligned}$$

Observe that the estimate for P_3 involves the essential boundedness for the gradient of the pressure P_n^{n+1}. Assumptions (A5.2)-(A5.5) ensure that the problem remains non-degenerate and therefore, the pressures have essential bounded gradients (see e.g. [Cao and Pop, 2015]). These estimates can be extended to the time discrete problems, with the time derivative of the saturation being replaced by the finite difference approximation, noting that these divided differences satisfy the same bounds as $\partial_t s$ (see [Cao and Pop, 2016]). The extension to the finite element approximation follows from [Nitsche and Wheeler, 1981/82] (also see [Li, 2015]).

Combining the estimates for $|P_1|$ to $|P_4|$, and choosing $\epsilon_3 = \sigma_n$ and $\epsilon_1 = \epsilon_2 = \epsilon_4 = \frac{\lambda_n}{3}$, we get the following estimate for the non-wetting phase:

$$
\begin{aligned}
&- \sum_{T_r \in \mathcal{T}} \int_{T_r} (\partial^- e_s^i) \phi e_{p_n}^i + \frac{\underline{\lambda_n}}{2} \sum_{T_r \in \mathcal{T}} \|K^{\frac{1}{2}} \nabla e_{p_n}^i\|_{T_r,0}^2 \\
&+ \left(\frac{\sigma_n}{2} - (1-\theta)^2 \frac{3\overline{\lambda_n}^2 C_t^2 \tilde{C}^2}{2\underline{\lambda_n}} \right) \sum_{F_r \in \mathcal{F}} \frac{f(k_p)}{|F_r|} \|[\![e_{p_n}^i]\!]\|_{F_r,0}^2 \\
&\leq \left(C_{n,1} + C_{n,2} \frac{\theta^2}{|F_r|^2} \right) \sum_{T_r \in \mathcal{T}} \|e_{\lambda_n}^{i-1}\|_{T_r,0}^2
\end{aligned} \tag{5.18}
$$

for some $C_{n,1}, C_{n,2}$ not depending on the discretization parameters.

5.3.2 Estimate for the wetting phase

We choose $\psi_w = e_{p_w}^i$ in (5.16), and proceed in a similar way as for the non-wetting phase, to get the following estimate for the wetting phase:

$$
\begin{aligned}
&\sum_{T_r \in \mathcal{T}} \int_{T_r} (\partial^- e_s^i) \phi e_{p_w}^i + \frac{\underline{\lambda_w}}{2} \sum_{T_r \in \mathcal{T}} \|K^{\frac{1}{2}} \nabla e_{p_w}^i\|_{T_r,0}^2 \\
&+ (\frac{\sigma_w}{2} - (1-\theta)^2 \frac{3\overline{\lambda_w}^2 C_t^2 \tilde{C}^2}{2\underline{\lambda_w}}) \sum_{F_r \in \mathcal{F}} \frac{f(k_p)}{|F_r|} \|[\![e_{p_w}^i]\!]\|_{F_r,0}^2 \\
&\leq \left(C_{w,1} + C_{w,2} \frac{\theta^2}{|F_r|^2} \right) \sum_{T_r \in \mathcal{T}} \|e_{\lambda_w}^{i-1}\|_{T_r,0}^2
\end{aligned} \tag{5.19}
$$

for some $C_{w,1}, C_{w,2}$ not depending on the discretization parameters.

5.3.3 Estimate for the capillary pressure

With $\psi_s = e_s^i$ in (5.17), we obtain,

$$
\begin{aligned}
&\sum_{T_r \in \mathcal{T}} \int_{T_r} L_s (S_w^{n+1,i} - S_w^{n+1,i-1}) e_s^i + \sum_{T_r \in \mathcal{T}} \int_{T_r} L_{s,T} \left(\frac{S_w^{n+1,i} - S_w^{n+1,i-1}}{\Delta t} \right) e_s^i \\
&+ \sum_{T_r \in \mathcal{T}} \int_{T_r} e_{p_c}^i e_s^i - \sum_{T_r \in \mathcal{T}} \int_{T_r} (p_{c,eq}(S_w^{n+1,i-1}) - p_{c,eq}(S_w^{n+1})) e_s^i \\
&+ \sum_{T_r \in \mathcal{T}} \int_{T_r} (\partial^- T(S_w^{n+1,i-1}) - \partial^- T(S_w^{n+1})) e_s^i = 0
\end{aligned} \tag{5.20}
$$

Note that, from (5.13)-(5.14), we can write

$$
\partial^- T(S_w^{n+1,i-1}) - \partial^- T(S_w^{n+1}) = \frac{1}{\Delta t} (T(S_w^{n+1,i-1}) - T(S_w^{n+1})) \, .
$$

Using (3.9) in (5.20), we get,

$$\begin{aligned}
&\frac{L_s}{2}\sum_{T_r\in\mathcal{T}}\|e_s^i\|_{T_r,0}^2+\frac{L_{s,T}}{2}\Delta t\sum_{T_r\in\mathcal{T}}\|\partial^- e_s^i\|_{T_r,0}^2+\sum_{T_r\in\mathcal{T}}\int_{T_r}e_{p_c}^i e_s^i\\
&+\frac{L_s}{2}\sum_{T_r\in\mathcal{T}}\|e_s^i-e_s^{i-1}\|_{T_r,0}^2+\frac{L_{s,T}}{2}\Delta t\sum_{T_r\in\mathcal{T}}\|\partial^- e_s^i-\partial^- e_s^{i-1}\|_{T_r,0}^2\\
&-\sum_{T_r\in\mathcal{T}}\int_{T_r}e_{p_{c,eq}}^{i-1}e_s^i+\sum_{T_r\in\mathcal{T}}\int_{T_r}\frac{1}{\Delta t}e_T^{i-1}e_s^i\\
&=\frac{L_s}{2}\sum_{T_r\in\mathcal{T}}\|e_s^{i-1}\|_{T_r,0}^2+\frac{L_{s,T}}{2}\Delta t\sum_{T_r\in\mathcal{T}}\|\partial^- e_s^{i-1}\|_{T_r,0}^2\,. \qquad (5.21)
\end{aligned}$$

Following Assumption (A5.3), $p_{c,eq}(\cdot)$ is monotonous and we have,

$$-(p_{c,eq}(x)-p_{c,eq}(y))(x-y)=|p_{c,eq}(x)-p_{c,eq}(y)|\cdot|x-y|\,,$$

Similar argument holds for $T(\cdot)$. Using the above equalities for $p_{c,eq}(\cdot)$ and $T(\cdot)$, (5.21) becomes,

$$\begin{aligned}
&\frac{L_s}{2}\sum_{T_r\in\mathcal{T}}\|e_s^i\|_{T_r,0}^2+\frac{L_{s,T}}{2}\Delta t\sum_{T_r\in\mathcal{T}}\|\partial^- e_s^i\|_{T_r,0}^2+\sum_{T_r\in\mathcal{T}}\int_{T_r}e_{p_c}^i e_s^i\\
&+\frac{L_s}{2}\sum_{T_r\in\mathcal{T}}\|e_s^i-e_s^{i-1}\|_{T_r,0}^2+\frac{L_{s,T}}{2}\Delta t\sum_{T_r\in\mathcal{T}}\|\partial^- e_s^i-\partial^- e_s^{i-1}\|_{T_r,0}^2\\
&+\sum_{T_r\in\mathcal{T}}\int_{T_r}|e_{p_{c,eq}}^{i-1}|\cdot|e_s^{i-1}|+\sum_{T_r\in\mathcal{T}}\int_{T_r}|\frac{1}{\Delta t}e_T^{i-1}|\cdot|e_s^{i-1}|\\
&=\frac{L_s}{2}\sum_{T_r\in\mathcal{T}}\|e_s^{i-1}\|_{T_r,0}^2+\frac{L_{s,T}}{2}\Delta t\sum_{T_r\in\mathcal{T}}\|\partial^- e_s^{i-1}\|_{T_r,0}^2\\
&+\sum_{T_r\in\mathcal{T}}\int_{T_r}e_{p_{c,eq}}^{i-1}(e_s^i-e_s^{i-1})+\sum_{T_r\in\mathcal{T}}\int_{T_r}\frac{1}{\Delta t}e_T^{i-1}(e_s^{i-1}-e_s^i)\,.
\end{aligned}$$

Using the Lipschitz continuity of $p_{c,eq}(\cdot)$ and $T(\cdot)$, and the Young's inequality, we get,

$$\begin{aligned}
&\frac{L_s}{2}\sum_{T_r\in\mathcal{T}}\|e_s^i\|_{T_r,0}^2+\frac{L_{s,T}}{2}\Delta t\sum_{T_r\in\mathcal{T}}\|\partial^- e_s^i\|_{T_r,0}^2+\sum_{T_r\in\mathcal{T}}\int_{T_r}e_{p_c}^i e_s^i\\
&+\frac{L_s}{2}\sum_{T_r\in\mathcal{T}}\|e_s^i-e_s^{i-1}\|_{T_r,0}^2+\frac{L_{s,T}}{2}\Delta t\sum_{T_r\in\mathcal{T}}\|\partial^- e_s^i-\partial^- e_s^{i-1}\|_{T_r,0}^2\\
&+\frac{1}{L_{P_c}}\sum_{T_r\in\mathcal{T}}\|e_{p_{c,eq}}^{i-1}\|_{T_r,0}^2+\frac{1}{L_T\Delta t}\sum_{T_r\in\mathcal{T}}\|e_T^{i-1}\|_{T_r,0}^2\\
&\le\frac{L_s}{2}\sum_{T_r\in\mathcal{T}}\|e_s^{i-1}\|_{T_r,0}^2+\frac{L_{s,T}}{2}\Delta t\sum_{T_r\in\mathcal{T}}\|\partial^- e_s^{i-1}\|_{T_r,0}^2\\
&+\frac{1}{2L_s}\sum_{T_r\in\mathcal{T}}\|e_{p_{c,eq}}^{i-1}\|_{T_r,0}^2+\frac{L_s}{2}\sum_{T_r\in\mathcal{T}}\|e_s^i-e_s^{i-1}\|_{T_r,0}^2
\end{aligned}$$

$$+\frac{1}{2L_{s,T}\Delta t}\sum_{T_r\in\mathfrak{T}}\|e_T^{i-1}\|^2_{T_r,0}+\frac{L_{s,T}\Delta t}{2}\sum_{T_r\in\mathfrak{T}}\|\frac{1}{\Delta t}(e_s^{i-1}-e_s^i)\|^2_{T_r,0}\,.$$

Finally, using (5.6), we get the following estimate for the capillary pressure:

$$\begin{aligned}
&\frac{L_s}{2}\sum_{T_r\in\mathfrak{T}}\|e_s^i\|^2_{T_r,0}+\frac{L_{s,T}}{2}\Delta t\sum_{T_r\in\mathfrak{T}}\|\partial^- e_s^i\|^2_{T_r,0}+\sum_{T_r\in\mathfrak{T}}\int_{T_r}e^i_{p_c}e^i_s\\
&+\frac{1}{2L_s}\sum_{T_r\in\mathfrak{T}}\|e^{i-1}_{p_{c,eq}}\|^2_{T_r,0}+\frac{1}{2L_{s,T}\Delta t}\sum_{T_r\in\mathfrak{T}}\|e_T^{i-1}\|^2_{T_r,0}\\
&\le\frac{L_s}{2}\sum_{T_r\in\mathfrak{T}}\|e_s^{i-1}\|^2_{T_r,0}+\frac{L_{s,T}}{2}\Delta t\sum_{T_r\in\mathfrak{T}}\|\partial^- e_s^{i-1}\|^2_{T_r,0}\,.
\end{aligned}\tag{5.22}$$

5.3.4 Combined estimates

Multiplying (5.22) with $\frac{\phi}{\Delta t}$, and adding the resulting equation to the sum of (5.18) and (5.19), and observing that,

$$\begin{aligned}
&\sum_{T_r\in\mathfrak{T}}\int_{T_r}\frac{\phi}{\Delta t}e^i_{p_c}e^i_s+\sum_{T_r\in\mathfrak{T}}\int_{T_r}\partial^- e^i_s(\phi e^i_{p_w}-\phi e^i_{p_n})\\
=&\sum_{T_r\in\mathfrak{T}}\int_{T_r}\frac{\phi}{\Delta t}e^i_{p_c}e^i_s-\sum_{T_r\in\mathfrak{T}}\int_{T_r}\partial^- e^i_s e^i_{p_c}\\
=&0
\end{aligned}$$

leads to,

$$\begin{aligned}
&\frac{L_s}{2}\frac{\phi}{\Delta t}\sum_{T_r\in\mathfrak{T}}\|e_s^i\|^2_{T_r,0}+\frac{L_{s,T}\phi}{2}\sum_{T_r\in\mathfrak{T}}\|\partial^- e_s^i\|^2_{T_r,0}\\
&+\frac{\phi}{2L_s\Delta t}\sum_{T_r\in\mathfrak{T}}\|e^{i-1}_{p_{c,eq}}\|^2_{T_r,0}+\frac{\phi}{2L_{s,T}\Delta t^2}\sum_{T_r\in\mathfrak{T}}\|e_T^{i-1}\|^2_{T_r,0}\\
&+\frac{\underline{\lambda_n}}{2}\sum_{T_r\in\mathfrak{T}}\|K^{\frac{1}{2}}\nabla e^i_{p_n}\|^2_{T_r,0}+\left(\frac{\sigma_n}{2}-(1-\theta)^2\frac{3\overline{\lambda_n}^2C_t^2\tilde{C}^2}{2\underline{\lambda_n}}\right)\sum_{F_r\in\mathfrak{F}}\frac{f(k_p)}{|F_r|}\|[\![e^i_{p_n}]\!]\|^2_{F_r,0}\\
&+\frac{\underline{\lambda_w}}{2}\sum_{T_r\in\mathfrak{T}}\|K^{\frac{1}{2}}\nabla e^i_{p_w}\|^2_{T_r,0}+\left(\frac{\sigma_w}{2}-(1-\theta)^2\frac{3\overline{\lambda_w}^2C_t^2\tilde{C}^2}{2\underline{\lambda_w}}\right)\sum_{F_r\in\mathfrak{F}}\frac{f(k_p)}{|F_r|}\|[\![e^i_{p_w}]\!]\|^2_{F_r,0}\\
&\le\left(C_{n,0}+C_{n,1}+\frac{C_{n,2}\theta^2}{|F_r|^2}\right)\sum_{T_r\in\mathfrak{T}}\|e^{i-1}_{\lambda_n}\|^2_{T_r,0}\\
&+\left(C_{w,0}+C_{w,1}+\frac{C_{w,2}\theta^2}{|F_r|^2}\right)\sum_{T_r\in\mathfrak{T}}\|e^{i-1}_{\lambda_w}\|^2_{T_r,0}\\
&+\frac{L_s\phi}{2\Delta t}\sum_{T_r\in\mathfrak{T}}\|e_s^{i-1}\|^2_{T_r,0}+\frac{L_{s,T}\phi}{2}\sum_{T_r\in\mathfrak{T}}\|\partial^- e_s^{i-1}\|^2_{T_r,0}\,.
\end{aligned}$$

After multiplying with Δt and rearranging the terms, we get,

$$
\begin{aligned}
&\frac{L_s\phi}{2}\sum_{T_r\in\mathfrak{T}}\|e_s^i\|_{T_r,0}^2+\frac{\Delta t L_{s,T}\phi}{2}\sum_{T_r\in\mathfrak{T}}\|\partial^- e_s^i\|_{T_r,0}^2\\
&+\frac{\phi}{2L_s}\sum_{T_r\in\mathfrak{T}}\|e_{p_{c,eq}}^{i-1}\|_{T_r,0}^2+\frac{\phi}{2L_{s,T}\Delta t}\sum_{T_r\in\mathfrak{T}}\|e_T^{i-1}\|_{T_r,0}^2\\
&+\frac{\Delta t\underline{\lambda_n}}{2}\sum_{T_r\in\mathfrak{T}}\|K^{\frac{1}{2}}\nabla e_{p_n}^i\|_{T_r,0}^2+\frac{\Delta t\underline{\lambda_w}}{2}\sum_{T_r\in\mathfrak{T}}\|K^{\frac{1}{2}}\nabla e_{p_w}^i\|_{T_r,0}^2\\
&+\Delta t\left(\frac{\sigma_n}{2}-(1-\theta)^2\frac{3\overline{\lambda_n}^2C_t^2\tilde{C}^2}{2\underline{\lambda_n}}\right)\sum_{F_r\in\mathfrak{F}}\frac{f(k_p)}{|F_r|}\|[\![e_{p_n}^i]\!]\|_{F_r,0}^2\\
&+\Delta t\left(\frac{\sigma_w}{2}-(1-\theta)^2\frac{3\overline{\lambda_w}^2C_t^2\tilde{C}^2}{2\underline{\lambda_w}}\right)\sum_{F_r\in\mathfrak{F}}\frac{f(k_p)}{|F_r|}\|[\![e_{p_w}^i]\!]\|_{F_r,0}^2\\
&\le\Delta t\left(C_{n,0}+C_{n,1}+\frac{C_{n,2}\theta^2}{|F_r|^2}\right)\sum_{T_r\in\mathfrak{T}}\|e_{\lambda_n}^{i-1}\|_{T_r,0}^2\\
&+\Delta t\left(C_{w,0}+C_{w,1}+\frac{C_{w,2}\theta^2}{|F_r|^2}\right)\sum_{T_r\in\mathfrak{T}}\|e_{\lambda_w}^{i-1}\|_{T_r,0}^2\\
&+\frac{L_s\phi}{2}\sum_{T_r\in\mathfrak{T}}\|e_s^{i-1}\|_{T_r,0}^2+\frac{\Delta t L_{s,T}\phi}{2}\sum_{T_r\in\mathfrak{T}}\|\partial^- e_s^{i-1}\|_{T_r,0}^2\,.
\end{aligned}
$$

Using the Lipschitz continuity of λ_n, λ_w, T^{-1}, and $p_{c,eq}^{-1}$, we can rewrite this as,

$$
\begin{aligned}
&\frac{L_s\phi}{2}\sum_{T_r\in\mathfrak{T}}\|e_s^i\|_{T_r,0}^2+\frac{\Delta t L_{s,T}\phi}{2}\sum_{T_r\in\mathfrak{T}}\|\partial^- e_s^i\|_{T_r,0}^2\\
&+\frac{l_{p_{c,eq}}^2\phi}{2L_s}\sum_{T_r\in\mathfrak{T}}\|e_s^{i-1}\|_{T_r,0}^2+\frac{l_T^2\Delta t\phi}{2L_{s,T}}\sum_{T_r\in\mathfrak{T}}\|\partial^- e_s^{i-1}\|_{T_r,0}^2\\
&+\frac{\Delta t\underline{\lambda_n}}{2}\sum_{T_r\in\mathfrak{T}}\|K^{\frac{1}{2}}\nabla e_{p_n}^i\|_{T_r,0}^2+\frac{\Delta t\underline{\lambda_w}}{2}\sum_{T_r\in\mathfrak{T}}\|K^{\frac{1}{2}}\nabla e_{p_w}^i\|_{T_r,0}^2\\
&+\Delta t\left(\frac{\sigma_n}{2}-(1-\theta)^2\frac{3\overline{\lambda_n}^2C_t^2\tilde{C}^2}{2\underline{\lambda_n}}\right)\sum_{F_r\in\mathfrak{F}}\frac{f(k_p)}{|F_r|}\|[\![e_{p_n}^i]\!]\|_{F_r,0}^2\\
&+\Delta t\left(\frac{\sigma_w}{2}-(1-\theta)^2\frac{3\overline{\lambda_w}^2C_t^2\tilde{C}^2}{2\underline{\lambda_w}}\right)\sum_{F_r\in\mathfrak{F}}\frac{f(k_p)}{|F_r|}\|[\![e_{p_w}^i]\!]\|_{F_r,0}^2\\
&\le\frac{L_s\phi}{2}\sum_{T_r\in\mathfrak{T}}\|e_s^{i-1}\|_{T_r,0}^2+\frac{\Delta t L_{s,T}\phi}{2}\sum_{T_r\in\mathfrak{T}}\|\partial^- e_s^{i-1}\|_{T_r,0}^2\\
&+\Delta t\left(L_{\lambda_n}^2C_n+L_{\lambda_w}^2C_w\right)\left(2+\frac{\theta^2}{|F_r|^2}\right)\sum_{T_r\in\mathfrak{T}}\|e_s^{i-1}\|_{T_r,0}^2\,.
\end{aligned}
$$

From this we obtain,

$$
\begin{aligned}
&\frac{L_s\phi}{2}\sum_{T_r\in\mathcal{T}}\|e_s^i\|_{T_r,0}^2+\frac{\Delta t L_{s,T}\phi}{2}\sum_{T_r\in\mathcal{T}}\|\partial^- e_s^i\|_{T_r,0}^2\\
&+\left[\frac{l_{p_{c,eq}}^2\phi}{2L_s}-\Delta t C\left(2+\frac{\theta^2}{|F_r|^2}\right)\right]\sum_{T_r\in\mathcal{T}}\|e_s^{i-1}\|_{T_r,0}^2+\frac{l_T^2\Delta t\phi}{2L_{s,T}}\sum_{T_r\in\mathcal{T}}\|\partial^- e_s^{i-1}\|_{T_r,0}^2\\
&+\frac{\Delta t\underline{\lambda_n}}{2}\sum_{T_r\in\mathcal{T}}\|K^{\frac{1}{2}}\nabla e_{p_n}^i\|_{T_r,0}^2+\frac{\Delta t\underline{\lambda_w}}{2}\sum_{T_r\in\mathcal{T}}\|K^{\frac{1}{2}}\nabla e_{p_w}^i\|_{T_r,0}^2\\
&+\Delta t\left(\frac{\sigma_n}{2}-(1-\theta)^2\frac{3\overline{\lambda_n}^2C_t^2\tilde{C}^2}{2\underline{\lambda_n}}\right)\sum_{F_r\in\mathcal{F}}\frac{f(k_p)}{|F_r|}\|[\![e_{p_n}^i]\!]\|_{F_r,0}^2\\
&+\Delta t\left(\frac{\sigma_w}{2}-(1-\theta)^2\frac{3\overline{\lambda_w}^2C_t^2\tilde{C}^2}{2\underline{\lambda_w}}\right)\sum_{F_r\in\mathcal{F}}\frac{f(k_p)}{|F_r|}\|[\![e_{p_w}^i]\!]\|_{F_r,0}^2\\
&\leq\frac{L_s\phi}{2}\sum_{T_r\in\mathcal{T}}\|e_s^{i-1}\|_{T_r,0}^2+\frac{\Delta t L_{s,T}\phi}{2}\sum_{T_r\in\mathcal{T}}\|\partial^- e_s^{i-1}\|_{T_r,0}^2,
\end{aligned}
$$

which can be reformulated as,

$$
\begin{aligned}
&\frac{L_s\phi}{2}\sum_{T_r\in\mathcal{T}}\|e_s^i\|_{T_r,0}^2+\frac{\Delta t L_{s,T}\phi}{2}\sum_{T_r\in\mathcal{T}}\|\partial^- e_s^i\|_{T_r,0}^2\\
&+\frac{\Delta t\underline{\lambda_n}}{2}\sum_{T_r\in\mathcal{T}}\|K^{\frac{1}{2}}\nabla e_{p_n}^i\|_{T_r,0}^2+\frac{\Delta t\underline{\lambda_w}}{2}\sum_{T_r\in\mathcal{T}}\|K^{\frac{1}{2}}\nabla e_{p_w}^i\|_{T_r,0}^2\\
&+\Delta t\left(\frac{\sigma_n}{2}-(1-\theta)^2\frac{3\overline{\lambda_n}^2C_t^2\tilde{C}^2}{2\underline{\lambda_n}}\right)\sum_{F_r\in\mathcal{F}}\frac{f(k_p)}{|F_r|}\|[\![e_{p_n}^i]\!]\|_{F_r,0}^2\\
&+\Delta t\left(\frac{\sigma_w}{2}-(1-\theta)^2\frac{3\overline{\lambda_w}^2C_t^2\tilde{C}^2}{2\underline{\lambda_w}}\right)\sum_{F_r\in\mathcal{F}}\frac{f(k_p)}{|F_r|}\|[\![e_{p_w}^i]\!]\|_{F_r,0}^2\\
&\leq\left[\frac{L_s\phi}{2}-\left(\frac{l_{p_{c,eq}}^2\phi}{2L_s}-\Delta t C\left(2+\frac{\theta^2}{|F_r|^2}\right)\right)\right]\sum_{T_r\in\mathcal{T}}\|e_s^{i-1}\|_{T_r,0}^2\\
&+\left(\frac{\Delta t L_{s,T}\phi}{2}-\frac{l_T^2\Delta t\phi}{2L_{s,T}}\right)\sum_{T_r\in\mathcal{T}}\|\partial^- e_s^{i-1}\|_{T_r,0}^2\,.
\end{aligned}
$$

For Δt small enough, this leads to a contraction for the terms $\sum_{T_r\in\mathcal{T}}\|e_s^i\|_{T_r,0}^2$ and $\sum_{T_r\in\mathcal{T}}\|\partial^- e_s^i\|_{T_r,0}^2$, which concludes the proof for the convergence of the proposed linearization scheme.

Remark 4 To obtain the contraction, it is required that the time-step is chosen s.t.,

$$
\Delta t<\frac{l_{p_{c,eq}}^2\phi}{2L_sC\left(2+\frac{\theta^2}{|F_{\min}|^2}\right)} \tag{5.23}
$$

where, $|F_{\min}|$ is the measure of the smallest face. This restriction is milder when compared to the typical stability conditions imposed for explicit methods (like IMPES), or for the Newton method (see e.g. [Radu et al., 2006] for the analysis for a simplified two-phase model). Moreover, for the IIP dG-scheme, in which $\theta = 0$, the constraint on the time-step does not depend on the mesh size at all and is similar to the one for the L-method for standard, equilibrium two-phase flows with $\tau = 0$ (see [Radu et al., 2015a]).

Remark 5 To guarantee the convergence, the parameters L_s and $L_{s,T}$ must satisfy (5.6). For degenerate problems, if e.g. the equilibrium capillary pressure function is not Lipschitz, one needs to first regularize the problem in order to ensure the convergence of the scheme.

Remark 6 The convergence result can be extended to conforming discretizations, like finite elements, when the approximation lies in $W^{1,2}(\Omega)$. On can carry out the similar steps as above, but now jumps and averages over faces do not appear anymore. As with the IIP dG-method, for the conforming discretizations the restriction on the time step does not depend on the mesh size, leading to results similar to [Radu et al., 2015a].

5.4 Numerical Example

In this section, we present a numerical example to show the effectiveness of the proposed L-scheme. The numerical scheme is implemented in C++ based DUNE-PDELab framework [Bastian et al., 2008a,b, 2010, 2011]. We chose a test problem with a known analytical solution. The test setting is described in Section 5.4.1. In Section 5.4.2, we make a parameter study to compare the behaviour of the L-scheme with the Newton-method.

5.4.1 Test-setting

We consider the domain $\Omega = (0,2) \times (0,2) \subset \mathbb{R}^2$ and the time interval $[0,3]$. The other parameters are listed in Table 5.1. The right hand sides (i.e. sources) in the governing equations, and the boundary and initial conditions are chosen such, that the following are the exact solutions of the model

$$\begin{aligned}
p_n(t,x,y) &= \frac{1}{4}\cos((x+y)\pi - t) + \frac{1}{2}, \\
S_w(t,x,y) &= \frac{1}{4}\sin((x+y)\pi - t) + \frac{1}{2}, \\
p_c(t,x,y) &= p_{c,eq}(S_w(t,x,y)) - \partial_t T(S_w(t,x,y)).
\end{aligned}$$

We chose $\theta = 0$ and the penalty parameters as $\sigma_w = \sigma_n = 10$. We set

$$T(S_w(t,x,y)) := \tau S_w(t,x,y)\ ,$$

which corresponds to a constant damping factor τ. $h-p$ convergence for this example is shown in [Karpinski and Pop, 2017].

5.4.2 Parameter study

For each combination of no. of elements $N = \{8\times 8, 16\times 16, 32\times 32\}$ and timestep-size $\Delta t[s] = \left\{\frac{1}{8}, \frac{1}{16}, \frac{1}{32}\right\}$, and polynomial order $k_s = 1$ and $k_p = 1$, we simulate the

Table 5.1: Example 1 - Properties

Phase Properties		
wetting phase dynamic viscosity	$\mu_w \left[\frac{kg}{ms}\right]$	1
non-wetting phase dynamic viscosity	$\mu_n \left[\frac{kg}{ms}\right]$	1
wetting phase density	$\rho_w \left[\frac{kg}{m^3}\right]$	1
non-wetting phase density	$\rho_n \left[\frac{kg}{m^3}\right]$	1
Hydraulic Properties		
absolute permeability	$K \ [m^2]$	1
residual wetting phase saturation	S_{rw}	0
residual non-wetting phase saturation	S_{rn}	0
porosity	φ	0.4
damping coefficient	$\tau \ [Pa \cdot s]$	1
Brooks-Correy Parameters		
entry pressure	$p_d \ [Pa]$	1
pore size distribution index	λ	2

test problem with Newton method and the L-scheme with different choices of L-parameter $L_s = \{4, 8, 16\}$. The L-parameters are chosen with respect to the theory, i.e. (5.6). In this example holds $0.7 \leq |p'_{c,eq}(s_w)| \leq 4$, so we choose $L_s \geq 4$. We also consider polynomial order $k_s = 2$ and $k_p = 2$, and simulate the test problem with Newton method and the L-scheme with $L_s = 4$ for each combination of N and Δt as above. As an initial guess for the non-linear solvers, we chose the solution of the previous timestep. The comparative performance of the Newton method and the L-scheme with different L-parameters is shown in Tables 5.2-5.5 in terms of average number of iterations per timestep, average computation time per timestep, and total computation time. As expected, the Newton scheme, which has a quadratic order of convergence, solves twice as fast as the L-scheme, which has a linear order of convergence.

In Figures 5.1-5.4, we compare the convergence at time $T = 1s$. Figure 5.1 shows the convergence of the Newton method compared with the L-Scheme in terms of the L^2-error of the residual, which we use as a convergence criterion for both the Newton and the L-scheme. Figures 5.2-5.4 compare the L^2-error of the pressures P_n, P_c and the saturation S_w, and also show the expected convergence rates. To obtain the expected convergence rates, we chose $\frac{1}{2}$ and $\frac{1}{4}$ of the rate obtained for $L = 16$ for $L = 8$ and $L = 4$, respectively. In our results we observe that the real convergence rate is at least as good as the expected convergence rate, and the convergence rates for pressures and saturation coincide. We also observe that with half the parameter L we get double the convergence rate. It is interesting to see that for the pressures in Figure 5.3 and 5.4 the first step does not fit the expected trend, but for the saturation the expected convergence rates are obtained within the first step. In each Figure 5.2-5.4 the convergence rate in horizontal direction, i.e. with timestep refinement, increases with the decreasing timestep size. Half the time step leads to double the convergence rate. In vertical direction, i.e. with spatial refinement, a similar trend is not observed. The convergence rates are constant with respect to change of the refinement level h. This result reflects the

Table 5.2: Comparison between Newton method and L-scheme with $L_s = 4$
Polynomial orders $k_s = 1$ and $k_p = 1$

N	**L-Scheme** $\Delta t = \frac{1}{8}$	$\Delta t = \frac{1}{16}$	$\Delta t = \frac{1}{32}$	**Newton method** $\Delta t = \frac{1}{8}$	$\Delta t = \frac{1}{16}$	$\Delta t = \frac{1}{32}$
Number of iterations per timestep $[-]$						
8×8	6	4	3	2	2	1.5
16×16	5	4	3	2	2	1
32×32	5	3	2	2	2	1
Computation time per step $[s]$						
8×8	1.79	1.45	0.85	0.51	0.71	0.55
16×16	5.81	4.61	3.56	2.84	2.05	1.44
32×32	28.28	17.65	11.61	13.58345	13.44	7.88
Total computation time $[s]$						
8×8	42.96	69.78	81.67	12.52	29.26	39.62
16×16	139.53	221.36	342.13	69.28	120.70	140.45
32×32	678.66	847.39	1114.45	293.39	612.21	722.29

independence of the convergence on the spatial discretization and shows the dependence only with respect to the timestep Δt. This is in accordance with our theoretical findings.

We repeat the above simulations for polynomial order $k_p = k_s = 1$ starting with a *bad initial guess* of $s_w = 0.5$ for the non-linear solver. In this case, we observe that the Newton method does not converge at all. The L-scheme still shows convergence due to its property of global convergence, however, only for $\Delta t = \dfrac{1}{32}$. For larger timesteps the L-scheme does not converge due to the restriction on the timestep size (5.23). The performance of the L-scheme in terms of average number of iterations per timestep, average computation time per timestep, and total computation time is tabulated in Table 5.6. In Figures 5.5 and 5.6, we show the convergence behaviour at $T = 1s$. It is interesting to observe that the scheme takes a few steps to find a close enough solution, after which it converges as expected. Here we see a clear advantage of the proposed L-scheme over the Newton method for solving realistic problems where the solution from last timestep may not always be a good initial guess. This also presents a possibility to combine the L-scheme with the Newton scheme, where the L-scheme can be used to find a good initial guess for the Newton scheme. This approach is also discussed in [List and Radu, 2016].

Table 5.3: Comparison between Newton method and L-scheme with $L_s = 8$
Polynomial orders $k_s = 1$ and $k_p = 1$

N	**L-Scheme** $\Delta t = \frac{1}{8}$	$\Delta t = \frac{1}{16}$	$\Delta t = \frac{1}{32}$	**Newton method** $\Delta t = \frac{1}{8}$	$\Delta t = \frac{1}{16}$	$\Delta t = \frac{1}{32}$
Number of iterations per timestep $[-]$						
8×8	8	5	4	2	2	1.5
16×16	8	5	3	2	2	1
32×32	7	4	3	2	2	1
Computation time per step $[s]$						
8×8	2.57	1.52	1.08	0.51	0.71	0.55
16×16	9.59	5.86	3.45	2.84	2.05	1.44
32×32	38.93	22.92	17.21	13.58345	13.44	7.88
Total computation time $[s]$						
8×8	61.75	72.89	104.05	12.52	29.26	39.62
16×16	230.19	281.31	330.81	69.28	120.70	140.45
32×32	934.29	1099.97	1652.56	293.39	612.21	722.29

Table 5.4: Comparison between Newton method and L-scheme with $L_s = 16$
Polynomial orders $k_s = 1$ and $k_p = 1$

N	**L-Scheme** $\Delta t = \frac{1}{8}$	$\Delta t = \frac{1}{16}$	$\Delta t = \frac{1}{32}$	**Newton method** $\Delta t = \frac{1}{8}$	$\Delta t = \frac{1}{16}$	$\Delta t = \frac{1}{32}$
Number of iterations per timestep $[-]$						
8×8	14	8	5	2	2	1.5
16×16	13	7	4	2	2	1
32×32	12	7	4	2	2	1
Computation time per step $[s]$						
8×8	4.30	2.64	1.69	0.51	0.71	0.55
16×16	17.08	9.33	5.26	2.84	2.05	1.44
32×32	72.93	45.56	25.14	13.58345	13.44	7.88
Total computation time $[s]$						
8×8	103.17	126.58	162.28	12.52	29.26	39.62
16×16	409.96	447.62	504.65	69.28	120.70	140.45
32×32	1750.22	2187.12	2413.52	293.39	612.21	722.29

Table 5.5: Comparison between Newton method and L-scheme with $L_s = 4$
Polynomial orders $k_s = 2$ and $k_p = 2$

N	**L-Scheme** $\Delta t = \frac{1}{8}$	$\Delta t = \frac{1}{16}$	$\Delta t = \frac{1}{32}$	**Newton method** $\Delta t = \frac{1}{8}$	$\Delta t = \frac{1}{16}$	$\Delta t = \frac{1}{32}$
Number of iterations per timestep $[-]$						
8×8	6	4	3	2	2	1.5
16×16	5	4	3	2	2	1
32×32	5	3	2	2	2	1
Computation time per step $[s]$						
8×8	3.59	2.26	1.81	0.51	0.71	0.55
16×16	14.81	11.56	8.66	2.84	2.05	1.44
32×32	114.73	67.74	45.64	13.58345	13.44	7.88
Total computation time $[s]$						
8×8	86.04	108.40	173.76	12.52	29.26	39.62
16×16	355.38	554.69	831.02	69.28	120.70	140.45
32×32	2753.48	3251.66	4381.63	293.39	612.21	722.29

Table 5.6: L-scheme with bad initial guess
Polynomial orders $k_s = 1$ and $k_p = 1$

N	L_s =16	L_s =8	L_s =4
Number of iterations per timestep $[-]$			
8×8	9	7	6
16×16	8	7	6
32×32	8	6	5
Computation time per step $[s]$			
8×8	2.56	2.04	1.73
16×16	9.36	8.14	6.90
32×32	45.97	35.63	28.04
Total computation time $[s]$			
8×8	245.66	195.45	165.71
16×16	898.24	781.01	662.81
32×32	6261.64	3420.12	2691.76

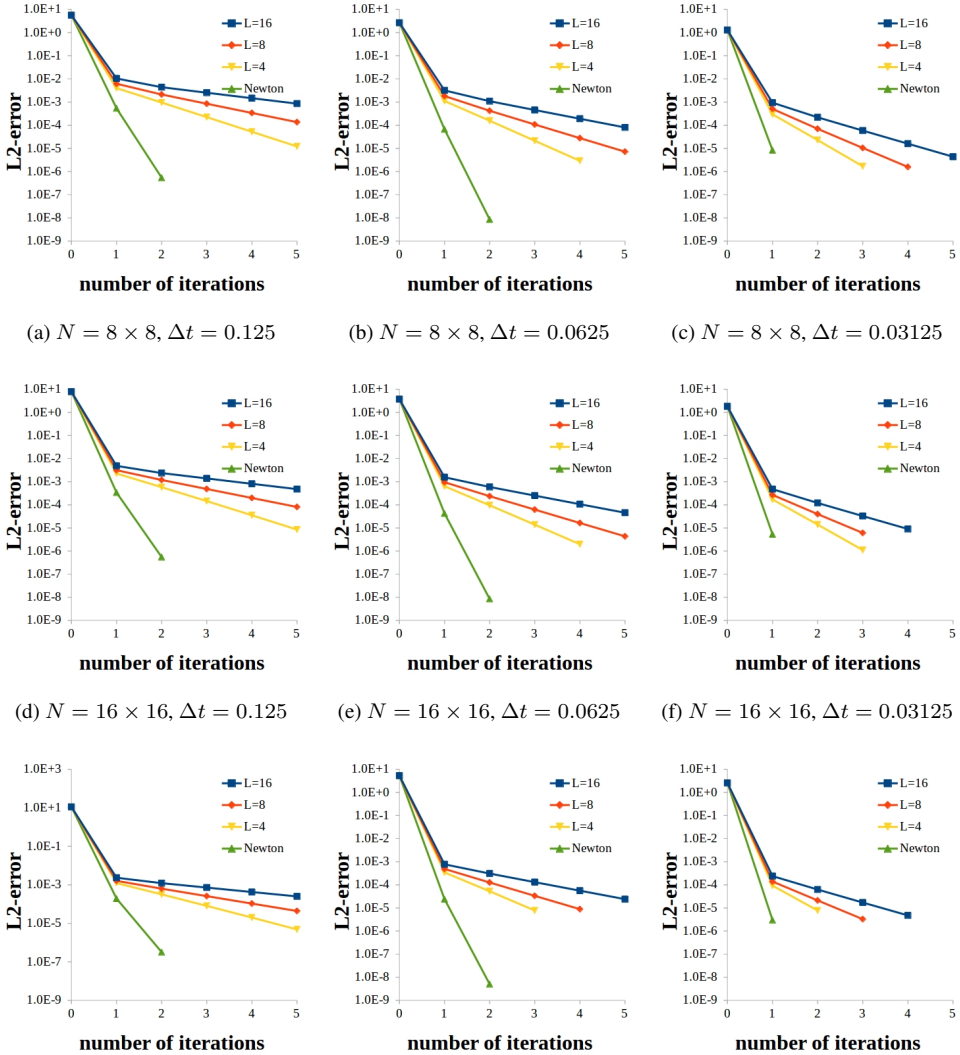

(a) $N = 8 \times 8$, $\Delta t = 0.125$ (b) $N = 8 \times 8$, $\Delta t = 0.0625$ (c) $N = 8 \times 8$, $\Delta t = 0.03125$

(d) $N = 16 \times 16$, $\Delta t = 0.125$ (e) $N = 16 \times 16$, $\Delta t = 0.0625$ (f) $N = 16 \times 16$, $\Delta t = 0.03125$

(g) $N = 32 \times 32$, $\Delta t = 0.125$ (h) $N = 32 \times 32$, $\Delta t = 0.0625$ (i) $N = 32 \times 32$, $\Delta t = 0.03125$

Figure 5.1: Residual at $T = 1s$ and polynomial order $k_s = k_p = 1$

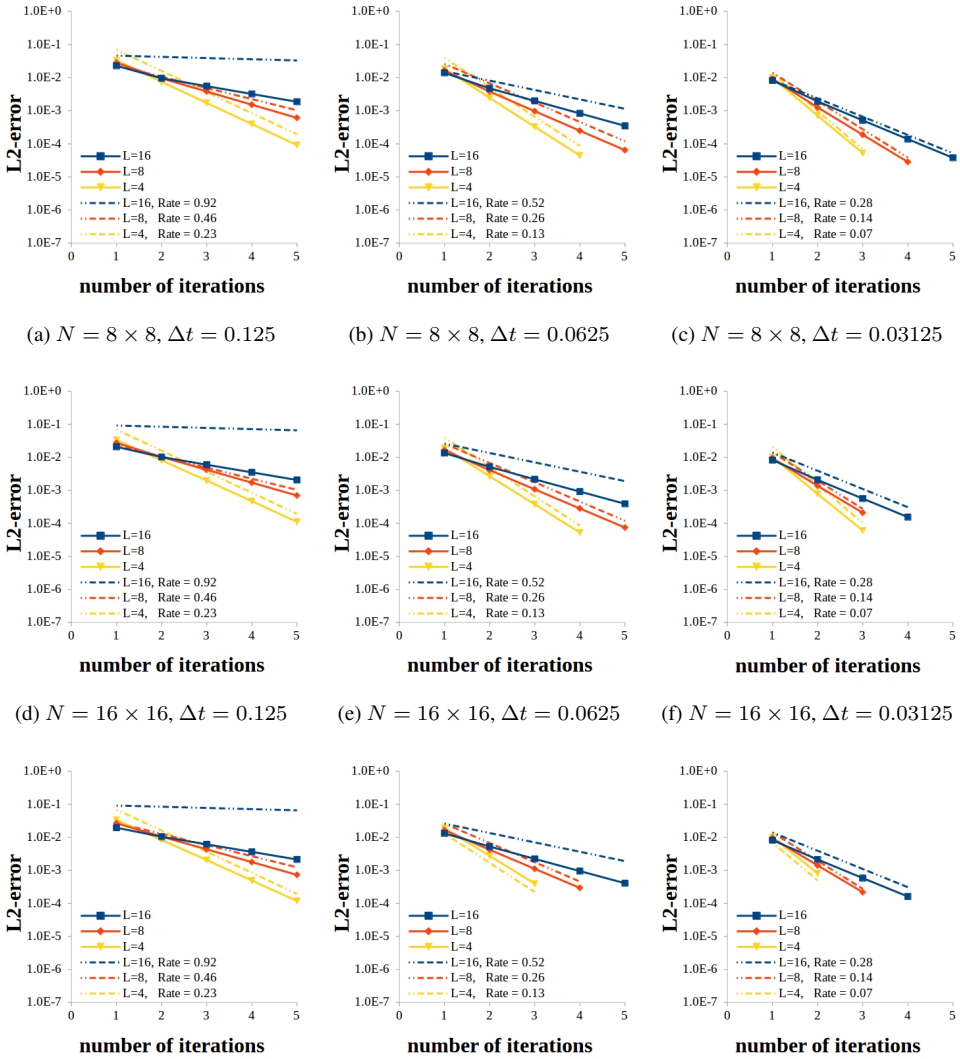

(a) $N = 8 \times 8$, $\Delta t = 0.125$ (b) $N = 8 \times 8$, $\Delta t = 0.0625$ (c) $N = 8 \times 8$, $\Delta t = 0.03125$

(d) $N = 16 \times 16$, $\Delta t = 0.125$ (e) $N = 16 \times 16$, $\Delta t = 0.0625$ (f) $N = 16 \times 16$, $\Delta t = 0.03125$

(g) $N = 32 \times 32$, $\Delta t = 0.125$ (h) $N = 32 \times 32$, $\Delta t = 0.0625$ (i) $N = 32 \times 32$, $\Delta t = 0.03125$

Figure 5.2: L^2-Error for S_w at $T = 1s$ and polynomial order $k_s = 1$

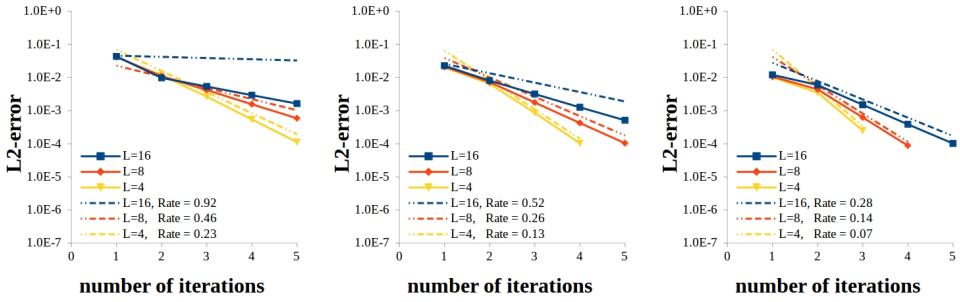

(a) $N = 8 \times 8$, $\Delta t = 0.125$

(b) $N = 8 \times 8$, $\Delta t = 0.0625$

(c) $N = 8 \times 8$, $\Delta t = 0.03125$

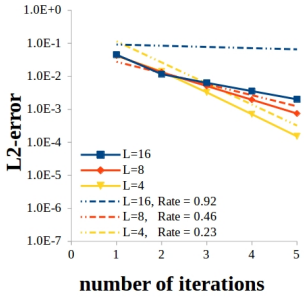

(d) $N = 16 \times 16$, $\Delta t = 0.125$

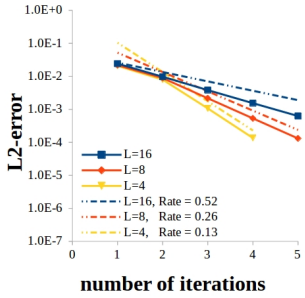

(e) $N = 16 \times 16$, $\Delta t = 0.0625$

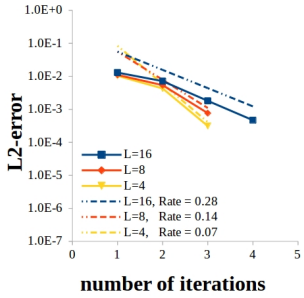

(f) $N = 16 \times 16$, $\Delta t = 0.03125$

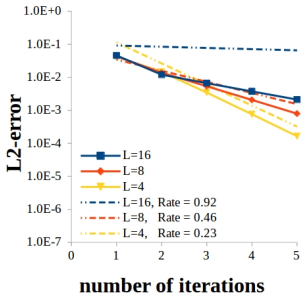

(g) $N = 32 \times 32$, $\Delta t = 0.125$

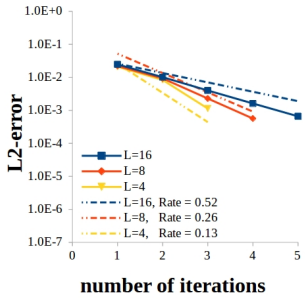

(h) $N = 32 \times 32$, $\Delta t = 0.0625$

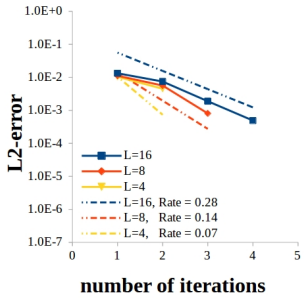

(i) $N = 32 \times 32$, $\Delta t = 0.03125$

Figure 5.3: L^2-Error for P_n at $T = 1s$ and polynomial order $k_p = 1$

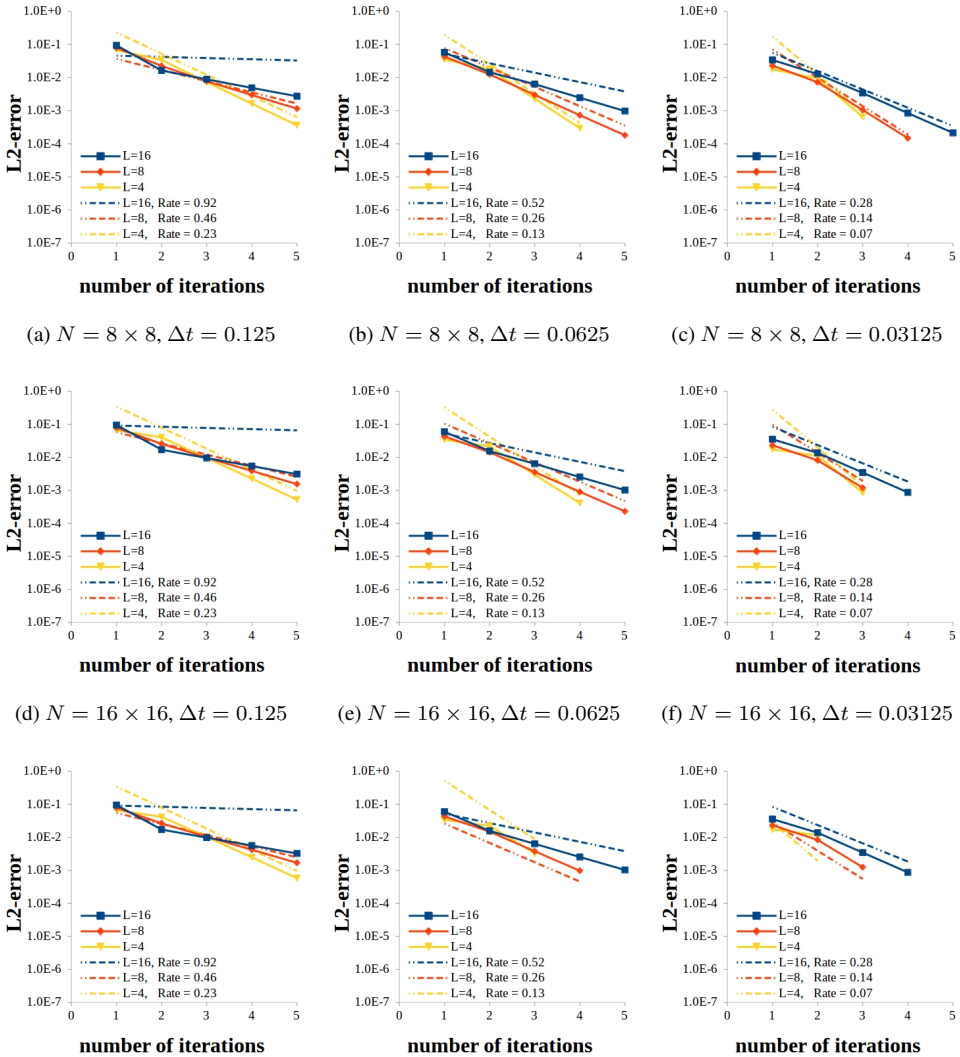

(a) $N = 8 \times 8$, $\Delta t = 0.125$ (b) $N = 8 \times 8$, $\Delta t = 0.0625$ (c) $N = 8 \times 8$, $\Delta t = 0.03125$

(d) $N = 16 \times 16$, $\Delta t = 0.125$ (e) $N = 16 \times 16$, $\Delta t = 0.0625$ (f) $N = 16 \times 16$, $\Delta t = 0.03125$

(g) $N = 32 \times 32$, $\Delta t = 0.125$ (h) $N = 32 \times 32$, $\Delta t = 0.0625$ (i) $N = 32 \times 32$, $\Delta t = 0.03125$

Figure 5.4: L^2-Error for P_c at $T = 1s$ and polynomial order $k_p = 1$

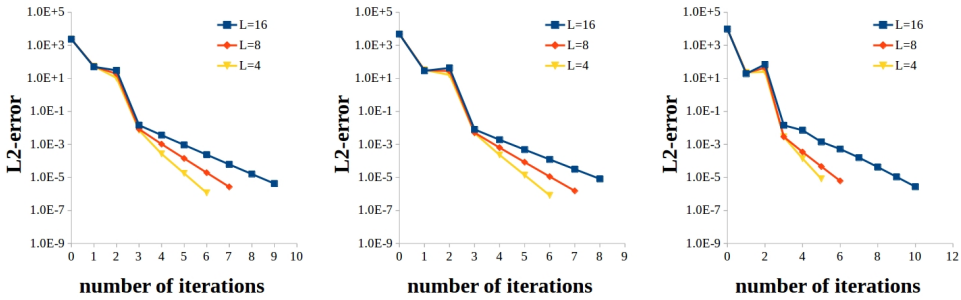

(a) $N = 8 \times 8$ (b) $N = 16 \times 16$ (c) $N = 32 \times 32$

Figure 5.5: L^2-Error for Residuals at $T = 1s$ for $\Delta t = 0.03125$ and polynomial order $k_p = k_s = 1$ for the case of a bad initial guess

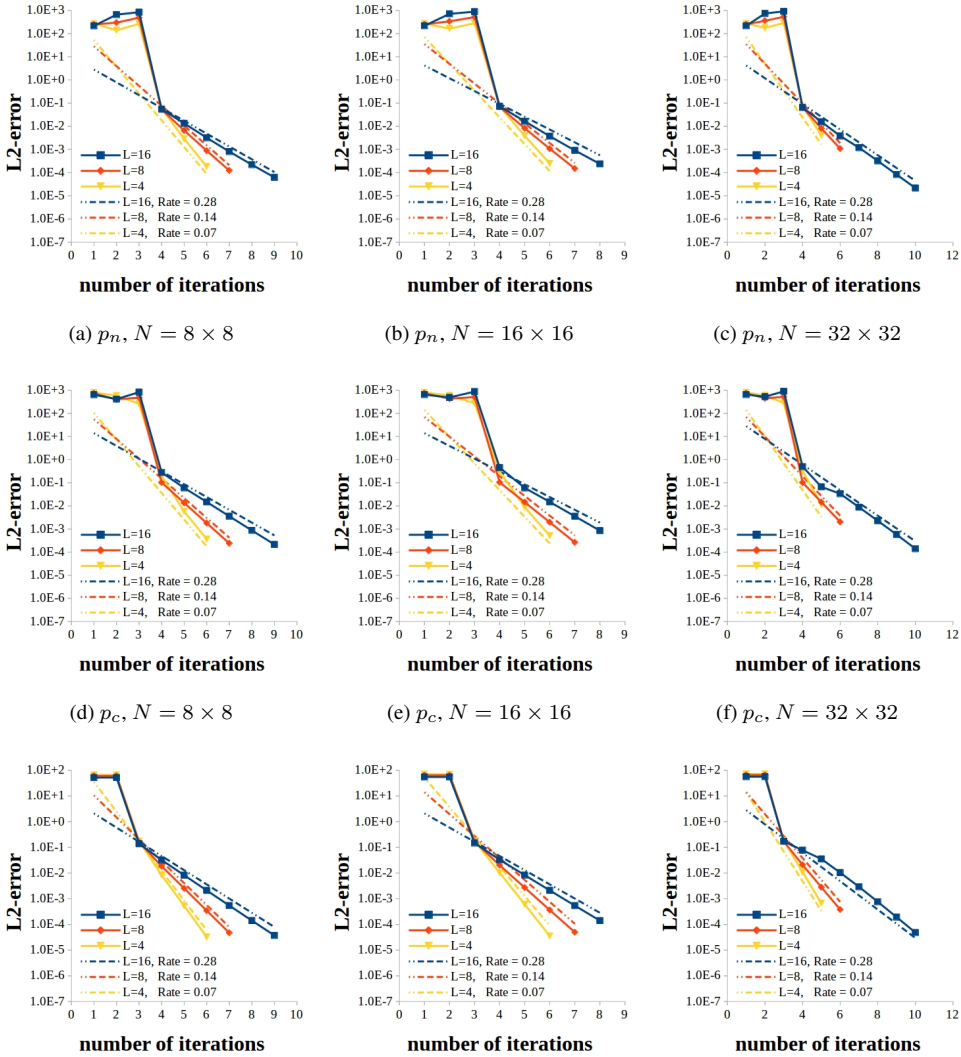

(a) p_n, $N = 8 \times 8$ (b) p_n, $N = 16 \times 16$ (c) p_n, $N = 32 \times 32$

(d) p_c, $N = 8 \times 8$ (e) p_c, $N = 16 \times 16$ (f) p_c, $N = 32 \times 32$

(g) s_w, $N = 8 \times 8$ (h) s_w, $N = 16 \times 16$ (i) s_w, $N = 32 \times 32$

Figure 5.6: L^2-Error for p_n, p_c, and s_w at $T = 1s$ for $\Delta t = 0.03125$ and polynomial order $k_p = k_s = 1$ for the case of a bad initial guess

Chapter 6

Numerical Examples in Heterogeneous Media

In this chapter, we show the capabilities of our scheme through different numerical examples in heterogeneous media.

In Example 1, Section 6.1, we consider a $2D$ problem with homogeneous and heterogeneous permeability fields, and continuous capillary pressure. In Example 2, Section 6.2, we verify our numerical scheme for heterogeneous porous media with discontinuous capillary pressure. For this, we consider a $1D$ problem from the text book by Rainer Helmig [Helmig, 1997]. Next, in Example 3, Section 6.3, we simulate a $1D$ inflow problem and compare the performance of the L-scheme and the Newton scheme. Finally, in Example 4, Section 6.4, we simulate a $2D$ lens problem with heterogeneous permeability field, discontinuous capillary pressure and capillary barrier effects, and gravitational effects to show the capabilities of our schemes.

6.1 Example 1: Inflow problem with homogeneous and heterogeneous permeability fields

We consider an inflow problem in a domain $\Omega = (0m, 1m) \times (0m, 1m)$, over a time interval $[0s, 2500s]$. The material properties and model parameters are listed in Table 6.1. We consider two cases: a homogeneous medium (**case A**) and a non-homogeneous (**case B**) one. The initial and the boundary conditions are listed in Table 6.2.

We discretize the domain into $50 \times 50 = 2500$ elements and chose a time-step of $dt = 10s$. For the L-scheme we take $L_s = 0.1$. Since the dynamic term is linear, no additional linearization is needed. We again chose $\theta = 0$ and $\sigma_w = \sigma_n = 10$.

The result for case A at $t = 1500s$ is shown in Figure 6.1a, and for case B at $t = 2500s$ is shown in Figure 6.1b. In case A, a straight finger is formed, propagating with the flow (from left to right). In case B, given the choice of the absolute permeability field K, a preferential flow path is formed along the medium with higher permeability, i.e. from the lower left to

Table 6.1: Example 1 - Properties

		case A	case B
Phase Properties			
water dynamic viscosity	μ_w $\left[\frac{kg}{ms}\right]$	10^{-3}	10^{-3}
oil dynamic viscosity	μ_n $\left[\frac{kg}{ms}\right]$	10^{-3}	10^{-3}
water density	ρ_w $\left[\frac{kg}{m^3}\right]$	10^3	10^3
oil density	ρ_n $\left[\frac{kg}{m^3}\right]$	$1.623 \cdot 10^3$	$1.623 \cdot 10^3$
Hydraulic Properties			
absolute permeability	K $[m^2]$	10^{-11}	$\begin{cases} 10^{-11} & \text{if } x < 0.5, y < 0.5 \\ 10^{-11} & \text{if } x > 0.5, y > 0.5 \\ 10^{-12} & \text{elsewhere} \end{cases}$
residual water saturation	S_{rw}	0	0
residual oil saturation	S_{rn}	0	0
porosity	φ	0.2	0.2
damping coefficient	τ $[Pa \cdot s]$	10^5	10^5
Brooks-Corey Parameters			
entry pressure	p_d $[Pa]$	$2.5 \cdot 10^3$	$2.5 \cdot 10^3$
pore size distribution index	λ	2	2

Table 6.2: Example 1 - Boundary and initial conditions

		case A	case B
Boundary values			
$x = 0m$			
water saturation	S_w	$\begin{cases} 0.6 & \text{if } 0.2 < y < 0.4 \\ 0.2 & \text{else} \end{cases}$	$\begin{cases} 0.6 & \text{if } 0.4 < y < 0.6 \\ 0.2 & \text{else} \end{cases}$
oil pressure	p_n $[Pa]$	$1.5 \cdot 10^5$	$1.5 \cdot 10^5$
$x = 1m$			
water saturation	S_w	0.2	0.2
oil pressure	p_n $[Pa]$	$1.0 \cdot 10^5$	$1.0 \cdot 10^5$
$y = 0m$ and $y = 1m$			
flow rate of water	q_w $\left[\frac{kg}{m^2 s}\right]$	0.0	0.0
flow rate of oil	q_n $\left[\frac{kg}{m^2 s}\right]$	0.0	0.0
Initial values			
water saturation	S_w	0.2	0.2

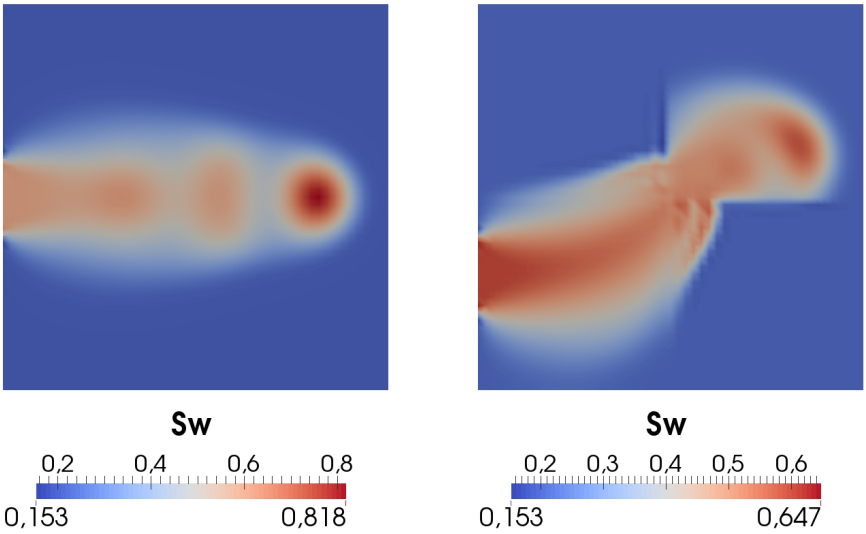

(a) S_w at $t = 1500s$ for case A.

(b) S_w at $t = 2500s$ for case B.

Figure 6.1: Example 1 - Saturation profiles at time t = 2500s for a homogeneous medium (left) and a heterogeneous one (right).

the upper right quadrant. The saturation overshoots in both cases are a manifestation of the dynamic capillarity. For both cases, the L-scheme performs as expected.

6.2 Example 2: Benchmark problem for verification of the numerical scheme with discontinuous capillary pressure

We consider the benchmark problem described in [Helmig, 1997], p. 275, section 5.5. The problem considers infiltration of non-aqueous phase liquid (NAPL) into a fully water saturated domain. A schematic of the problem is shown in Figure 6.2. The domain is $0.5m$ in length, and is divided into three parts with interfaces at $x = 0.15m$ and $x = 0.35m$. Sub-domain 1 $(0 \leq x < 0.15)$ and sub-domain 3 $(0.35m \leq x < 0.5m)$ are made of a porous material with lower entry pressure P_e, while the subdomain 2 $(0.15 \leq x < 0.35)$ is made of a porous material with a higher entry pressure P_e. The properties of the fluids and the materials in each sub-domain are listed in Table 6.3.

On the boundary Γ_L we prescribe an inflow condition, and on the boundary Γ_R we prescribe Dirichlet conditions for p_n and S_w. The initial condition for the S_w corresponds to a fully saturated porous media. An overview of the initial and boundary conditions can be found in Table 6.4.

We solve the problem in $1D$, discretize the domain into 320 elements of size $h = 0.003125$ with polynomial degrees of $k_p = k_s = 1$, and chose a timestep of $\Delta t = 1s$.

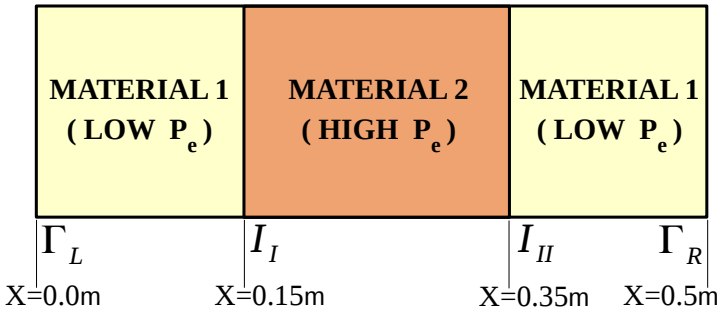

Figure 6.2: Example 2 - Test schematic.
Here, Γ_L and Γ_R are the left and the right boundary, respectively, and I_I and I_{II} are the material interfaces.

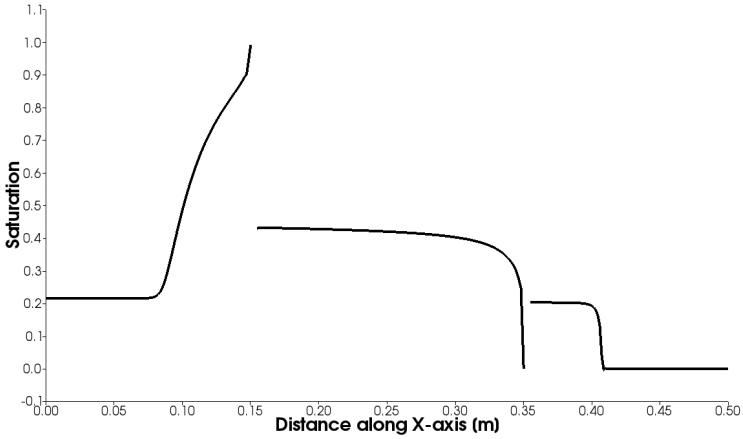

Figure 6.3: Example 2 - S_n profile at $t = 2150$ s.

The result of the simulation is given in Figure 6.3. The comparison to the results of Helmig [Helmig, 1997, p. 286, fig 5.39] shows a good match, which verifies the correctness of our implementation.

6.3 Example 3: Comparison of Newton scheme and L-scheme with discontinuous capillary pressure

We consider a $1D$ infiltration problem similar to Example 2, and compare the performance of the Newton scheme and the L-scheme with additional dynamic capillary pressure effects. The schematic for the problem is shown in Figure 6.4. We again divide the domain into three sub-domains to cover both transitions: from low to high entry pressure, and from high to low entry pressure. The domain has a length of $2m$ and has material interfaces at $x = 0.5m$ and $x = 1m$. The phase and the material properties are listed in Table 6.5. The problem is simulated without additional gravitational effects.

Table 6.3: Example 2 - Material properties.

Fluid Phase Properties			
dyn. viscosity wetting phase	$\mu_w \left[\frac{kg}{ms}\right]$	0.001	
dyn. viscosity non-wetting phase	$\mu_n \left[\frac{kg}{ms}\right]$	0.001	
density wetting phase	$\rho_w \left[\frac{kg}{m^3}\right]$	1000	
density non-wetting phase	$\rho_n \left[\frac{kg}{m^3}\right]$	1400	
Hydraulic Properties		**Material 1**	**Material 2**
abs. permeability	$K \left[m^2\right]$	$5.04 \cdot 10^{-10}$	$5.26 \cdot 10^{-11}$
res. wetting phase saturation	S_{rw}	0.08	0.1
res. non-wetting phase saturation	S_{rn}	0	0
porosity	φ	0.4	0.39
Brooks-Correy Parameters		**Material 1**	**Material 2**
entry pressure	$p_d \ [Pa]$	370	1324
pore size distr. index	λ	3.86	2.49

Table 6.4: Example 2 - Boundary and initial conditions.

Boundary values		
$x = 0m$		
wetting phase flow	$q_w \left[\frac{kg}{sm^2}\right]$	0
non-wetting phase flow	$q_n \left[\frac{kg}{sm^2}\right]$	0.05
$x = 0.5m$		
wetting phase saturation	S_w	1.
non-wetting fluid pressure	$p_n \ [Pa]$	$1.99630 \cdot 10^5$
Initial values		
wetting phase saturation	S_w	1

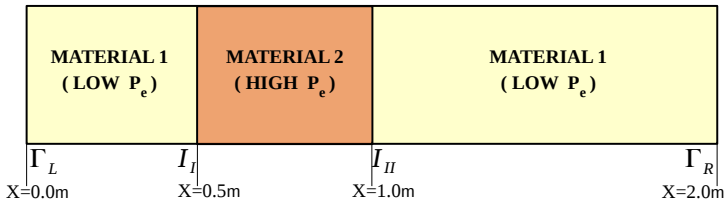

Figure 6.4: Example 3 - Schematic

The initial and the boundary conditions are given in Table 6.6. At $t = 0$, the domain is saturated with the wetting phase for $x > 0.25$. For $x \leq 0.25$, we define a cubic profile for wetting phase saturation (see Table 6.6). At the boundaries, for $t \geq 0$, Dirichlet conditions are prescribed.

We solve the problem for all combinations of time step sizes $\Delta t[s] = [0.125,\ 0.25,\ 0.5]$ and number of elements $N = [100,\ 200\quad 400]$. We chose a minimal residual of $\epsilon_{RES} < 10^{-6}$ for convergence. For the L-scheme, we choose $L = 0.1$.

We compare the performance of the Newton scheme and the L-scheme in terms of the average computation time, average iteration steps necessary, and the total computation time for different time and spatial discretizations. Table 6.7 shows the average number of iterations needed for convergence, Table 6.8 shows the average computation time per time-step, and Table 6.9 shows the total computation time for each scheme. We can observe that as the mesh size and the time step size decrease, the performance of the L-scheme approaches that of the Newton scheme.

In Figure 6.5, we plot the non-wetting phase saturation profiles in the domain at selected time steps for the simulation run with $\Delta t = 0.125s$ and $N = 400$. Due to the dynamic capillary effects, we obtain saturation overshoots as the front propagates. The retardation coefficient τ was chosen high enough to allow a plateau to build up. To compare the Newton and L-schemes, we plot both simulation results over each other. The continuous lines represent the results of the L-scheme, while the dots represent the results of the Newton scheme.

The accuracy of both schemes is similar, where as the number of iterations necessary for convergence for the L-scheme are twice as many as those for the Newton scheme which is due to the linear convergence of the L-scheme against the quadratic convergence of the Newton scheme.

6.4 Example 4: $2D$ Lens problem

We consider a two dimensional problem where a non-wetting fluid (e.g. NAPL) is infiltrating a domain which is initially fully saturated with the wetting fluid (e.g. water). The schematic of the problem is shown in Figure 6.6. The computational domain contains two distinct zones, each composed of a different material, signifying the material heterogeneity.

Table 6.5: Example 3 - Material properties

Phase Properties			
dyn. viscosity wetting phase	$\mu_w \left[\frac{kg}{ms}\right]$	10^{-3}	
dyn. viscosity non-wetting phase	$\mu_n \left[\frac{kg}{ms}\right]$	$0.9 \cdot 10^{-3}$	
density wetting phase	$\rho_w \left[\frac{kg}{m^3}\right]$	10^3	
density non-wetting phase	$\rho_n \left[\frac{kg}{m^3}\right]$	1.460	
Hydraulic Properties		**Material 1**	**Material 2**
abs. permeability	$K \ [m^2]$	$6 \cdot 10^{-10}$	$1.5 \cdot 10^{-10}$
res. wetting phase saturation	S_{rw}	0	0
res. non-wetting phase saturation	S_{rn}	0	0
porosity	φ	0.4	0.4
retardation coefficient	$\tau \ [Pa \cdot s]$	10^4	2×10^4
Brooks-Correy Parameters		**Material 1**	**Material 2**
entry pressure	$p_d \ [Pa]$	2500	5000
pore size distr. index	λ	2	2

Table 6.6: Example 3 - Boundary and initial conditions

Boundary values			
$x = 0m$			
wetting phase saturation	S_w	0.5	
non-wetting fluid pressure	$p_n \ [Pa]$	$1.5 \cdot 10^5$	
$x = 0.5m$			
wetting phase saturation	S_w	$1.$	
non-wetting fluid pressure	$p_n \ [Pa]$	$1.0 \cdot 10^5$	
Initial values			
wetting phase saturation	S_w	1	if $x > 0.25$
		$1 - 0.5 \cdot (128x^3 - 48x^2 + 1)$	otherwise

Table 6.7: Example 3 - Comparison of average number of iterations

	L-Scheme			**Newton-Scheme**		
N	$\Delta t = 0.5$	$\Delta t = 0.25$	$\Delta t = 0.125$	$\Delta t = 0.5$	$\Delta t = 0.25$	$\Delta t = 0.125$
100	6	4.4	3.5	2.6	2	1.7
200	5.8	4.1	3.2	3	2.3	1.8
400	5.7	3.8	3	3.8	2.7	2

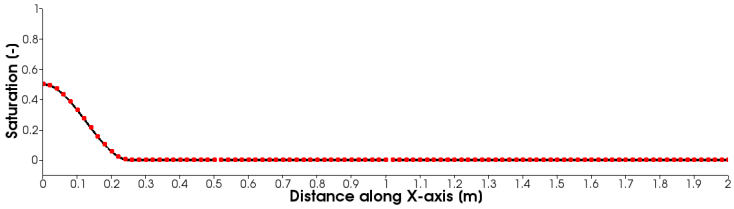

(a) $t = 0$ s

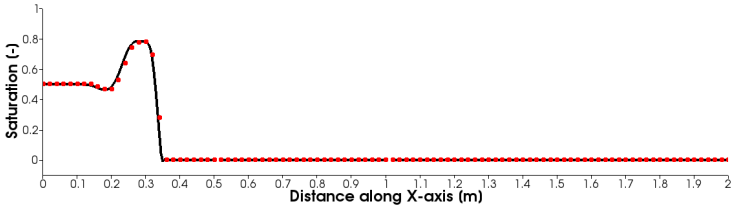

(b) $t = 10$ s

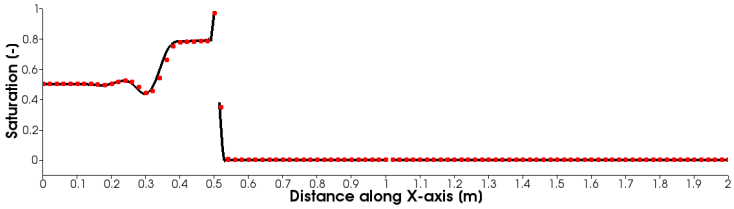

(c) $t = 20$ s

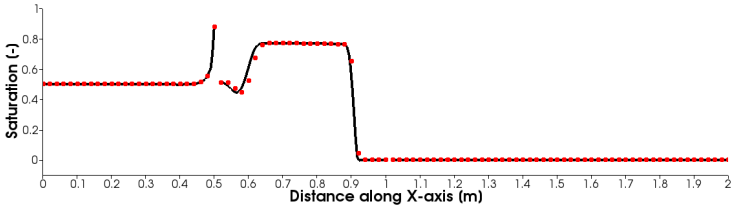

(d) $t = 50$ s

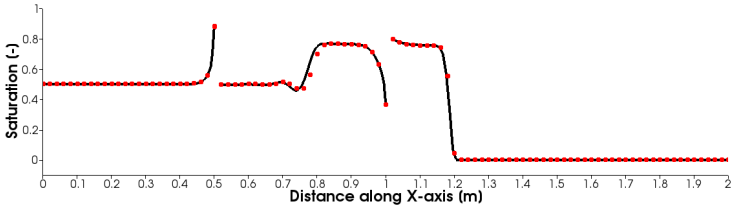

(e) $t = 75$ s

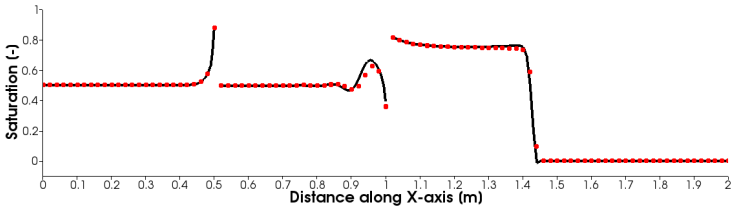

(f) $t = 100$ s

Figure 6.5: Example 3 - Non-wetting saturation profiles for $N = 400$ and $\Delta t = 0.125$ s

Table 6.8: Example 3 - Comparison of average computation time per step in seconds $[s]$

	L-Scheme			**Newton-Scheme**		
N	$\Delta t = 0.5$	$\Delta t = 0.25$	$\Delta t = 0.125$	$\Delta t = 0.5$	$\Delta t = 0.25$	$\Delta t = 0.125$
100	2.19	1.49	1.06	0.86	0.69	0.63
200	3.90	2.64	1.88	1.84	1.57	1.19
400	7.42	4.43	2.68	4.28	3.39	2.57

Table 6.9: Example 3 - Comparison of total computation time in seconds $[s]$

	L-Scheme			**Newton-Scheme**		
N	$\Delta t = 0.5$	$\Delta t = 0.25$	$\Delta t = 0.125$	$\Delta t = 0.5$	$\Delta t = 0.25$	$\Delta t = 0.125$
100	451.36	601.066	839.497	171.278	276.7	515.319
200	801.253	1098.01	1544.75	369.994	625.383	954.94
400	1560.24	1852.81	2161.04	854.712	1334.55	2021.59

The *material II* has a higher capillary pressure than *material I* in the sense of the description in Section 2.7. All relevant properties of both the materials are listed in Table 6.10. The infiltration of the non-wetting fluid is prescribed as a Dirichlet value at the upper boundary, while the lower boundary is assumed to be *blind*. On the left and right boundaries, no-flow condition is prescribed. Gravitational effects are also included.

We simulate two different scenarios to demonstrate the effects of the standard and non-standard capillary pressure relationships in the presence of a material heterogeneity:

Case A: without dynamic capillary pressure effects, i.e. $\tau = 0$, and

Case B: with dynamic capillary pressure effects. The values for τ are listed in Table 6.10.

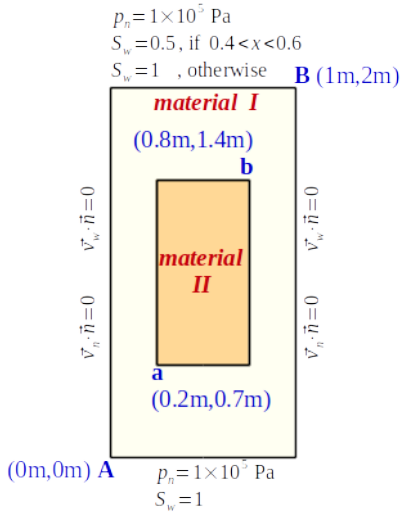

Figure 6.6: Example 4 - Schematic

Case A: $\tau = 0$ The results are presented in Figures 6.7a - 6.7e. We use a refinement of $h = 0.025$ and $\Delta t = 0.5$. As in the one dimensional examples, the non-wetting phase front propagates until the interface (Figure 6.7a). There it first has to accumulate due to the capillary barrier (Figure 6.7b). While a direct infiltration is not possible, a certain amount of the non-wetting phase flows around the lense leading to two additional fronts (Figure 6.7c). Those additional fronts can not infiltrate the lense from the side, as the threshold capillary pressure for infiltration is not reached. As soon as the entry condition on the upper interface is fulfilled, the main non-wetting phase front starts flowing through the domain at a lower speed, due to the higher lower intrinsic permeability. (Figure 6.7d) At the lower interface, leaving the interface no

Table 6.10: Example 4 - Material properties

Fluid Phase Properties			
dyn. viscosity wetting phase	$\mu_w \left[\frac{kg}{ms}\right]$	10^{-3}	
dyn. viscosity non-wetting phase	$\mu_n \left[\frac{kg}{ms}\right]$	$0.9 \cdot 10^{-3}$	
density wetting phase	$\rho_w \left[\frac{kg}{m^3}\right]$	10^3	
density non-wetting phase	$\rho_n \left[\frac{kg}{m^3}\right]$	1.460	
Hydraulic Properties		**Material 1**	**Material 2**
abs. permeability	$K \ [m^2]$	$6 \cdot 10^{-10}$	$1.5 \cdot 10^{-10}$
res. wetting phase saturation	S_{rw}	0	0
res. non-wetting phase saturation	S_{rn}	0	0
porosity	φ	0.4	0.4
retardation coefficient	$\tau \ [Pa \cdot s]$		
	Case A	0	0
	Case B	10^5	$2 \cdot 10^5$
Brooks-Correy Parameters		**Material 1**	**Material 2**
entry pressure	$p_d \ [Pa]$	2500	5000
pore size distr. index	λ	2	2

barrier occurs and flow is directly possible.(Figure 6.7e)

Case B: $\tau > 0$ With dynamic capillary pressure effects we get similar results as in case A. The results are presented in Figures 6.7f - 6.7j. We again use a refinement of $h = 0.025$ and $\Delta t = 0.5$. The additional dynamic term leads to a retardation effect, resulting in a slower propagation of the front. Mass accumulates at the tip of the resulting inflow-finger (Figure 6.7f). Like in the standard case, reaching the upper interface an info is not directly possible and non-wetting phase saturation accumulates (Figure 6.7g). Again two fingers are formed flowing around the lense each of them with an overshoot at the tip (Figure 6.7h). As soon as an inflow is possible, the main front propagates forward, forming again an overshoot. At the lower boundary we once again don't observe a capillary barrier, and the flow is directly possible (Figure 6.7j).

Figure 6.8 makes the retardation effect of the dynamic capillary pressure more clearly, we plotted the results next to each other in and used the same time in each figure, to visualize the difference in infiltration speed.

Figure 6.7: Example 4 - Results
bottom: with $\tau > 0$, top: without $\tau = 0$

(a) $t = 37.5$ s (b) $t = 100$ s (c) $t = 175$ s (d) $t = 250$ s (e) $t = 375$ s

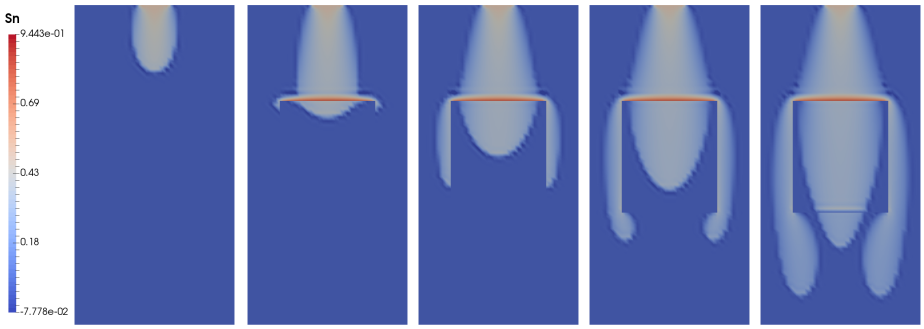

(f) $t = 125$ s (g) $t = 200$ s (h) $t = 300$ s (i) $t = 400$ s (j) $t = 500$ s

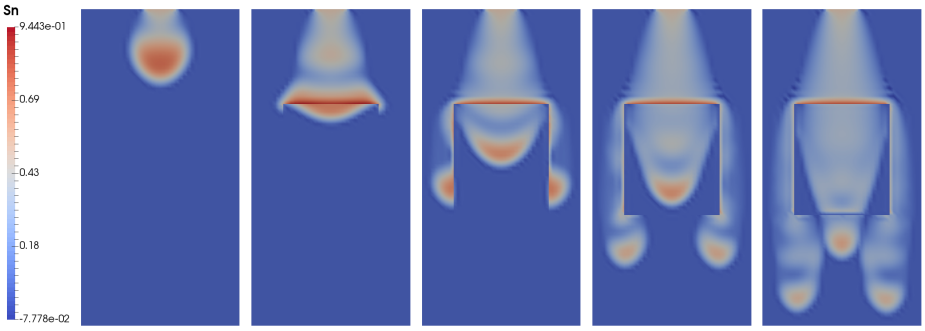

Figure 6.8: Example 4 - Effect of the retardation coefficient
left: $\tau = 0$, right: $\tau > 0$

(a) $t = 125$ s

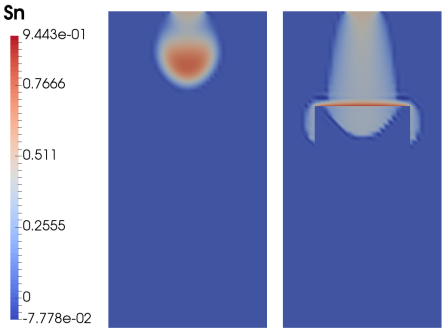

(b) $t = 200$ s

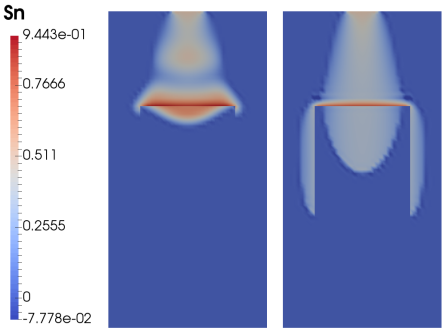

(c) $t = 300$ s

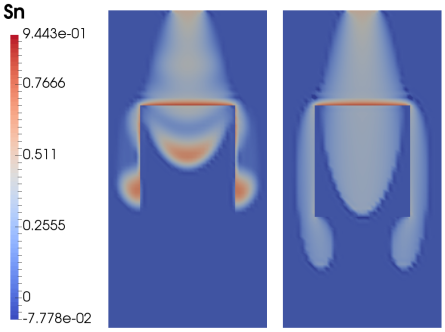

(d) $t = 400$ s

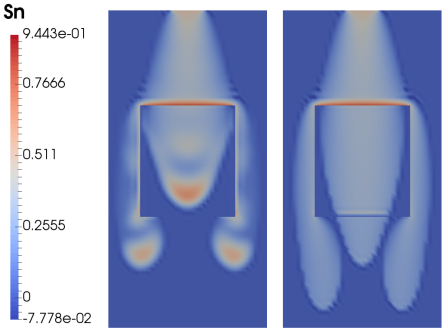

Chapter 7

Outlook

In this thesis, we presented a discontinuous Galerkin (dG) based numerical discretization for a two phase flow model in heterogeneous porous media with dynamic and discontinuous capillary pressure. For the mathematical model, we elaborated on the interface conditions to account for the discontinuities in the capillary pressure due to heterogeneities in the porous media, and presented an extension for our dG scheme to include these interface conditions. In the numerical model, the governing mass balance equations were not reformulated and no un-physical primary variable, like total pressure, was used. We rigorously proved existence, stability, and convergence of our numerical scheme for the homogeneous case. We were able to obtain h-p error estimates, which we were able to test and verify numerically. Further, we developed a linearization scheme for the discrete non-linear system which is based on a fixed point iteration. The performance of the linearization can be adjusted by a parameter L. Some advantages of this scheme are that it does not require computation of derivatives, is globally convergent and converges even for ill conditioned problems. The scheme was rigorously analysed and we were able to prove convergence. We showed that the scheme converges linearly under a mild time step restriction independent of the spatial discretization. The performance of the linearization method was also numerically tested in an extensive parameter study. Finally, we presented several $1D$ and $2D$ numerical examples in heterogeneous media with and without discontinuous capillary pressure to show the capabilities of our numerical scheme.

The numerical scheme was developed to easily incorporate nonlinearities and non-standard extensions to the capillary pressure. However, within the scope of this thesis, we restricted the model to include only linear dynamic capillary pressure effects. We made regularity assumptions on the equilibrium capillary pressure curve and the relative permeability functions, and restricted the numerical treatment to the non-degenerate case. It will be interesting to extend the current model towards a degenerate case, i.e., when one phase vanishes, and based on this, we could directly extend the model to multiphase flows, and possibly also to multicomponent flows. Hysteresis in capillary pressure is also a problem of great interest. Another natural extension for the mathematical model is to include nonlinear retardation coefficients. This leads to one very interesting possibility of defining the retardation coefficients as nonsmooth functions which can implicitly mimic a hysteretic effect without using scanning curves

from the previous timestep. With these model extensions, of course the regularity assumptions on the constitutive relations do not hold anymore and the convergence proof would also then need to be adapted to account for the nonsmooth, nonlinear capillary pressure curves.

For numerical solution of the problem and to get the correct interface behaviour, we need very fine meshes. This is computationally quite expensive, particularly also because in our problem formulation, we have an extra equation to solve for the capillary pressure. To make the solution less expensive without compromising the quality of the solution at interface, one option would be to consider h-p adaptivity. Another possibility would be to use domain decomposition with different refinement levels together with moving meshes.

In this thesis, we use generic linear solvers, which are not optimized for our problem. We can greatly improve the performance of our numerical scheme by implementing problem specific pre-conditioners. Also, parallel domain decomposition methods might be a valuable improvement for the solution of our linear system.

Lastly, we showed that our proposed linearization scheme converges globally for any initial guess value for the solution, whereas the Newton scheme converges quadratically, but only locally and can have issues with convergence for ill behaved, realistic problems. It will be interesting to investigate the possibility of combining the linearization scheme with the Newton scheme to make the Newton scheme more robust for application to realistic problems.

List of Figures

List of Tables

Bibliography

M. Acosta, C. Merten, G. Eigenberger, H. Class, R. Helmig, B. Thoben, and H. Müller-Steinhagen. Modeling non-isothermal two-phase multicomponent flow in the cathode of PEM fuel cells. *Journal of Power Sources*, 2(159):1123–1141, 2006.

R.A. Adams and J.J.F. Fournier. *Sobolev Spaces*. Pure and Applied Mathematics. Elsevier Science, 2003.

M.M. Arzanfudi, R. Al-Khoury, and L.J. Sluys. A computational model for fluid leakage in heterogeneous layered porous media. *Advances in Water Resources*, 73:214 – 226, 2014.

I. Babuska and M. Suri. The $h - p$ version of the finite element method with quasiuniform meshes. *ESAIM: Mathematical Modelling and Numerical Analysis*, 21(2):199–238, 1987.

G.I. Barenblatt, T.W. Patzek, D.B. Silin, et al. The mathematical model of nonequilibrium effects in water-oil displacement. *Society of Petroleum Engineers Journal*, 8(04):409–416, 2003.

P. Bastian. A fully-coupled discontinuous galerkin method for two-phase flow in porous media with discontinuous capillary pressure. *Computational Geosciences*, 18(5):779–796, 2014.

P. Bastian and B. Riviere. Superconvergence and H(div) projection for discontinuous Galerkin methods. *International Journal for Numerical Methods in Fluids*, 42(10):1043–1057, 2003.

P. Bastian, M. Blatt, A. Dedner, C. Engwer, R. Klöfkorn, R. Kornhuber, M. Ohlberger, and O. Sander. *A generic grid interface for parallel and adaptive scientific computing*. DFG Research Center MATHEON, 2007.

P. Bastian, M. Blatt, A. Dedner, C. Engwer, R. Klöfkorn, R. Kornhuber, M. Ohlberger, and O. Sander. A generic grid interface for parallel and adaptive scientific computing. part ii: Implementation and tests in DUNE. *Computing*, 82(2):121–138, 2008a.

P. Bastian, M. Blatt, A. Dedner, C. Engwer, R. Klöfkorn, M. Ohlberger, and O. Sander. A generic grid interface for parallel and adaptive scientific computing. Part i: Abstract framework. *Computing*, 82(2):103–119, 2008b.

P. Bastian, F. Heimann, and S. Marnach. Generic implementation of finite element methods in the distributed and unified numerics environment (DUNE). *Kybernetika*, 46(2):294–315, 2010.

P. Bastian, M. Blatt, A. Dedner, Ch. Engwer, J. Fahlke, C. Gräser, R. Klöfkorn, M. Nolte, M. Ohlberger, and O. Sander. DUNE Web page, 2011. http://www.dune-project.org.

M. Bause, U. Koecher, and F.A. Radu. Space-time finite element approximation of the Biot poroelasticity system with iterative coupling. *Computer Methods in Applied Mechanics and Engineering*, 2017.

J. Bear. *Dynamics of Fluids in Porous Media*. Dover Civil and Mechanical Engineering. Dover Publications, 2013.

L. Bergamaschi and M. Putti. Mixed finite elements and Newton-type linearizations for the solution of Richards' equation. *International Journal for Numerical Methods in Engineering*, 45(1):1025–1046, 1999.

M. Bertsch, R. Dal Passo, and C.J. van Duijn. Analysis of oil trapping in porous media flow. *SIAM Journal on Mathematical Analysis*, 35(1):245–267, 2003.

J.W. Both, M. Borregales, J.M. Nordbotten, K. Kumar, and F.A. Radu. Robust fixed stress splitting for Biot's equations in heterogeneous media. *Applied Mathematics Letters*, 68: 101–108, 2017.

A. Bourgeat and M. Panfilov. Effective two-phase flow through highly heterogeneous porous media: Capillary nonequilibrium effects. *Computational Geosciences*, 2(3):191–215, 1998.

A.T. Brooks, R.H. Corey. Hydraulic properties of porous media. *Hydrology papers (Colorado State University)*, 3, 1964.

N.T. Burdine. Relative permeability calculations from pore size distribution data. *Journal of Petroleum Technology*, 5(3):71 – 78, 1953.

F. Buzzi, M. Lenzinger, and B. Schweizer. Interface conditions for degenerate two-phase flow equations in one space dimension. *Analysis. International Mathematical Journal of Analysis and its Applications*, 29(3):299–316, 2009.

C. Cancès. *Two-phase flows in heterogeneous porous media: Modeling and analysis of the flows of the effects involved by the discontinuities of the capillary pressure.* PhD thesis, Université de Provence-Aix-Marseille I, 2008.

C. Cancès, T. Gallouët, and A. Porretta. Two-phase flows involving capillary barriers in heterogeneous porous media. *Interfaces and Free Boundaries*, 11:239–258, 2009.

X. Cao and I.S. Pop. Two-phase porous media flows with dynamic capillary effects and hysteresis : Uniqueness of weak solutions. *Computers and Mathematics with Applications*, 69(2015)(7):688–695, 2015.

X. Cao and I.S. Pop. Degenerate two-phase porous media flow model with dynamic capillarity. *Journal of Differential Equations*, 260(3):2418 – 2456, 2016.

X. Cao, S.F. Nemadjieu, and I.S. Pop. A multipoint flux approximation finite volume scheme for two phase porous media flow with dynamic capillarity. *CASA-Report 15-33*, 2015.

M. Celia, E. Bouloutas, and R. Zarba. A general mass-conservative numerical solution for the unsaturated flow equation. *Water Resources Research*, 26:1483–1496, 1990.

G. Chavent and J. Jaffre. *Mathematical Models and Finite Elements for Reservoir Simulation Single Phase, Multiphase and Multicomponent Flows through Porous Media*, volume 17 of *Studies in Mathematics and Its Applications*. Elsevier, 1986.

Z. Chen. Degenerate two-phase incompressible flow: I. existence, uniqueness and regularity of a weak solution. *Journal of Differential Equations*, 171(2):203 – 232, 2001.

M.J. de Neef and J. Molenaar. Analysis of DNAPL infiltration in a medium with a low-permeable lens. *Computational Geosciences*, 1(2):191–214, 1997.

J.W. Demmel, J.R. Gilbert, and X.S. Li. SuperLU users' guide. Technical Report LBNL-44289, Lawrence Berkeley National Laboratory, September 1999.

P. Deuflhard. *Newton methods for nonlinear problems : affine invariance and adaptive algorithms*. Springer series in computational mathematics. Springer, Berlin, Heidelberg, New York, 2004.

D.A. Di Carlo. Experimental measurements of saturation overshoot on infiltration. *Water Resources Research*, 40(4), 2004.

D.A. Di Pietro and A. Ern. Discrete functional analysis tools for discontinuous Galerkin methods with application to the incompressible Navier-Stokes equations. *Mathematics of Computation*, 79(271):1303–1330, 2010.

D.A. Di Pietro and A. Ern. *Mathematical Aspects of Discontinuous Galerkin Methods*. Springer, 2012.

H.-J.G. Diersch, V. Clausnitzer, V. Myrnyy, R. Rosati, M. Schmidt, H. Beruda, B.J. Ehrnsperger, and R. Virgilio. Modeling unsaturated flow in absorbent swelling porous media: Part 1. theory. *Transport in Porous Media*, 83(3):437–464, 2010.

L.J. Durlofsky. A triangle based mixed finite element - finite volume technique for modeling two phase flow through porous media. *Journal of Computational Physics*, 105(2):252–266, 1993.

G. Enchéry, R. Eymard, and A. Michel. Numerical approximation of a two-phase flow problem in a porous medium with discontinuous capillary forces. *SIAM Journal on Numerical Analysis*, 43(6):2402–2422, 2006.

Y. Epshteyn and B. Riviere. Analysis of discontinuous Galerkin methods for incompressible two-phase flow. *Journal of Computational and Applied Mathematics*, 225(2):487 – 509, 2009.

A. Ern, I. Mozolevski, and L. Schuh. Discontinuous Galerkin approximation of two-phase flows in heterogeneous porous media with discontinuous capillary pressures. *Computer Methods in Applied Mechanics and Engineering*, 199(23–24):1491 – 1501, 2010.

L.C. Evans. *Partial Differential Equations*. Graduate studies in mathematics. American Mathematical Society, 1998.

R. Eymard, R. Herbin, and A. Michel. Mathematical study of a petroleum-engineering scheme. *Mathematical Modelling and Numerical Analysis*, 37:2003, 2003.

R. Eymard, D. Hilhorst, and M. Vohralík. A combined finite volume–finite element scheme for the discretization of strongly nonlinear convection–diffusion–reaction problems on non-matching grids. *Numerical Methods for Partial Differential Equations*, 26(3):612–646, 2010.

Y. Fan and I.S. Pop. A class of pseudo-parabolic equations: existence, uniqueness of weak solutions, and error estimates for the Euler-implicit discretization. *Mathematical Methods in the Applied Sciences*, 34:2329–2339, 2011.

R. Fucik and J. Mikyska. Numerical investigation of dynamic capillary pressure in two-phase flow in porous medium. *Mathematica Bohemica*, 136(4):395–403, 2011.

V. Girault and P.A. Raviart. *Finite element methods for Navier-Stokes equations: Theory and algorithms*. Springer-Verlag, 1986.

S. Gupta, R. Helmig, and H. Wohlmuth. Non-isothermal, multi-phase, multi-component flows through deformable methane hydrate reservoirs. *Computational Geosciences*, 5(19): 1063–1088, 2015.

S.M. Hassanizadeh and A.Yu. Beliaev. A theoretical model of hysteresis and dynamic effects in the capillary relation for two-phase flow in porous media. *Transport in Porous Media*, 43(3):487–510, 2001.

S.M. Hassanizadeh and W.G. Gray. General conservation equations for multi-phase systems: 1. Averaging procedure. *Advances in Water Resources*, 2:131 – 144, 1979a.

S.M. Hassanizadeh and W.G. Gray. General conservation equations for multi-phase systems: 2. Mass, momenta, energy, and entropy equations. *Advances in Water Resources*, 2:191 – 203, 1979b.

S.M. Hassanizadeh and W.G. Gray. Thermodynamic basis of capillary pressure in porous media. *Water Resources Research*, 29(10):3389–3405, 1993.

S.M. Hassanizadeh, M. Celia, and H.K. Dahle. Dynamic effect in the capillary pressure-saturation relationship and its impacts on unsaturated flow. *Vadose Zone Journal*, 1(1): 38–57, 2002.

R. Helmig. *Multiphase Flow and Transport Processes in the Subsurface: A Contribution to the Modeling of Hydrosystems*. Environmental engineering. Springer, 1997.

R. Helmig, A. Weiss, and B.I. Wohlmuth. Dynamic capillary effects in heterogeneous porous media. *Computational Geosciences*, 11(3):261–274, 2007.

R. Helmig, A. Weiss, and B.I. Wohlmuth. Variational inequalities for modeling flow in heterogeneous porous media with entry pressure. *Computational Geosciences*, 13(3):373–389, 2009.

U. Hornung. *Homogenization and Porous Media*. Springer, 2012.

H. Hoteit and A. Firoozabadi. Numerical modeling of two-phase flow in heterogeneous permeable media with different capillarity pressures. *Advances in Water Resources*, 31(1): 56–73, 2008.

B. Jha, L. Cueto-Felgueroso, and R. Juanes. Fluid mixing from viscous fingering. *Physical Review Letters*, 106, 2011.

S. Karpinski and I.S. Pop. Analysis of an interior penalty discontinuous Galerkin scheme for two phase flow in porous media with dynamic capillarity effects. *Numerische Mathematik*, 136(1):249–286, 2017.

S. Karpinski, I.S. Pop, and F.A. Radu. Analysis of a linearization scheme for an interior penalty discontinuous Galerkin method for two phase flow in porous media with dynamic capillarity effects. *International Journal for Numerical Methods in Engineering*, 2017. (accepted, available online).

J. Koch, A. Rätz, and B. Schweizer. Two-phase flow equations with a dynamic capillary pressure. *European Journal of Applied Mathematics*, 24:49–75, 2 2013.

J. Kou and S. Sun. A new treatment of capillarity to improve the stability of IMPES two-phase flow formulation. *Computers and Fluids*, 39:1923–1931, 2010a.

J. Kou and S. Sun. On iterative IMPES formulation for two-phase flow with capillarity in heterogeneous porous media. *International Journal of Numerical Analysis and Modeling Series B*, pages 20–40, 2010b.

S. Kraeutle. The semismooth Newton method for multicomponent reactive transport with minerals. *Advances in Water Resources*, 34(5):137–151, 2011.

B.H. Kueper and E.O. Frind. Two-phase flow in heterogeneous porous media: 1. Model development. *Water Resources Research*, 27(6):1049–1057, 1991a.

B.H. Kueper and E.O. Frind. Two-phase flow in heterogeneous porous media: 2. Model application. *Water Resources Research*, 27(6):1059–1070, 1991b.

F. Lehmann and Ph. Ackerer. Comparison of iterative methods for improved solutions of the fluid flow equation in partially saturated porous media. *Transport in Porous Media*, 31: 275–292, 1998.

B. Li. Maximum-norm stability and maximal L^p regularity of FEMs for parabolic equations with Lipschitz continuous coefficients. *Numerische Mathematik*, 131(3):489–516, 2015.

F. List and F.A. Radu. A study on iterative methods for solving Richards' equation. *Computational Geosciences*, 20(2):341–353, 2016.

S. Manthey. *Two-phase flow processes with dynamic effects in porous media - parameter estimation and simulation*, volume 157 of *Mitteilungen / Institut für Wasser- und Umweltsystemmodellierung*. Universität Stuttgart, Stuttgart, 2006. (Doctoral dissertation).

A. Mikelic. A global existence result for the equations describing unsaturated flow in porous media with dynamic capillary pressure. *Journal of Differential Equations*, 248(6):1561 – 1577, 2010.

I. Mozolevski and L. Schuh. Numerical simulation of two-phase immiscible incompressible flows in heterogeneous porous media with capillary barriers. *Journal of Computational and Applied Mathematics*, 242:12–27, 2013.

Y. Mualem. A new model for predicting the hydraulic conductivity of unsaturated porous media. *Water Resources Research*, 12:513–522, 1976.

R. Neumann, P. Bastian, and O. Ippisch. Modeling and simulation of two-phase two-component flow with disappearing nonwetting phase. *Computational Geosciences*, 17: 139–149, 2013.

J.A. Nitsche and M.F. Wheeler. L_∞-boundedness of the finite element Galerkin operator for parabolic problems. *Numerical Functional Analysis and Optimization*, 4(4):325–353, 1981/82.

J.M. Nordbotten and M.A. Celia. *Geological Storage of CO2: Modeling Approaches for Large-Scale Simulation*. Wiley, 2011.

E.J. Park. Mixed finite elements for nonlinear second-order elliptic problems. *SIAM Journal on Numerical Analysis*, 32:865–885, 1995.

M. Peszynska and S.-Y. Yi. Numerical methods for unsaturated flow with dynamic capillary pressure in heterogeneous porous media. *International Journal of Numerical Analysis and Modeling*, 5(Special Issue):126–149, 2008.

I.S. Pop, F.A. Radu, and P. Knabner. Mixed finite elements for the Richards' equations: Linearization procedure. *Journal of Computational and Applied Mathematics*, 168(1-2): 365–373, 2004.

F.A. Radu and I.S. Pop. Mixed finite element discretization and Newton iteration for a reactive contaminant transport model with non-equilibrium sorption: Convergence analysis and error estimates. *Computational Geosciences*, 15(3):431–450, 2011.

F.A. Radu, I.S. Pop, and P. Knabner. On the convergence of the Newton method for the mixed finite element discretization of a class of degenerate parabolic equation. *Numerical Mathematics and Advanced Applications. A. Bermudez de Castro et al. (editors), Springer.*, pages 1194–1200, 2006.

F.A. Radu, J.M. Nordbotten, I.S. Pop, and K. Kumar. A robust linearization scheme for finite volume based discretizations for simulation of two-phase flow in porous media. *Journal of Computational and Applied Mathematics*, 289(0):134 – 141, 2015a.

F.A. Radu, J.M. Nordbotten, I.S. Pop, and K. Kumar. A convergent mass conservative numerical scheme based on mixed finite elements for two-phase flow in porous media. *arXiv*, 1512.08387:1 – 32, 2015b.

A. Rätz and B. Schweizer. Hysteresis models and gravity fingering in porous media. *ZAMM-Journal of Applied Mathematics and Mechanics*, 94(7-8):645–654, 2014.

B. Riviere, M.F. Wheeler, and V. Girault. A priori error estimates for finite element methods based on discontinuous approximation spaces for elliptic problems. *SIAM Journal on Numerical Analysis*, 39(3):902–931, 2001.

M. Slodička. A robust and efficient linearization scheme for doubly nonlinear and degenerate parabolic problems arising in flow in porous media. *SIAM Journal of Scientific Computing*, 23(5):1593–1614, 2002.

M. Slodička. Approximation of a nonlinear degenerate parabolic equation via a linear relaxation scheme. *Numerical Methods for Partial Differential Equations*, 21(2):191–212, 2005a.

M. Slodička. A robust linearisation scheme for a nonlinear elliptic boundary value problem: Error estimates. *Anziam Journal*, 46(4):449–470, 2005b.

S. Sun and M.F. Wheeler. Symmetric and nonsymmetric discontinuous Galerkin methods for reactive transport in porous media. *SIAM Journal on Numerical Analysis*, 43(1):195–219, 2005.

R. Temam. *Navier-Stokes equations: Theory and numerical analysis*, volume 343. American Mathematical Soc., 2001.

C.J. van Duijn and M.J. de Neef. Similarity solution for capillary redistribution of two phases in a porous medium with a single discontinuity. *Advances in Water Resources*, 21(6):451–461, 1998.

C.J. van Duijn, J. Molenaar, and M.J. de Neef. The effect of capillary forces on immiscible two-phase flow in heterogeneous porous media. *Transport in Porous Media*, 21(1):71–93, 1995.

C.J. van Duijn, Y. Fan, L.A. Peletier, and I.S. Pop. Travelling wave solutions for degenerate pseudo-parabolic equations modelling two-phase flow in porous media. *Nonlinear Analysis: Real World Applications*, 14(3):1361 – 1383, 2013.

C.J. van Duijn, X. Cao, and I. S. Pop. Two-phase flow in porous media: Dynamic capillarity and heterogeneous media. *Transport in Porous Media*, 114(2):283 – 308, 2016.

M.Th. van Genuchten. A closed-form equation for predicting the hydraulic conductivity of unsaturated soils. *Journal of Soil Science Society of America*, 44(5):892–898, 1980.

T. Warburton and J.S. Hesthaven. On the constants in hp-finite element trace inverse inequalities. *Computer Methods in Applied Mechanics and Engineering*, 192(25):2765 – 2773, 2003.

W.A. Yong and I.S. Pop. A numerical approach to porous medium equations. *Preprint, IWR Heidelberg*, 95-50, 1996.